FEASIBILITY STUDY
30 WATTS PER POUND
ROLLUP SOLAR ARRAY

Second Quarterly Report

Contract No. 951971

REPORT NO. 40067-2 15 JANUARY 1968

This work was performed for the Jet Propulsion Laboratory, California Institute of Technology, as sponsored by the National Aeronautics and Space Administration under Contract NAS 7-100.

RYAN AERONAUTICAL COMPANY ◇ 5650 KEARNY MESA ROAD ◇ SAN DIEGO, CALIFORNIA

This report contains information prepared by the Ryan Aeronautical Company under JPL subcontract. Its content is not necessarily endorsed by the Jet Propulsion Laboratory, California Institute of Technology, or the National Aeronautics and Space Administration.

ABSTRACT

Principal efforts in this reporting period were applied to preparation of the detail design of the array structure and mechanisms and to manufacturing drawings for a demonstration model of the selected design concept. Analytical support focused on substantiation of the detail design. Additional studies were performed of dynamic criteron effects on components of the wrap drum. Thermal studies were extended to evaluate another thin film (preferred) material for the substrate and its influence on solar cell temperatures. Electrical design considerations included feasibility studies and ramifications of using a new, larger size, solar cell and a new coverglass application concept. Preliminary evaluations suggest improvement in the array power to weight characteristic and net savings in the estimated cost of cell installation. Weight estimates have been up-dated in keeping with refinements in detail design. Performance of this contractor's rollout solar array design is now projected as capable of producing 31.6 watts per pound of weight; excludes estimated improvements from use of new solar cell design.

CONTENTS

CONTENTS (Continued)

CONTENTS (Continued)

LIST OF ILLUSTRATIONS

LIST OF ILLUSTRATIONS

LIST OF ILLUSTRATIONS

1.0 INTRODUCTION

This second Quarterly Report is submitted by the Ryan Aeronautical Company to the Jet Propulsion Laboratory in accordance with Article I, item (a) (2) (iv) and Article II, item (a) (5) of Contract No. 951971. The report presents a summary of work accomplished from 1 November through 31 December 1967. The reporting period is abbreviated to coincide with the extended reporting period encompassed by the first Quarterly Report, reference 1, (i.e., from date of Contract through 31 October 1967).

The discussion presented herein reports the collective efforts of Ryan and its associate contractor, Spectrolab Division of Textron Electronics, Inc. The data describes the refinements and those improvements that have developed in advancing a preliminary design configuration towards a definitive, detail design.

2.0 TECHNICAL DISCUSSION

2.1 DESIGN

Definition of the detail design was the prime objective in this reporting period.

Ryan concentrated on preparing drawings for the structures and mechannisms which compose a 250 square foot array and certain models for test and demonstration purposes. Detail designs adhered to the configuration presented in the first Quarterly Report, (see Figure 1, sheets 1 and 2) except for a new arrangement in attachment of the substrate to the extendible beams.

Spectrolab investigated the feasibility of using a larger solar cell and how it would affect circuit layouts, power to weight ratios and relative cost considerations. A new coverglass arrangement and related fabrication techology are presented in subsequent discussions.

2.1.1 Mechanical/Structural

2.1.1.1 Substrate-to-Beam Attachment

A change has been made in the selected structural configuration which concerns the clip arrangement for attaching the thin-film substrate to the deployable beams. It was decided that the attachment scheme (the use of fold-over, metal clips) could be improved upon by using a device that was more tolerant of manufacturing variables and anticipated deviations in installation and operational characteristics.

The solution that was adopted was to substitute local, silicone impregnated fiberglass tabs that are bonded to both substrate and beam as shown in Figure 2.

PRECEDING PAGE BLANK NOT FILMED.

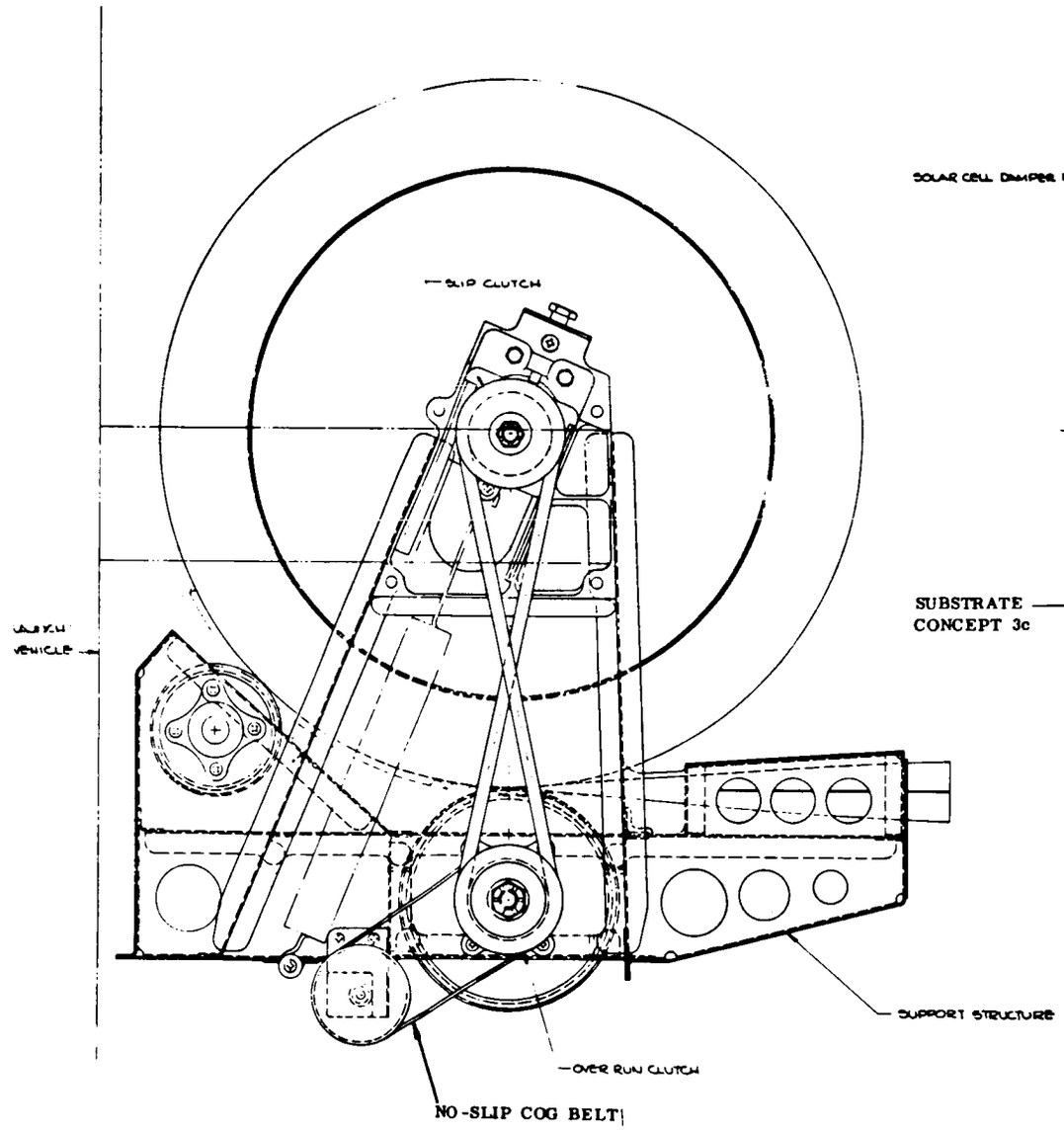

Fig 1-A

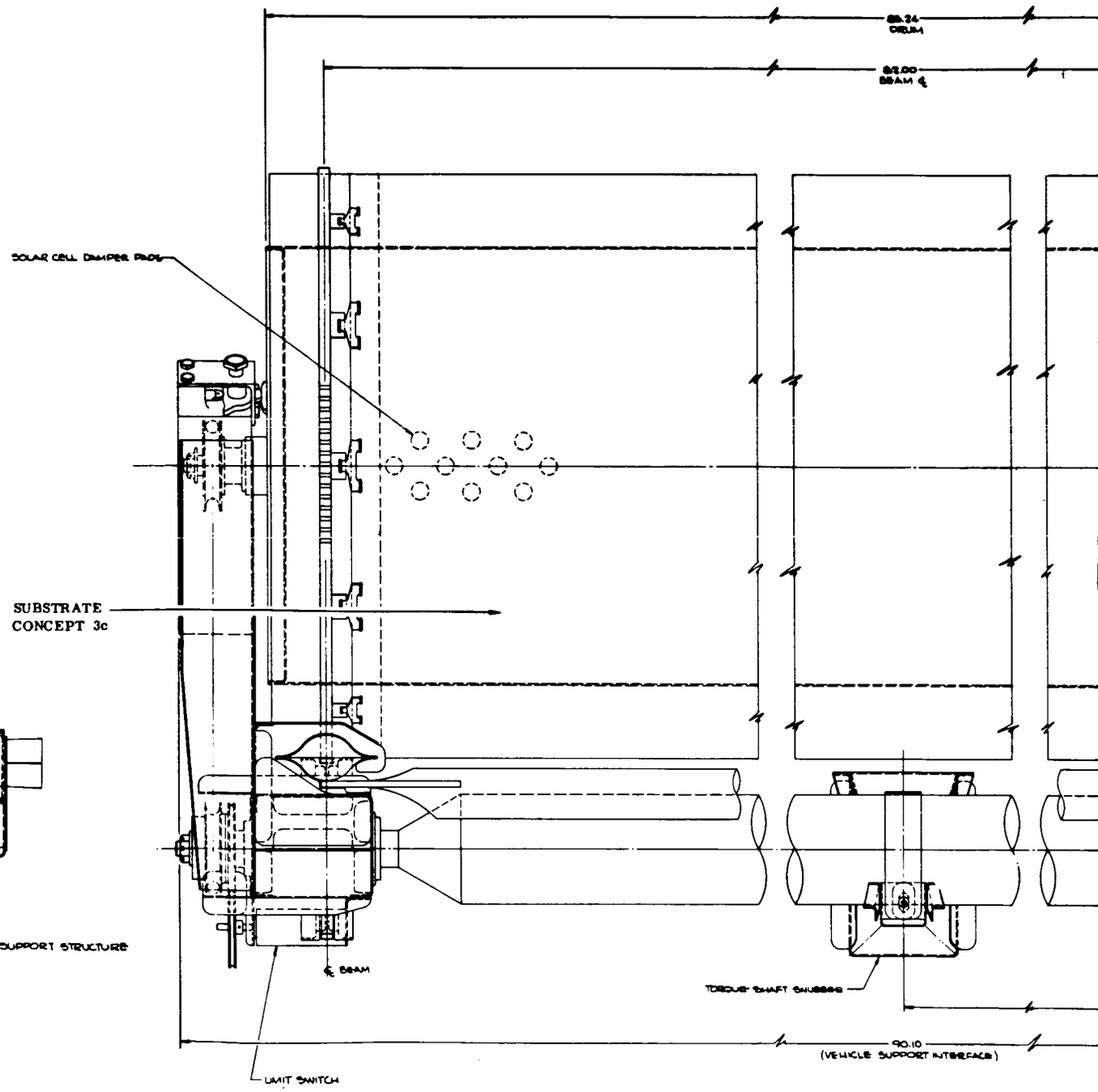

Fig 1-B

NOTE:

This end view illustrates Concept 1 b.

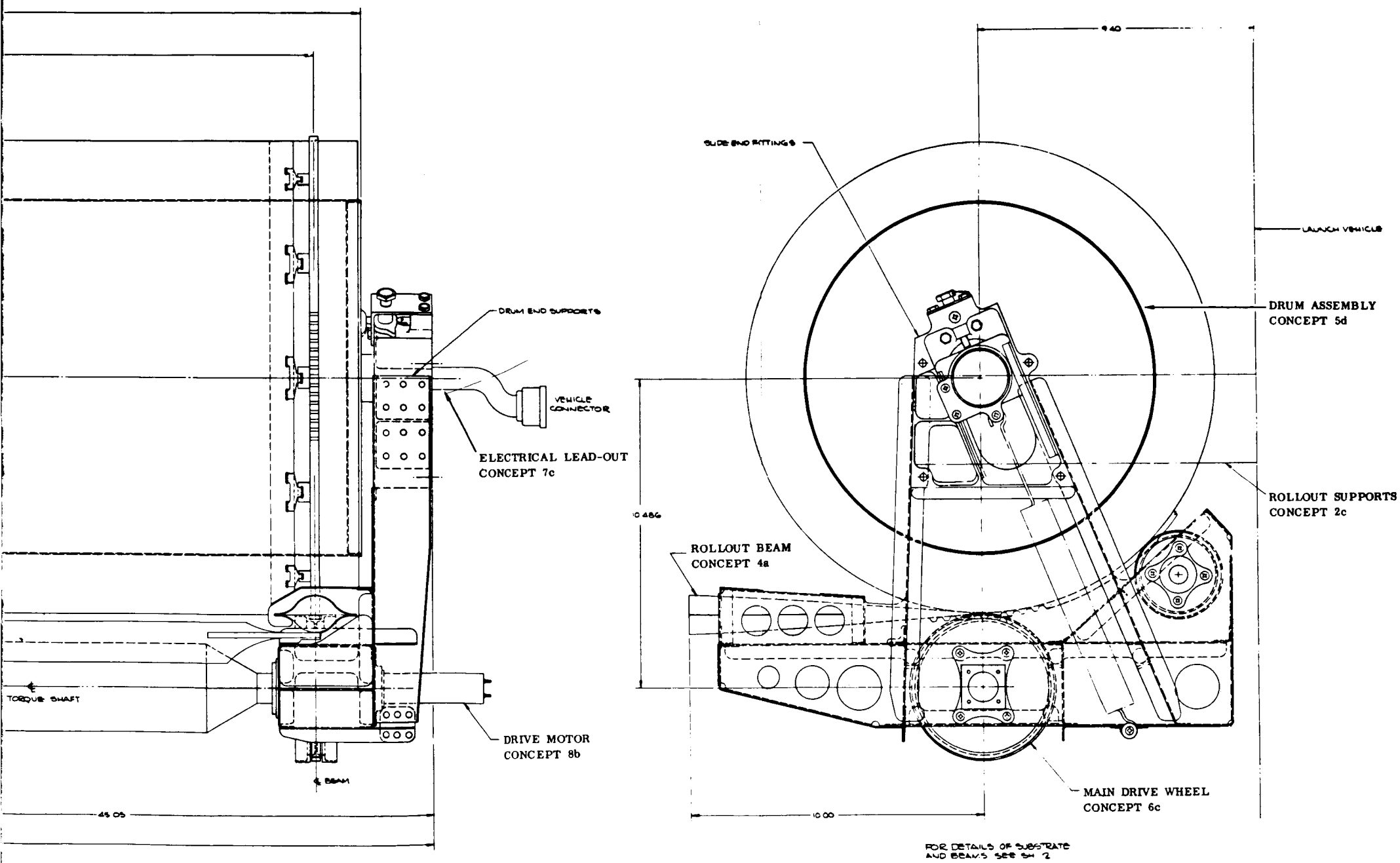

Figure 1 Roll-up Assembly - 250 Square Foot (Sheet 1 of 2)

Fig 1-C

PRECEDING PAGE BLANK NOT FILMED.

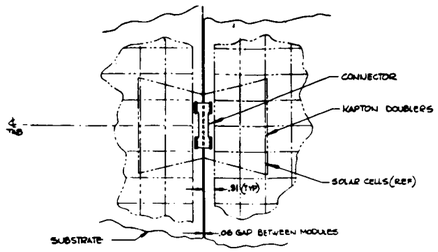

VIEW D INTER MODULE ATTACH
FULL SCALE

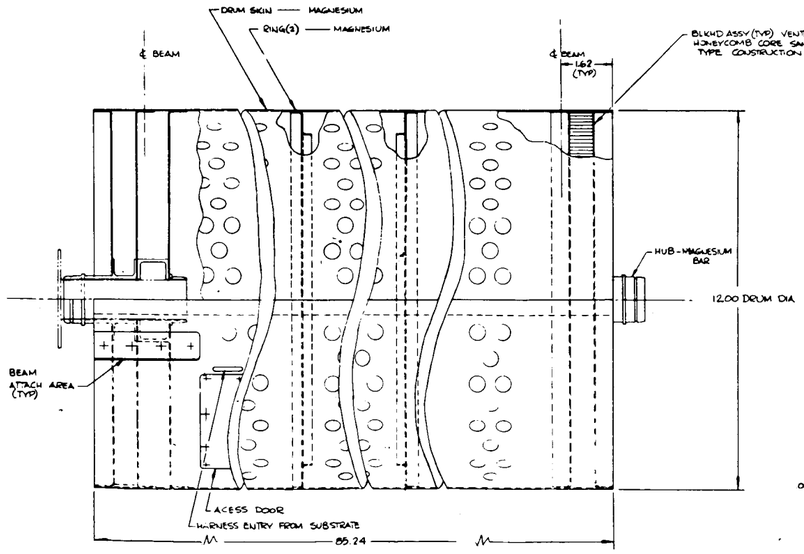

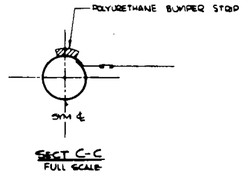

SECT C-C
FULL SCALE

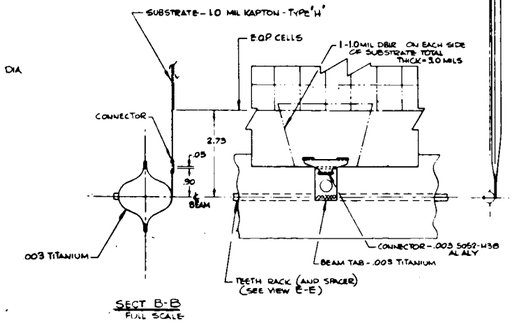

SECT B-B
FULL SCALE

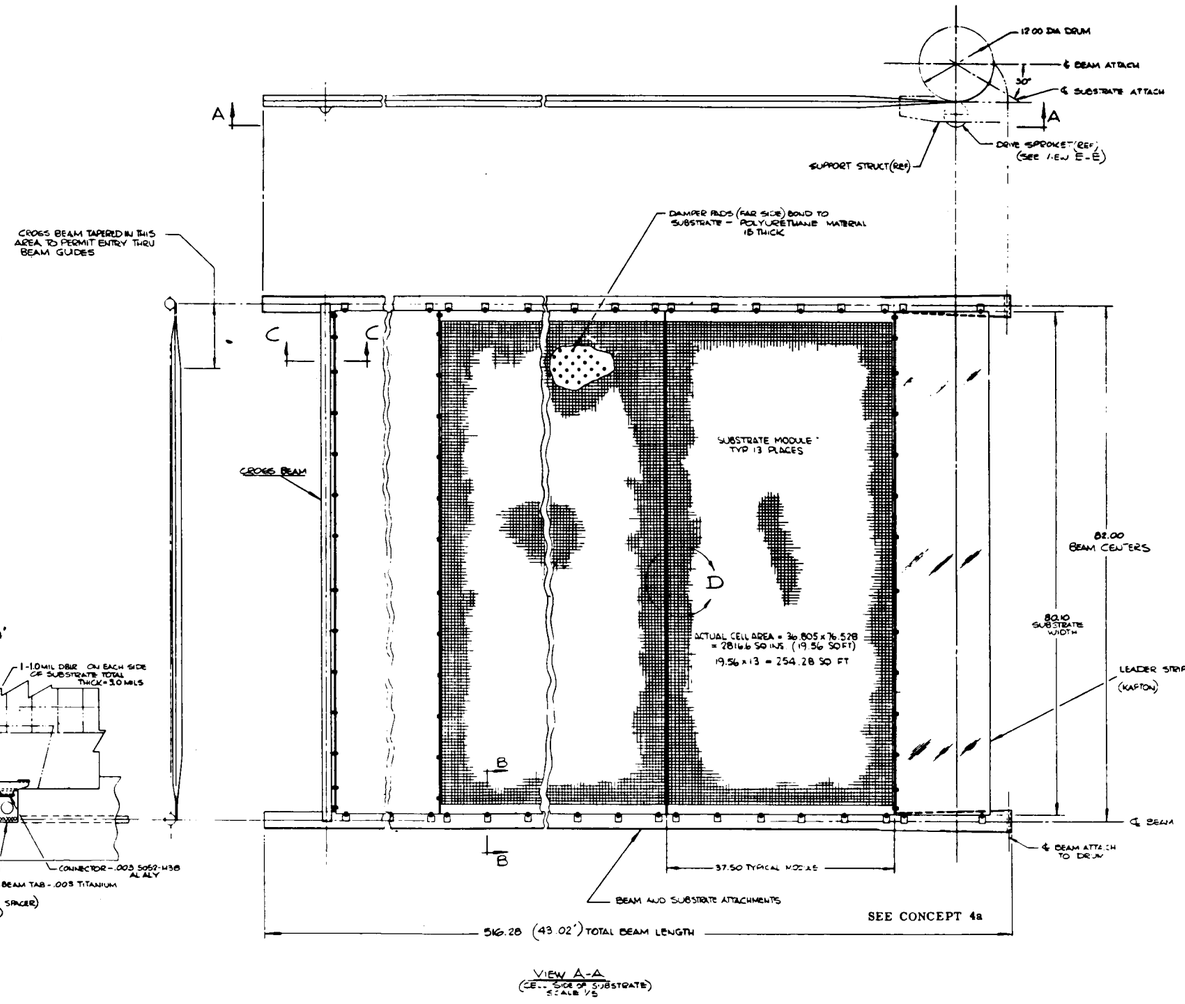

VIEW A-A
(SEE SIDE OF SUBSTRATE)
SCALE 1/6

Fig 1-A Sheet 2 of 2

Fig 1-B Sheet 2 of 2

Figure 1 Roll-up Assembly - 250 Square Foot (Sheet 2 of 2)

Fig 1-C
Sheet 2 of 2

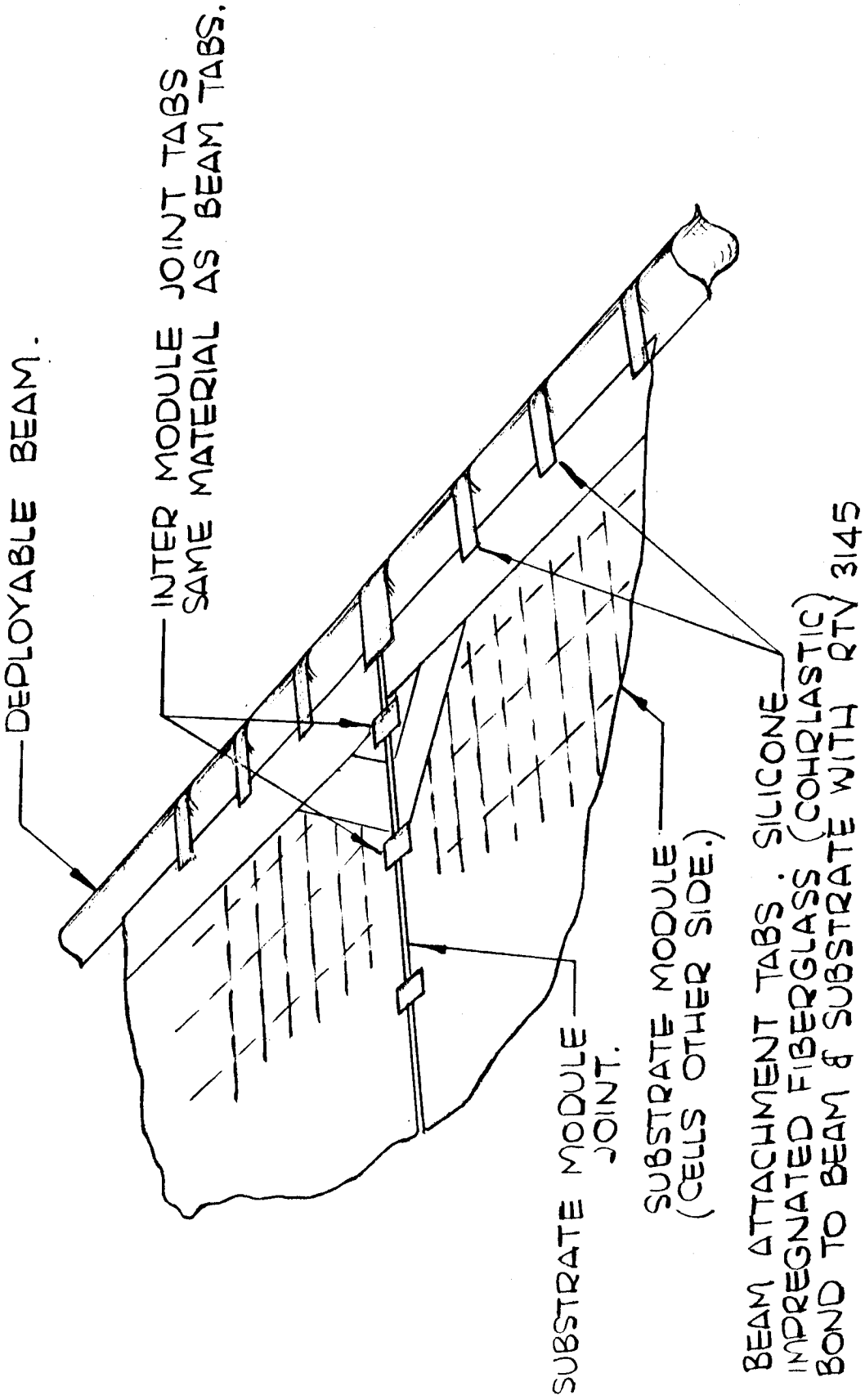

Figure 2 Substrate-to-Beam Tab Arrangement

2.1.1.2 Lateral Restraint for Wrapped Substrate

Further study of vibration effects on the wrapped substrate indicated that dynamic inputs, parallel to the axis of the wrap drum, could induce inter-layer shifting of substrate wraps and dislocation from the drum at the attachment interface. Therefore, it would be wise to incorporate a simple method for restraining the wrapped substrate.

The design selected consists of intermittently spaced channel sections attached to the crown of the beam on the side opposite of the corrugated drive rack. When the beam and substrate wrap about the drum these local channels engage the adjacent corrugation strip of the preceding wrap. By this interlocking scheme the lateral substrate loads are transmitted through the beams to the wrap drum. An additional restraint is provided to secure the first wrap on the drum.

2.1.2 Electrical Design

2.1.2.1 Circuit Layout

A new solar cell size is being considered to increase overall area efficiency and reduce fabrication costs.

A gain in the power per unit area ratio is obtained by increasing the overall cell size and maintaining the same contact area as the 2 x 6 cm silicon solar cell proposed in the first Quarterly Report. The efficiency of this larger solar cell (1.042 $\pm$.005 x 2.384 $\pm$.005 inches; 2.65 cm x 6.08 cm) compares favorably with the 2 x 2 cm corner dart contact cell.

This cell would necessitate a slight modification in the longitudinal module substrate dimension. The dimension would be reduced by approximately .500 inch. Overall circuit length will be 36.000 inches plus a .500 inch allowance for circuit termination. Each complete circuit

will consist of four 34 cell sub-circuits connected in series to total 136 cells in series. No significant changes in circuit layout are required due to this change in solar cell size.

Figure 3 shows a typical module layout for 2 x 2 or 2 x 6 cm solar cells. Figure 4 is the module arrangement for the large cell.

2.1.2.2 Interconnect Design

The same type of bus bars and interconnections selected for the 2 x 6 cm solar cell can be used with the special large cell.

Consideration has been given to standardizing the longitudinal bus for each substrate panel module to facilitate interchangeability. A more detailed review indicates that interchangeability is an important factor to be considered during a cost analysis.

Standardization would require using a constant width longitudinal bus for all thirteen modules. A constant cross-section is feasible if the major power bus in considered to be at a constant potential along its entire length. A compromise dimension of 2.00 inches in width was selected. This results in an increase in weight of approximately .001 pound per square foot over the original concept. Current density in the conductor will be increased slightly at the inboard modules but will not influence the overall array performance significantly. Standardization of this nature would simplify fabrication of the substrates and minimize tooling requirements. Figure 5 illustrates the two longitudinal bus arrangements that have been discussed.

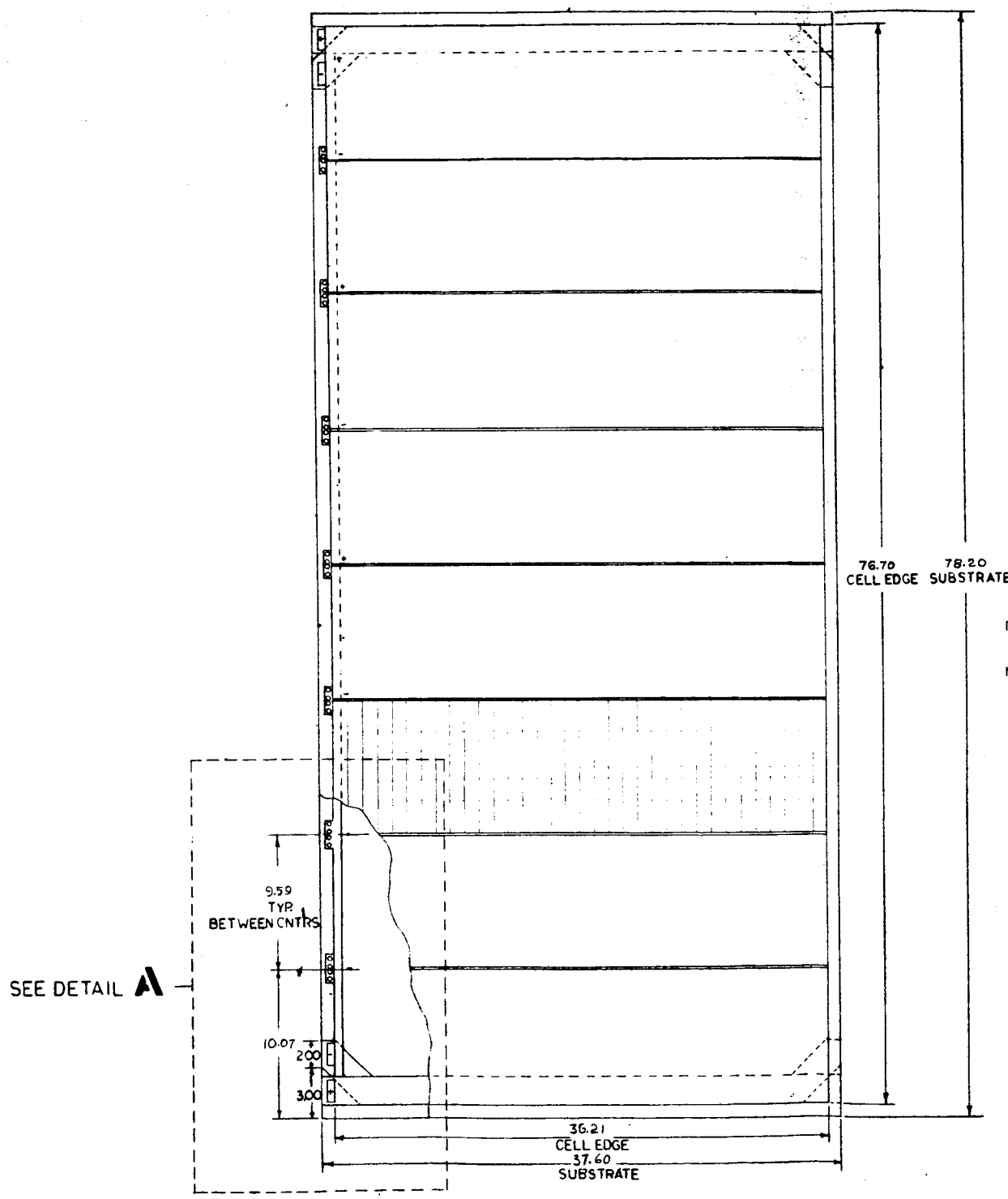

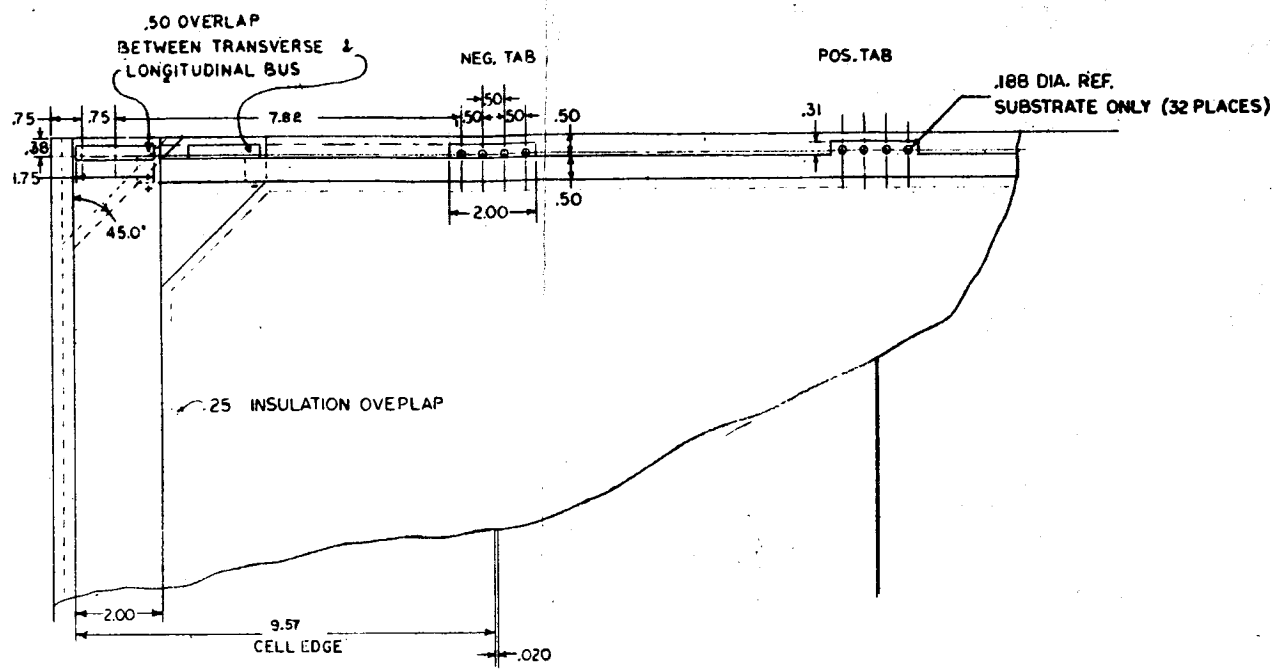

DETAIL A SCALE: 2-1

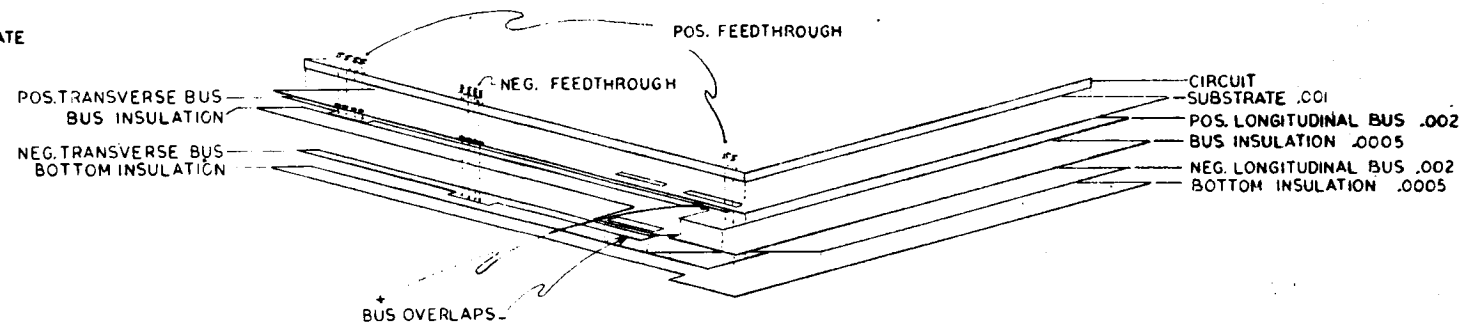

CROSS SECTION TYPICAL FOR:
(2X2 2X6 & SPECIAL CELL)

Figure 3 Solar Cell Module Layout for 2 X 2 or 2 X 6 cm Cells

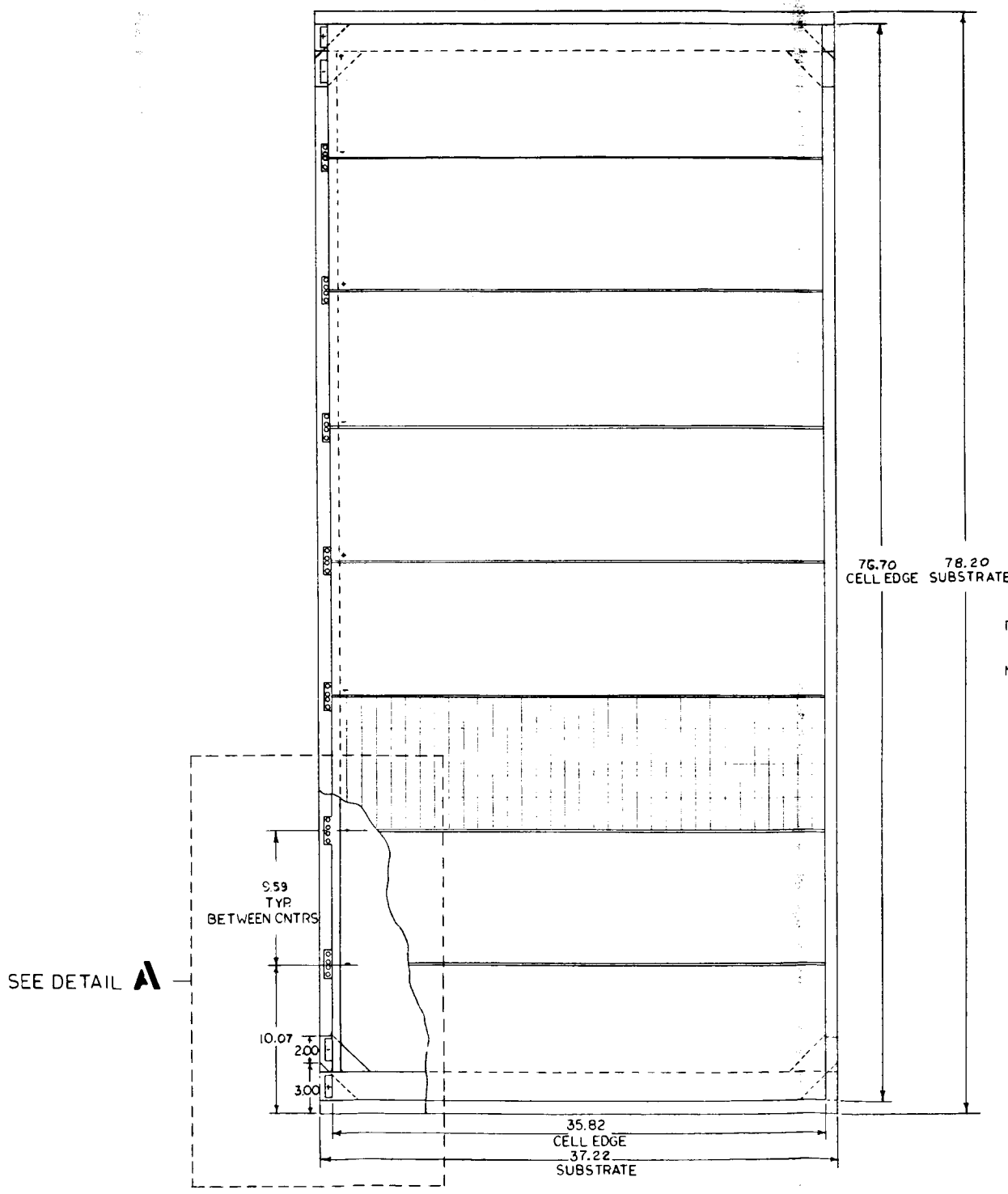

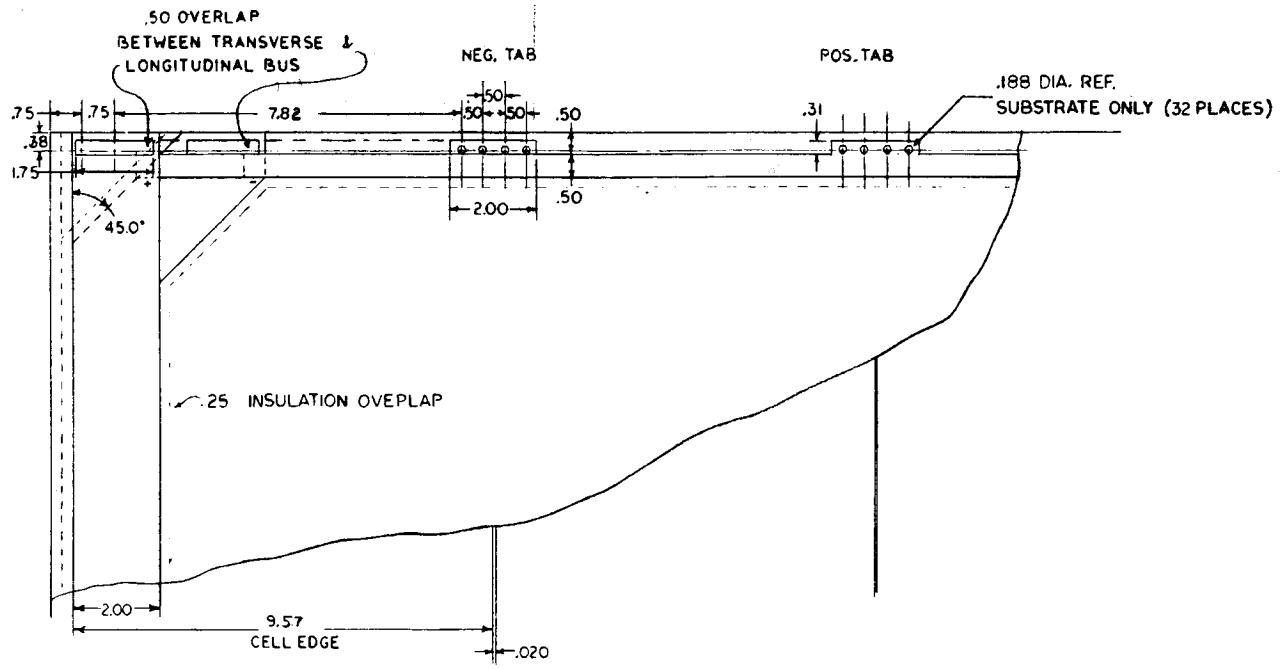

DETAIL A SCALE: 2-1

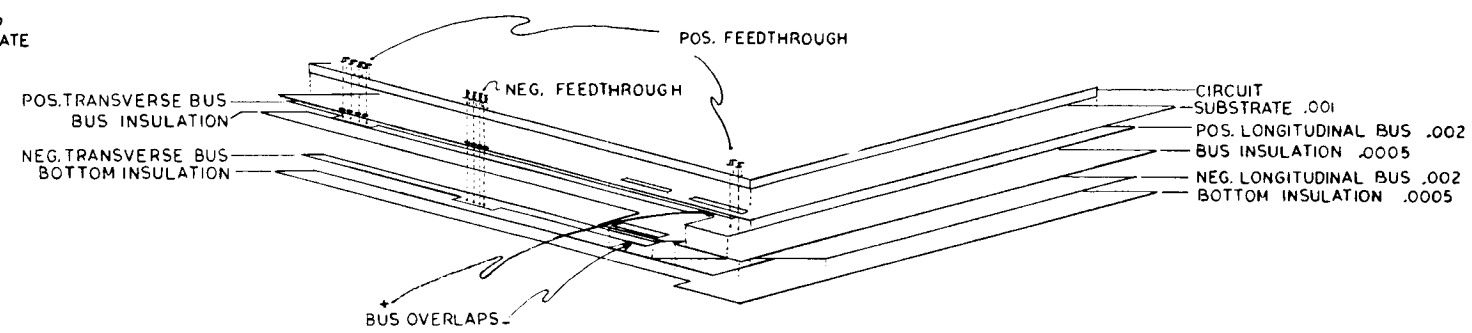

CROSS SECTION TYPICAL FOR:
(2X2 2X6 & SPECIAL CELL)

Figure 4 Solar Cell Module Layout for 1.042 x 2.384 inch Cells

PRECEDING PAGE BLANK NOT FILMED.

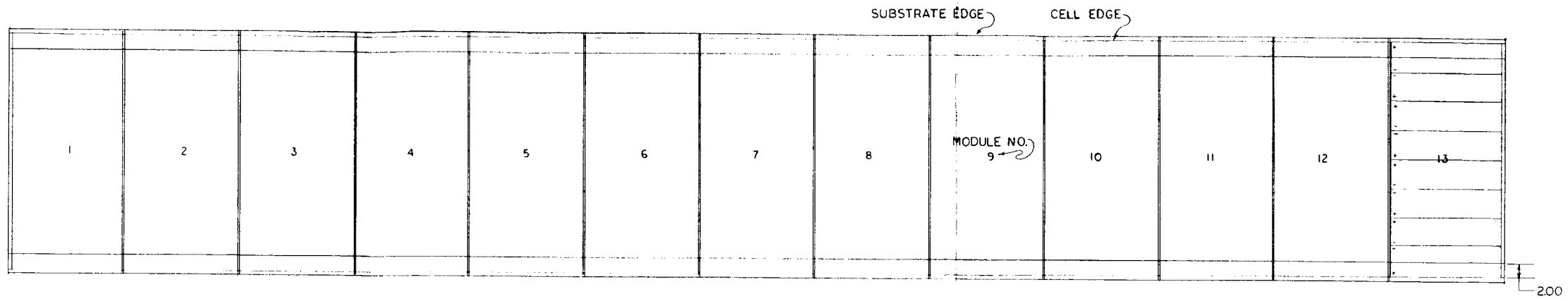

PROPOSED CONSTANT WIDTH BUS

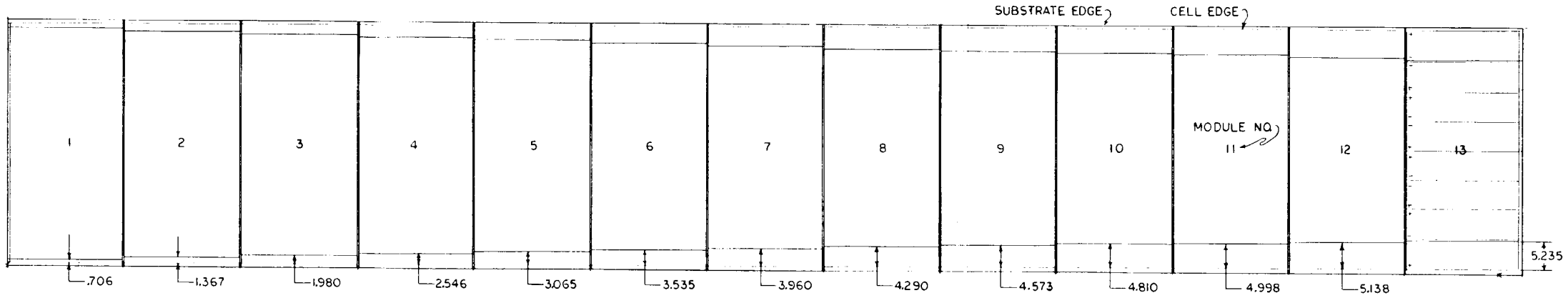

PROPOSED TAPERED BUS

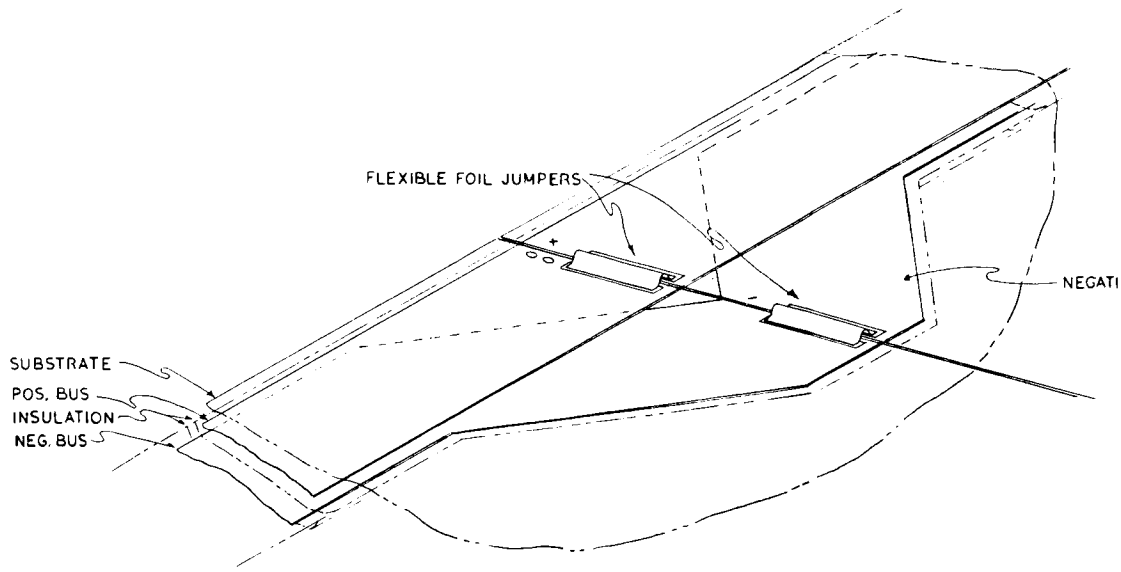

TYPICAL CONNECTION OF LONGITUDINAL BUS AT SUBSTRATE JOINT

Figure 5 Alternate Arrangements of Longitudinal Bus in Solar Array

2.1.3 Materials and Processes

2.1.3.1 Adhesive Systems

Evaluation of adhesive systems was continued with particular attention given to process methods for substrate assembly and application of solar cells. It has been reported (reference 1) that use of RTV 41 or RTV 511 with the Kapton substrate required a chromic acid etch pre-treatment. Preliminary tests indicated that RTV 3145 could produce higher peel values without chromic acid etch. However, use of primer on the Kapton surface was contradictory with the RTV 3145 system due to low peel strength values reported.

Peel tests were conducted to verify these results. Additional samples were prepared bonding the Kapton to solar cells and Kapton to aluminum. The solar cell bonding surface and the aluminum surface were primed with Dow Corning 1200 primer for all test coupons. The results of these tests are presented in Table 1 which follows.

TABLE 1

EFFECT OF PRIMER ON ADHESION OF SILICONE ADHESIVE TO KAPTON

CONFIGURATION	ADHESIVE/KAPTON SURFACE	PEEL STRENGTH LBS/IN WIDTH	FAILURE
Kapton to Solar Cell Bond	RTV 3145 - no primer	2.5	Adhesive to Kapton
	RTV 102 - no primer	0.8	" " "
Kapton to Aluminum Bond	RTV 3145 - no primer	3.3	Adhesive to Kapton
	RTV 3145/1200 primer	0.1	" " "
*Kapton to Solar Cell Bond	RTV 3145 - no primer	3.5	Adhesive to Kapton
	RTV 3145 /1200 primer	0.1	" " "

*Data from Spectrolab. Other data obtained at Ryan.

These results again indicate that when the Kapton surface is primed, the adhesion is completely lost.

Based on the adhesive work done on the previous quarter, TR-150-25 adhesive was selected to be used to fabricate a full size substrate. The method selected was to apply the adhesive in the areas to be bonded on the Kapton and B-stage the adhesive. The parts were then assembled and trial cures attempted in an oven, using a hot iron and an infra red lamp. Some difficulties were apparent with the use of this adhesive. These may be summarized as being caused by the adhesive shrinking during the B-staging operation which created distortion of the film and pillowing and buckling in certain areas. Control of the B-staging operation was also critical which frequently resulted in poor bonds. Because of these difficulties the use of TR-150-25 was discontinued.

Work was continued in evaluation of FM-1044R adhesive for substrate assembly. Sample assemblies exhibiting typical bus bar and Kapton doubler configurations were made up using soldered conductors and FM 1044R adhesive. The detail parts were tacked in place with a hot iron, after which the assembly was cured on a heated plate at 350°F for one hour under a vacuum bag. The results of this process were very satisfactory with no problems of film distortion.

2.1.3.2 Conductor Material Selection

One addditional material consisting of silver clad aluminum was investigated and appears to be a suitable material for bussing providing it is not subjected to any sharp bends. The material consists of .002 inch aluminum clad with .0002 inch of silver. The sample foil supplied by Wadsworth Pacific Manufacturing was received in an as-rolled condition and was susceptible to fracture if bent 150° on a .005 inch radius. Annealing at 650°F with a slow cool resulted in the silver being diffused into the aluminum which caused the surface to become mottled.

2.1.3.3 Edge Attachment

In a redesign of the substrate to beam attachment, a silicone rubber coated glass fabric was selected to provide a more flexible joint. The material selection for preliminary evaluation is Cahrlastic 1007-M803 (Connecticut Hard Rubber Co.) which is a dispersion coated glass fabric .002 inch thick weighing 8.5 ounces per square yard. The flexibility temperature range of the coated fabric is -110°F to 500°F. The film is to be bonded to the titanium beam and Kapton substrate with RTV 3145. Typical bonded joint samples have been designed to be tested to measure joint strength and failure modes.

2.1.4 Manufacturing Restraints

2.1.4.1 A Beryllium Wrap Drum Structure

The feasibility of using beryllium in a simple structure such as the wrap drum was discussed in the first Quarterly Report, but was summarily dismissed for lack of response to Ryan inquiries to potential fabricators.

However, discussions have been held with interested contractors in this latest reporting period with some degree of encouragement. There are no specific conclusions at this time except that there is general concurrence that a drum configuration could be fabricated without too great a compromise in design, but additional study is necessary.

Ryan proposes to pursue the study within reasonable limits as back-up information to its selected drum concept, that is, of magnesium sheet metal construction with aluminum honeycomb end plates. There are no plans for deviating from this concept at this time.

2.1.4.2 Manufacturing Feasibility - Solar Cell Considerations

No severe problem areas are anticipated at this time; however, two areas will require additional development time. The two areas that require development time are large area solar cells and a new technique of coverglass application.

Large Area Solar Cells

The large cell development program is considered due to an estimated reduction in the cost of power per unit area. The large solar cell (1.042 x 2.384 inches) compares very favorable with the 2 x 2 cm corner dart contact cell on a power per unit area basis. Active area of the large cell is approximately four times the active area of an individual 2 x 2 cm corner dart cell and is approximately 8% greater than the active area of 4 standard 2 x 2 cm bar contact cells. Estimated cost of this large solar cell, including tooling costs, is three times the cost of an individual production 2 x 2 cm corner dart cell. For a large solar cell array, 250 square feet or larger, this would result in a sizeable cost reduction. An additional cost reduction would be realized due to fewer handling and soldering operations.

Coverglass Application Technology

The second area that will require development effort is a new technique for applying the coverglass/filter to the solar cell. This technique will be submitted in a new technology report but will be reviewed briefly to present the concept. The original concept was developed due to the difficulty in fabricating thin coverslides. Several coverglass suppliers refused to quote on the large cell covers.

The concept consists of two parts both of which utilize 1-1/2 mil glass in a continuous roll or ribbon. The first process would be the application of a magnesium fluoride antireflective coating and/or a blue

reflecting filter on a continuous basis. A process of this type would reduce the basic coverglass cost for a large colar cell (1.042 x 2.384 inches) to that of a 2 x 2 cm solar cell.

The second step of the process involves the application of the coverglass/filter to the solar cell on a continuous basis. The process would begin with a roll of ribbon glass and solar cells mounted on a continuous belt and would be completed with the ejection of individual filtered cells.

The process will be divided into the following phases:

a. Adhesive deposition on glass and cell

b. Adhesive outgassing

c. Solar cell, glass indexing and rolling

d. Accelerated adhesive cure (partial)

e. Excess adhesive removal, trim and scribe glass

f. Final cure of coverglass adhesive

This process will maintain uniformity of the coverglass adhesive thickness and will simplify the handling of .0013 inch thick coverslides. Currently used coverglass handling techniques are inadequate for fabricating these thin covers.

The only problem anticipated at this time is the type of glass available in the .0013 inch thickness. It is a Corning Glass type 8871 which is a lead potash glass with a density of 3.60. This glass offers excellent radiation shielding but is slightly susceptible to ultraviolet browning. A sample cell was covered with type 8871 glass using RTV 602 as the adhesive and subjected to seventeen and one-half hours of U.V. radiation at a 5 sun level. A subsequent test revealed a 1/2 of 1% loss compared to the filtered solar cell before it was exposed to the

U.V. The 17.5 hour exposure time was selected because results of other U.V. degradation tests conducted by Spectrolab indicated a major percentage of the degradation was experienced during this period. This one test, though not conclusive, indicates that browning of glass in this thickness may not be a major source of degradation. Other types of glass such as the borosilicate family would not show susceptible browning, but this glass is not presently available in the .0013 inch thickness. Glass manufacturers indicate a development program would be acceptable.

2.1.4.3 Handling Fixture Design - Solar Cell Application

Handling frames and fixtures have been designed and drawings have been completed (see Figure 6). These fixtures will be used throughout the manufacturing testing and shipping phases of fabrication. The handling frame is basically a frame with a sheet of 1/2 inch thick removable honeycomb support member in the center of the frame. The honeycomb member will serve as a flat surface for cell bonding and will be removed for access to the rear module surface. Barring any unforeseen problems, a module substrate will remain in place in a handling frame throughout the manufacturing and test phases. The handling frame will be mounted in a suitable container for shipping.

2.1.4.4 Repair Procedure - Solar Cell Replacement

Sample modules utilizing standard fabrication techniques and materials evaluated in this effort and typical defects were produced in the modules. The defects were then corrected using state-of-the-art techniques.

The following outline illustrates the typical cell replacement technique employed on Kapton substrates.

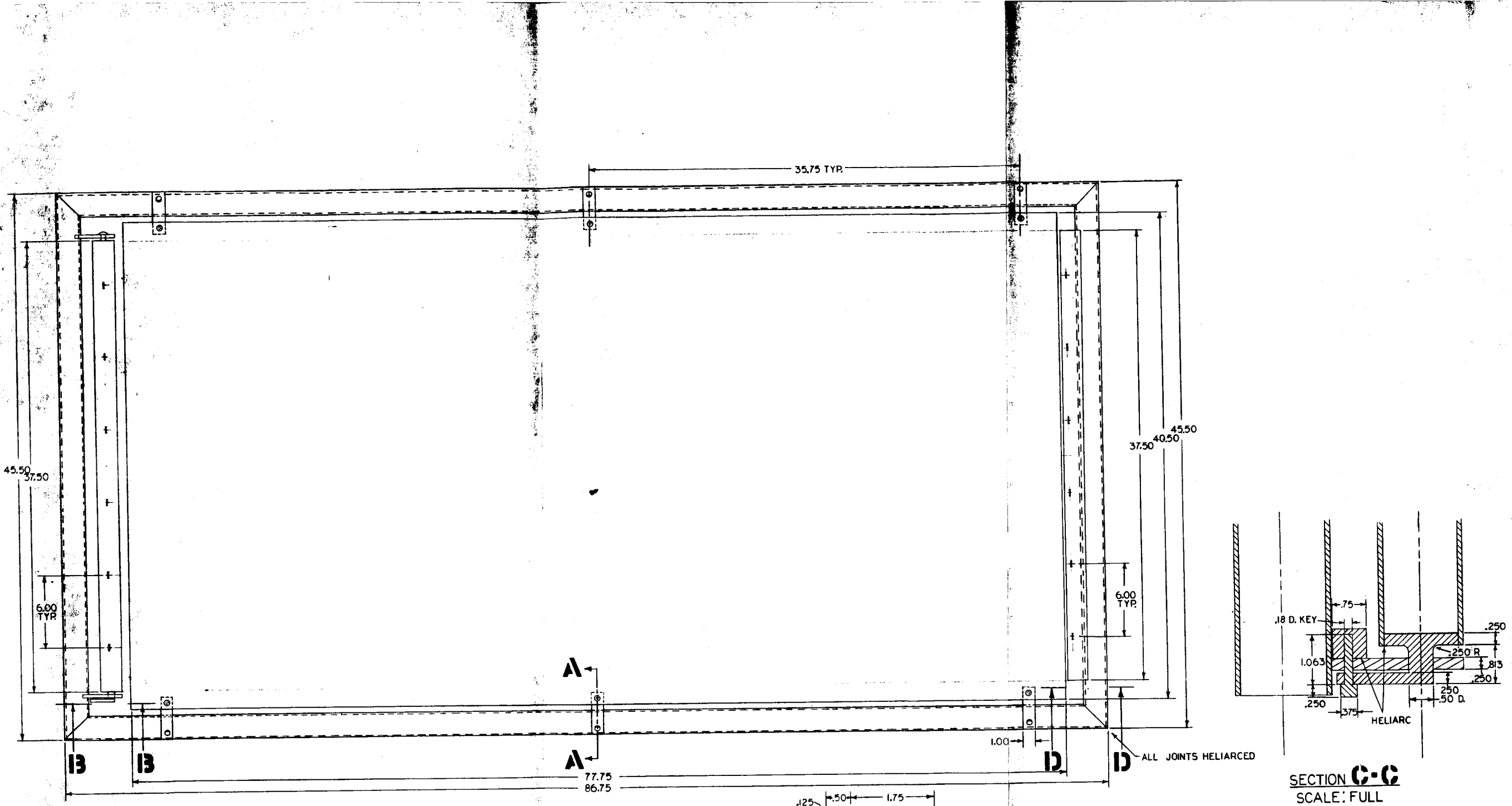

SECTION C-C
SCALE: FULL

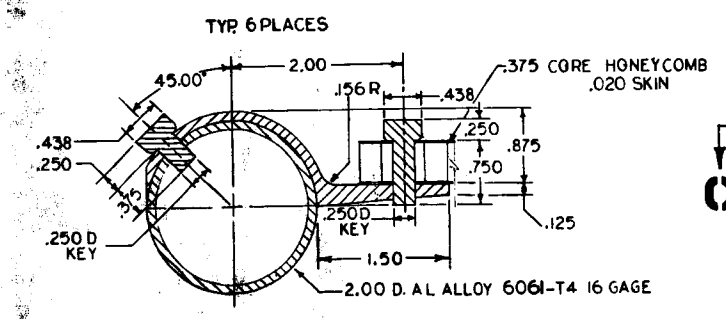

SECTION A-A SCALE: FULL

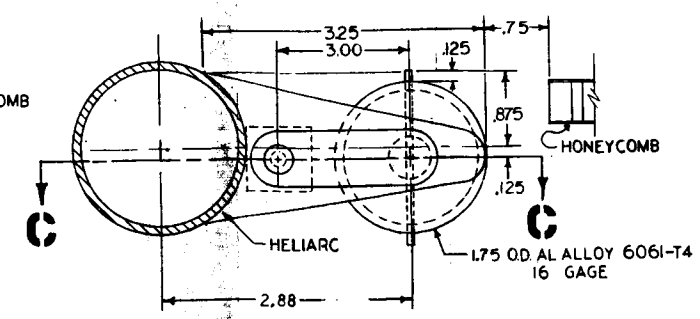

VIEW B-B SCALE: FULL

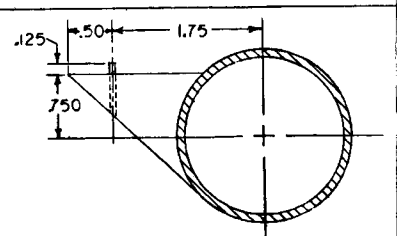

VIEW D-D
SCALE: FULL

Figure 6 Proposed Handling Fixture - Roll-up Array

a. Using a razor blade dipped in alcohol, remove the filter from the cell.

b. Apply flux to the face of the cell and with a well tinned soldering iron applied to the face of the cell and a lifting probe under the tabs, lift the tabs from the cell when the solder has melted. Then continue to apply heat to the cell until the adhesive bond is broken and the solder to the back tabs has melted. When this happens, place the lifting probe under an edge of the cell and lift the cell from the substrate.

c. With a cotton swab, alcohol, and a wooden probe, clean the adhesive from the area.

d. Remove the tabs from the bus bar.

e. Take a cell with the same electrical values and then solder replacement tabs to the back of the cell.

f. Lay the replacement cell in place and position it with masking tape - when correct alignment is achieved, solder the tabs from the cell to the bus bar.

g. With a cotton swab and alcohol, clean the area under the cell and the back surface of the cell. Prime the back side of the cell.

h. After the primer has dried for a sufficient amount of time, apply a metered amount of adhesive to the substrate. Press the cell into position, weight it down and tape it in position.

i. After the adhesive has cured, solder the front tabs into position.

2.2 TECHNICAL SUPPORT

Principal technical support rendered in this reporting period was concerned with substantiation of the selected configuration, as reported in the first Quarterly Report. Four primary areas relating to array structure include dynamics, loads, stress and thermal. Weight and materials are considered in separate sections. Both weight and materials however are a major consideration in the technical support area.

Most of the basic structural concepts have been established. Basic load paths, dynamic responses and dynamic loadings have been established, based upon preliminary design concepts. Thus, current efforts consist of refinement of these computations based on, and consistent with the design and structural optimization.

2.2.1 Drum Support and Guide Sleeve Mount Assembly

2.2.1.1 Dynamics

The dynamic analysis was presented in the first Quarterly Report, reference 1. The frequency f_n = 79.6 cps is not subject to any change other than a refinement of the value due to design detail changes.

2.2.1.2 Loads

The loads on the drum mounting fitting are dynamic loads due to 4g (0 - pk.) vibratory excitation. The structural elements which load this fitting are:

a. Beam guide structure

b. Wrap drum

c. Panel assembly

d. Solar cell installation

The primary load condition occurs in the retracted position during launch. A secondary loading condition can occur in the extended position of the solar array.

Weights

a.	Beam guide structure	7.214
	(W = 1.9219 + 3.2882 + 0.5196 + 1.4847)	
b.	Panel Assembly	10.916
c.	Wrap Drum Assembly	9.500
d.	Solar Cell Installation	47.500
	Total; (b) + (c) + (d)	67.916

A (1.20) factor is applied to P_n, which is the drum axial dynamic loading. This is to allow for possibly unequal distribution of the thrust load to the end bearings.

The loads were calculated using various transmissibilities based on vibration laboratory environmental tests of the fifty square foot deployable solar array. These transmissibilities were:

a.	Wrap drum laterial vibration	T.R. = 4.0
b.	Wrap drum axial vibration	T.R. = 5.0
c.	Beam guide structure	T.R. = 16.7

All loads are summarized in Figure 7 and Table 2.

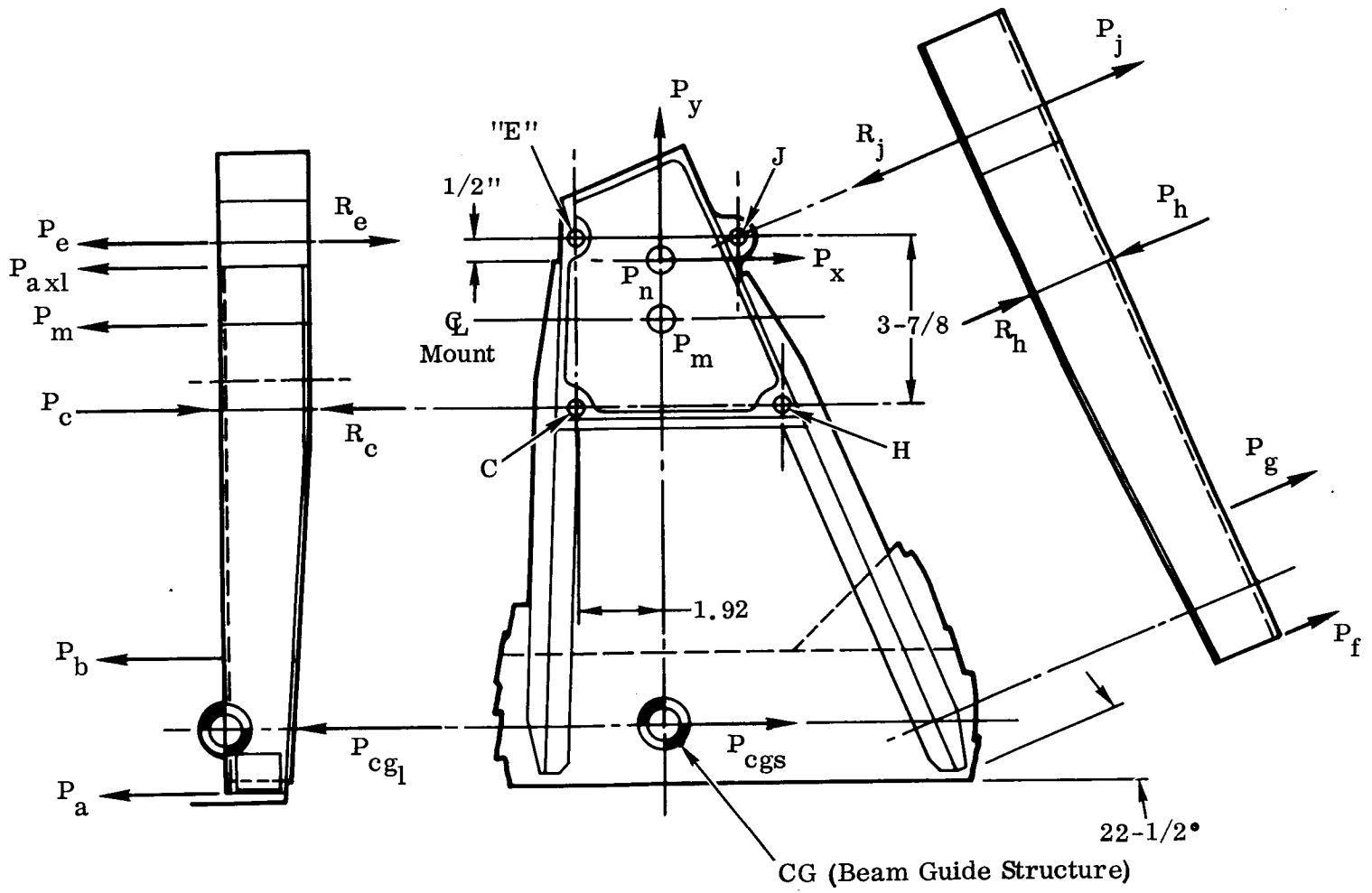

Figure 7 Load Applications on Drum Support and Guide Sleeve Mount Assembly

TABLE 2

CALCULATED DYNAMIC LOADS

ON DRUM SUPPORT AND GUIDE SLEEVE MOUNT ASSEMBLY

(Reference Figure 7)

P_{cg}	P_a	P_b	P_f	P_g
187.3	72.73	61.15	29.43	24.00

P_c	P_e	P_h	P_j	R_c	R_e
380.93	247.06	152.27	98.86	470.42	670.63

P_m	P_{axl}	P_x	P_y	R_h	R_j
53.60	814.99	458.36	458.36	214.53	522.43

The above loads are considered to be limit for a cyclic fatigue life of 10^4 cycles with corresponding cyclic fatigue stress limit for 10^4 cycles.

All of the above loads are considered to act simultaneously (dynamically in phase), for purposes of stress analysis. This is somewhat conservative.

2.2.1.3 Stress

All component parts have been sized on a preliminary basis, based on the loads given in Section 2.2.1.2. There was some increase in basic material sizes, but due to efficient usage of materials, the overall weight has been slightly reduced.

2.2.2 Beam Guide Sleeves

Detail design of this structure is nearly complete. Preliminary stress calculations have been made for the design and detail support effort. Final stress calculations will be made upon completion of the design details.

2.2.3 Wrap Drum Assembly

2.2.3.1 Drum End Plate Optimization Study

This section deals with the end plate only, considering that the mass of the drum, substrate, solar cells and beams constitutes a sprung mass with the end plate acting as a spring in the drum axial direction.

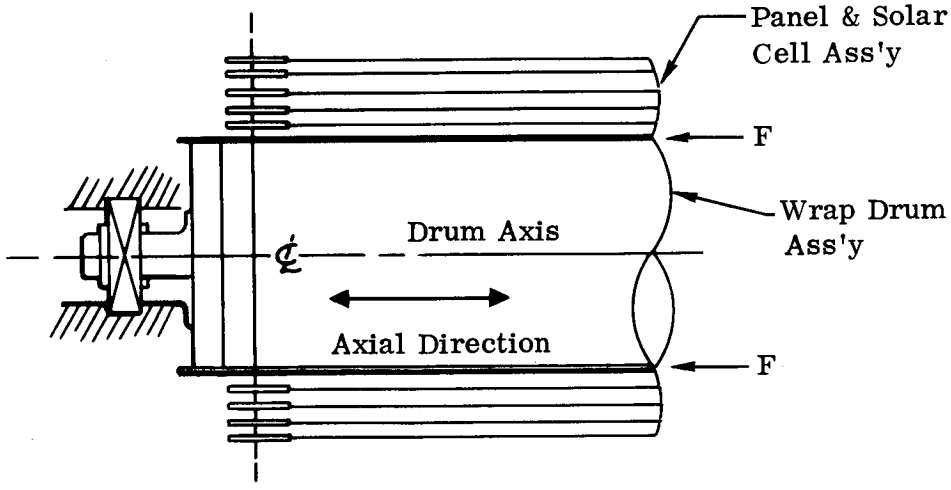

Viewed as a model:

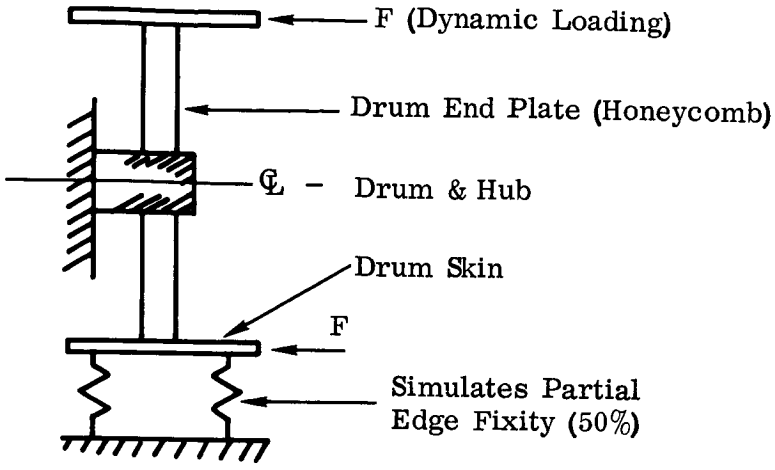

The study was conducted to determine what cross-section and facing thicknesses of the wrap drum end plates will provide a minimum weight end plate design and yet be sufficiently rigid to minimize sinusoidal excitation accelerations (in drum axial direction) to the wrapped panel. Large induced excitations to the wrapped panel would cause excessive motion of the wrapped panel layers in the axial direction, allowing the wraps to slip and displace relative to each other on the drum which could then prevent ease of deployment of the stowed panel. The end plate design used for weight analysis presented in the first quarter report had a cross-section thickness limited to 0.70 inch, compatible with the wire harness concept, while the facing thickness, honeycomb core, and attachment configuration were selected to improve structural stiffness and load carrying capacity. Based on end plate edge attach fixity of 50% and supporting a vibrating sprung mass comprising the wrapped panel and wrap drum of 33.3 pounds per end plate, that end plate would have vibrated at a fundamental frequency of 146 cps; shown in Figure 8. Since sinusoidal excitation exists up to 200 cps per JPL Specification, reference 3, a fundamental frequency of at least 222 cps (see Figure 8) is required to limit dynamic transmissibility through the end plate to the wrapped panel to a value of 4.0 which is about equal to the value that exists when the

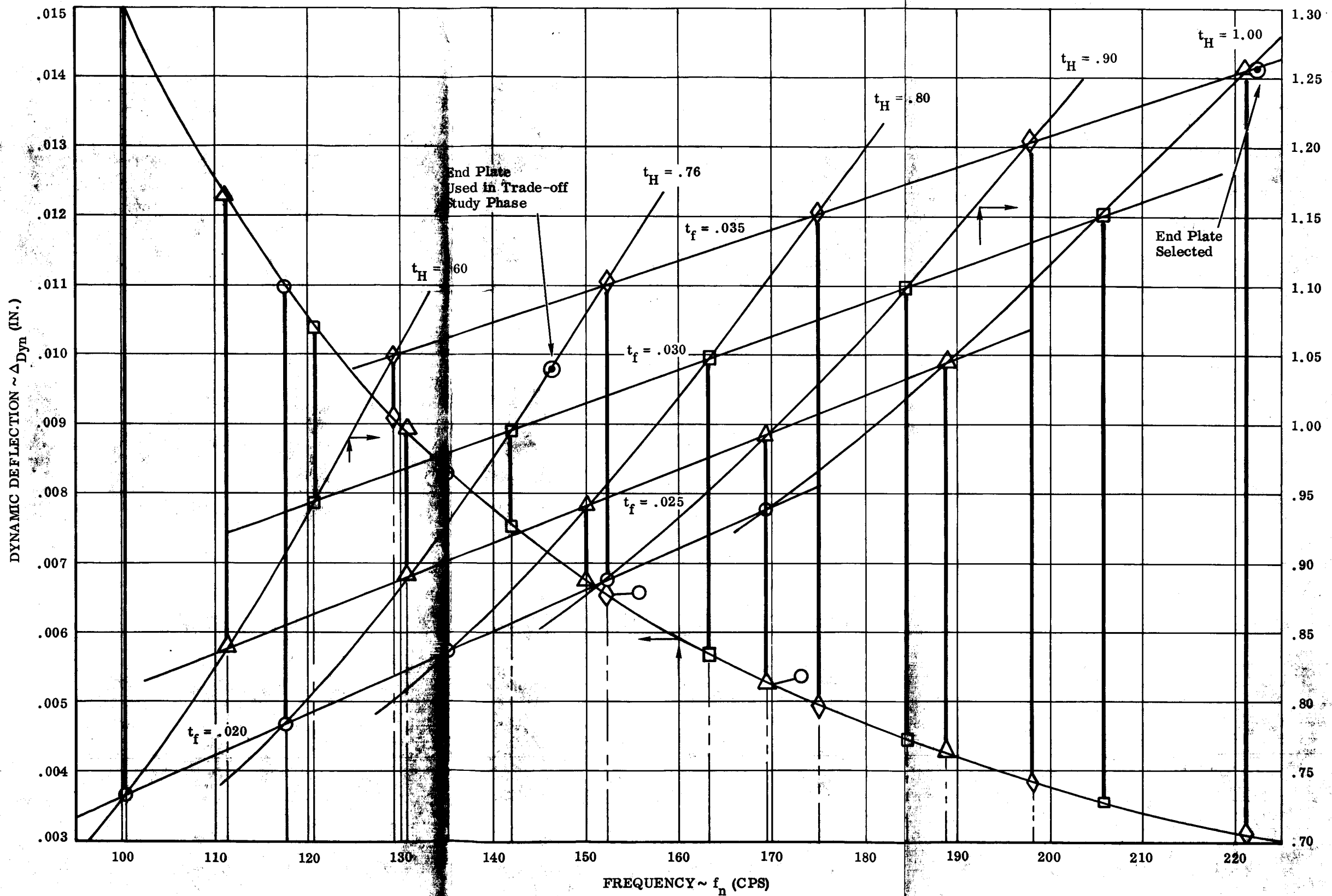

Figure 8 End Plate Optimization

wrapped panel layers are at resonance in the drum axial direction. (This is supported by transmissibilities obtained in test of the 50-square foot deployable solar array). To limit, then, dynamic transmissibility to the wrapped layers in the drum axisl direction to approximately 4.0, the end plate will be increased in thickness to 1.0 inch core thickness with aluminum facings of 0.035 inch thick required, in lieu at this time of a detail stress analysis for the loads induced. This end plate cross-section appears to be sufficient to prevent premature elastic dimpling of the face sheets during sinusoidal vibration. Satisfactory limitation of sinusoidal excitations to the wrapped panel layers is then predicated upon the spacecraft mounts being sufficiently stiff to prevent (1) modal coupling with the end plate mode or the wrapped panel layer axial mode and (2) spacecraft mount resonance in the sinusoidal range. Analysis presented in Section 8.2.2 of the first Quarterly Report gives a minimum mount frequency of 152 cps and a maximum of 426 cps in the critical plane. It is believed that sufficient conservatism exists in that analysis to allow consideration of the higher frequency as realistic, and, in that case, with a drum end plate natural frequency of 222 cps, a mount natural frequency of approximately 400 cps, and a wrapped panel natural frequency of 200 cps. The dynamic transmissibility in the wrapped panel will be limited to 6.0. A possible solution, if the spacecraft mount proves inadequate in stiffness, is to substitute beryllium for the proposed aluminum mount to increase its stiffness.

2.2.3.2 Drum Bearing and End Plate Loads Analysis

The loads on the wrap drum assembly consist of vibratory loads on the wrap drum in the lateral (X and Y), and axial directions as shown in the following illustration.

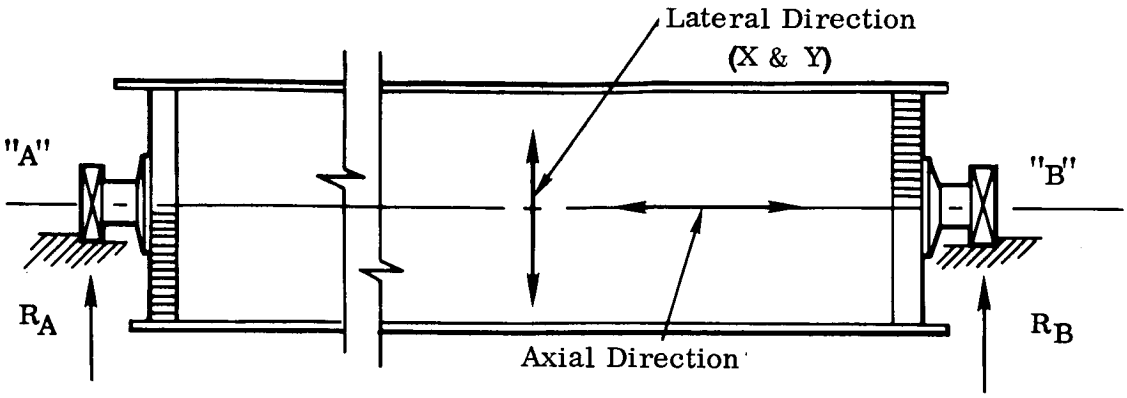

Dynamically the wrap drum is acted on by a 4g (0-pk.) sinusoidal dynamic excitation force in all directions. It is assumed that all dynamic loadings can occur simultaneously (dynamically in phase), and lateral vibration can occur bi-axially as shown by P_x and P_y in Figure 9. The loads were calculateed using various transmissibilities based on vibration laboratory environmental tests of the fifty square foot deployable solar array. These transmissabilities were:

a. Wrap drum lateral vibration T.R. = 4.0

b. Wrap drum axial vibration T.R. = 5.0

All loads are summarized in Figure 9 and Table 3 below. The drum is supported by bearings in the drum mount fitting. The sprung weight used in the calculations was 67.92#. A (K = 1.2) factor is used in the calculation of P_{ax}, to allow for unequal distribution of the axial thrust loading (P_{ax}) to the two end bearings.

TABLE 3

DRUM SPINDLE LOAD SUMMARY

P_x	P_y	$P_{a/d}$	$P_{p/t}$	P_r	θ
458.4 lb.	458.4 lb.	30.0 lb.	30.0 lb.	715.7 lb.	41°42'

P_{ax}	Pax_1	Pax_2	M_o	$P_{ma} = -P_{mb}$	Q_s
815.0 lb.	21.6 lb/in	129.7 lb/in	1252.4 in/lb	27.7 lb/in	36.7 lb/in

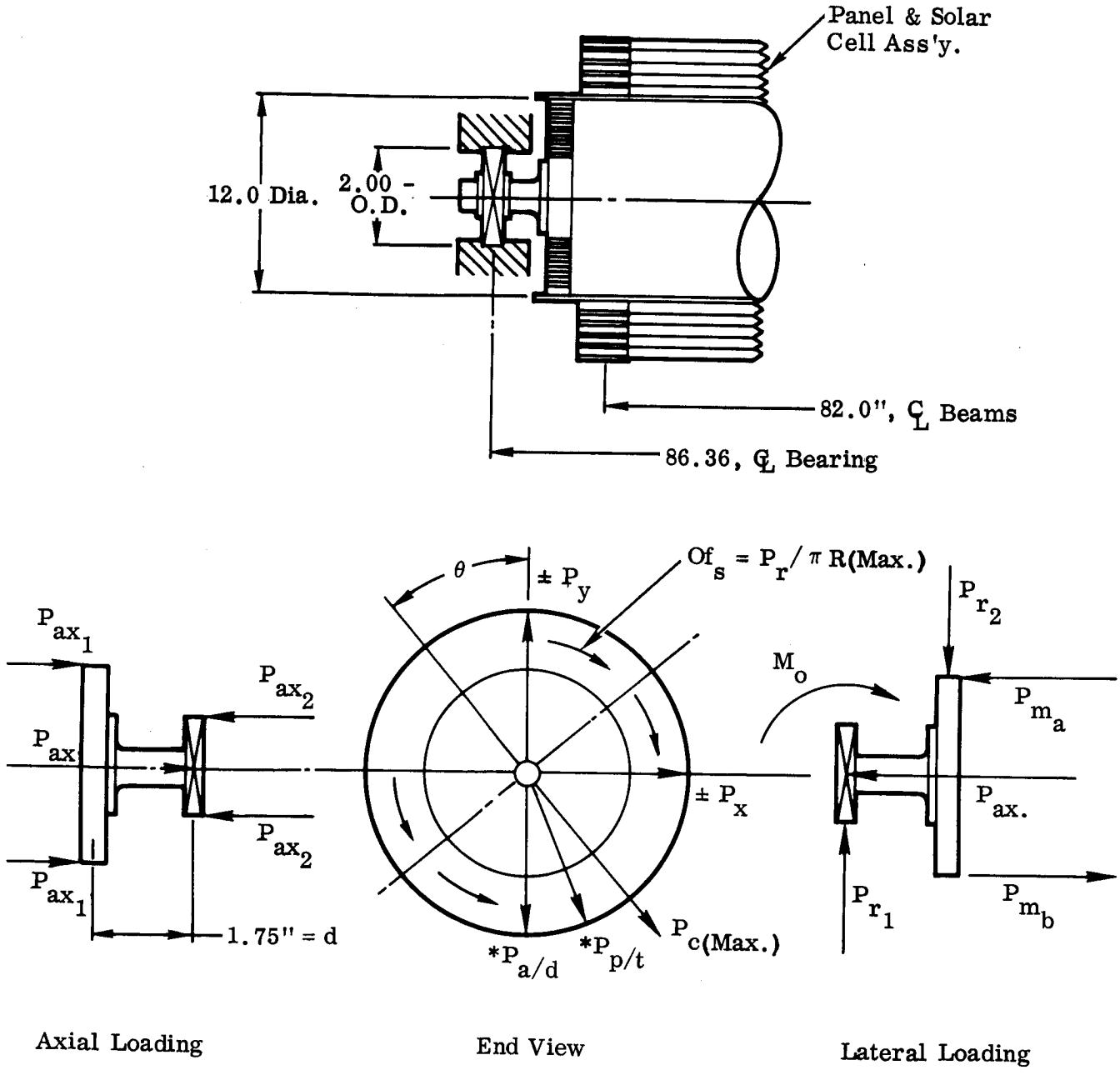

Figure 9 Drum Spindle Load Applications

The above loads are considered to be limit for a cyclic fatigue life of 10^4 cycles, with corresponding cyclic fatigue stress limit for 10^4 cycles.

2.2.4 Spacecraft Mount Assembly

Preliminary design for the spacecraft mount assembly has been completed. A dynamic analysis of the preliminary mount assembly was made in the first Quarterly Report, reference 1. The natural fundamental frequencies in the following directions were:

x) $f_n = 157$ cps

y) $f_n = 426$ cps

z) $f_n = 400$ cps

Final detail design is scheduled to start after completion of the wrap drum and drum support design. Preliminary stress calculations will be made based on the loads developed in Section 2.2.1.2 for Drum Support and Guide Sleeve Mount Assembly, since these loads will be transmitted directly into the spacecraft mount assembly, plus the dynamic inertial loads of the spacecraft mount assembly itself.

2.2.5 Panel Assembly

2.2.5.1 Axial Restraint Requirements for Wrapped Panel Layers

If the stowed panel is excited at launch by sinusoidal vibration in the drum axial direction, a dynamic transmissability of 6 is possible to the panel wrap layers (see Drum End Plate Optimization Study, Section 2.2.3.1). Tests were conducted to determine what axial force can be transmitted between wrapped layers before slippage (interplay) will occur. The test consisted of an in-plane load application by a graduated spring scale to a 9" x 11.5" sample panel specimen (same

specimen as used for vibration testing, Section 2.4.1). The specimen rested, back side down (polyurethane pad side) in a 1g field, on the solar cell side of a similar specimen.

With the assumption made that no more than an equivalent normal (radial) force between wraps of 2g is possible due to the way the panel will wrap on the drum, the axis force per wrap that can be transmitted between wraps under sinusoidal vibration is calculated from static test data as,

F = 2 (test force, psi, at 1g) (effective contact area each wrap)

F = 2 (.00367) (effective contact area each wrap)

while the comparative sinusoidal vibration force induced at each wrap is calculated from,

f = (g_{in}) (Q) (weight of wraps transmitting force to wrap in concern)

f = (4) (6) (weight of wraps transmitting force to wrap in concern), considered as a steady state limit force of 0-peak magnitude.

The induced forces and forces which can be transmitted at each wrap layer are tabulated in the following chart. An additional restraint force is required to prevent slippage at every wrap layer.

From the chart we can see that little effect is made on the additional restraint force required. Regardless of the value of normal wrap force available due to the way the panel wraps on the drum. Shaped metal clips are provided to transfer the additional load (which cannot be stopped by friction between the polyurethane pads and solar cells) into the deployable side beams. The side beams wrap with some

pre-tension to prevent axial motion, but until test data is available it will be assumed that all the load must be transferred to the drum through the shear clips at the inner wrapped beam layer.

WRAP NO. NUMBERING FROM INNER WRAP	PAD AREA, IN^2	WRAP WEIGHT, LBS.	F_1 LBS	f_1 LBS LIMIT	ADDITIONAL RESTRAINT FORCE REQUIRED PER WRAP, LBS.
1	2934	4.58	21.5	1247	1226
2	1147	4.31	8.4	1137	1129
3	1119	4.43	8.7	1033	1024
4	893	4.48	6.6	927	920
5	917	4.59	6.7	820	813
6	806	4.68	5.9	709	703
7	827	4.80	6.1	597	591
8	636	4.87	4.7	482	477
9	651	4.98	4.8	365	360
10	518	5.06	3.8	246	242
11	530	5.17	3.9	124	120

With the channel shaped restrains clips provided every 4 inches along the side beams, the average axial restraint wrap is given as:

WRAP NO. (NUMBERING FROM INNER WRAP)	AVG. FORCE AT EACH CLIP LBS. LIMIT
1	130
2	114
3	100
4	88
5	76
6	64
7	52
8	41
9	30
10	20
11	10

The above loads for the inner wraps are exceedingly high to consider transmitting into the thin .003 titanium beam and not distort the beam in the drum axial direction since each wrapped beam layer is stabilized

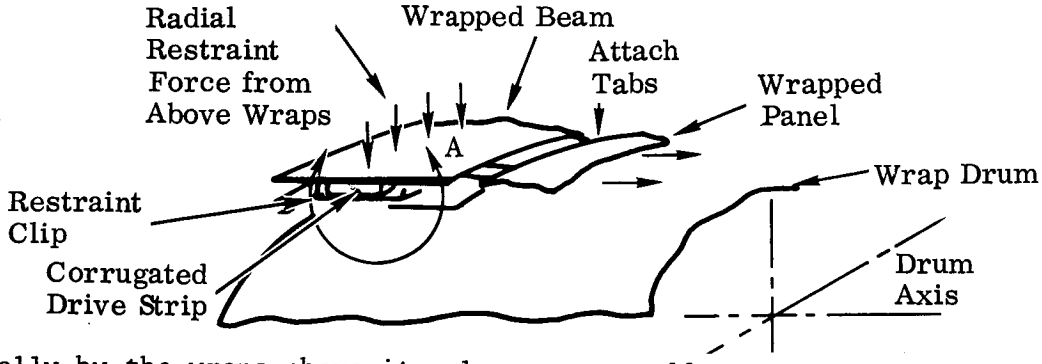

radially by the wraps above it only over a small percentage of the wrapped beam flat area.

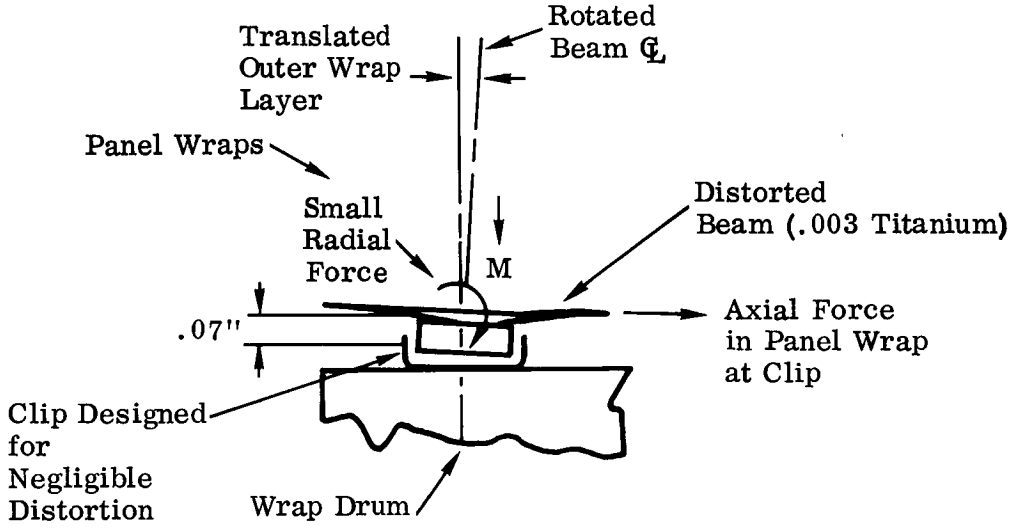

Therefore, the force at each clip will be transmitted to the wrap below through shear only in the clips, while moment restraint will be considered negligible. This means that with distortion occurring in the axial direction due to a moment in the wrapped beam, some wrapped panel layer translation relative to another layer will occur. The clip forces given in the chart above assume that the axial translation of the wrapped panel will occur due to shear deflection of the polyurethane sponge damping pads; with any reasonable load exhibited, though, translation will occur due to slippage between panel wrap layers allowed by the wrapped beam distorting

at the restraint clips. As a result, the wrapped panel natural frequency and transmissability may be changed, resulting in a change in the forces at the restraint clips. Until test data can verify the dynamic transmissability, the forces given in the chart will be used for design of the restraint clips and panel-to-beam attach tabs.

2.2.5.2 Dynamics-Wrapped Panel Axial Mode

This section considers the longitudinal vibration of the various wrap layers on the drum. These wrap layers are composed of the substrate and damper pads with the solar cells attached, as shown in Figure 10.

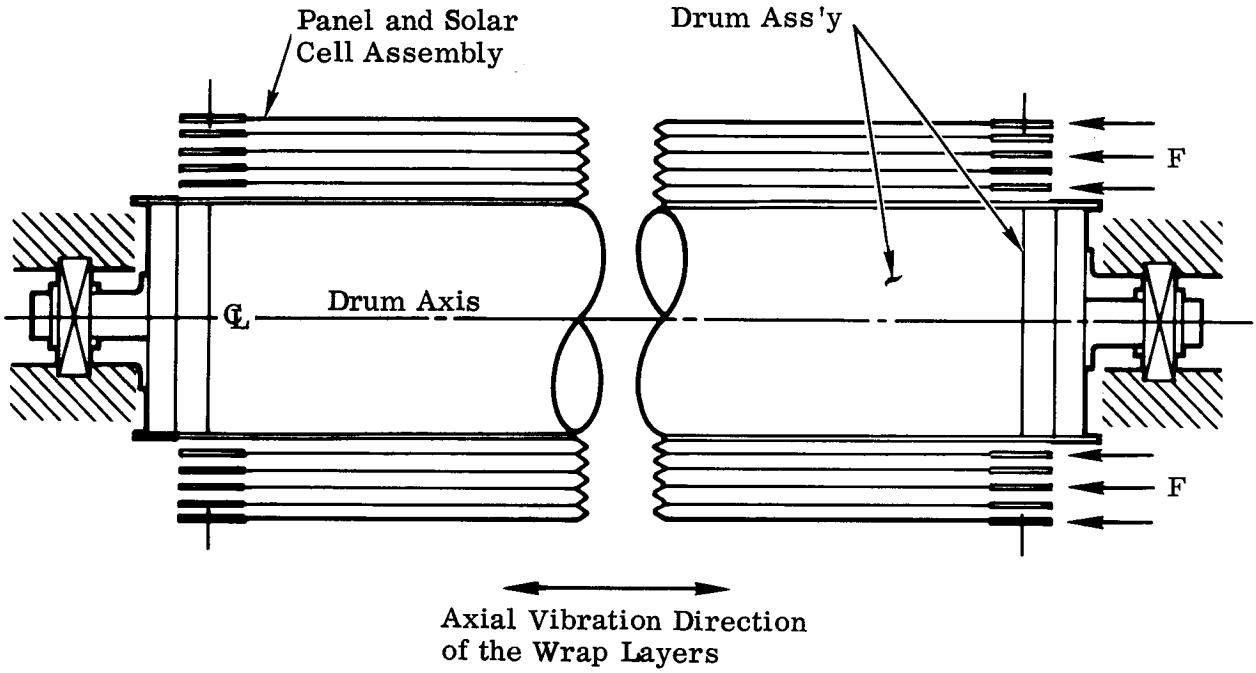

Figure 10 Axial Vibration of the Wrap Layers

The wrap layers have been idealized to individual concentric tubes with interlayed polyurethane layers, as shown in Figure 11.

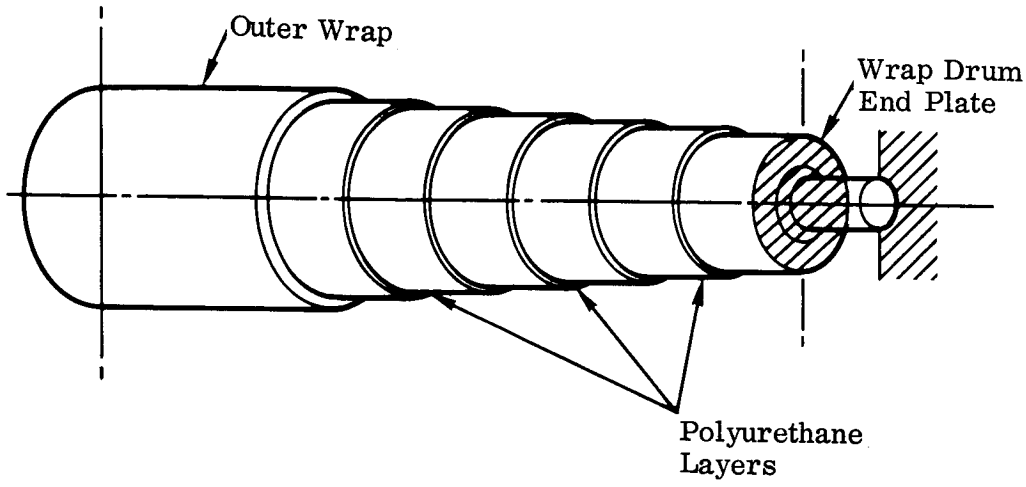

Figure 11 Model Wrap Configuration

The above system is the equivalent of multidegree of freedom spring-mass system, with the polyurethane layers in shear acting as spring as shown below.

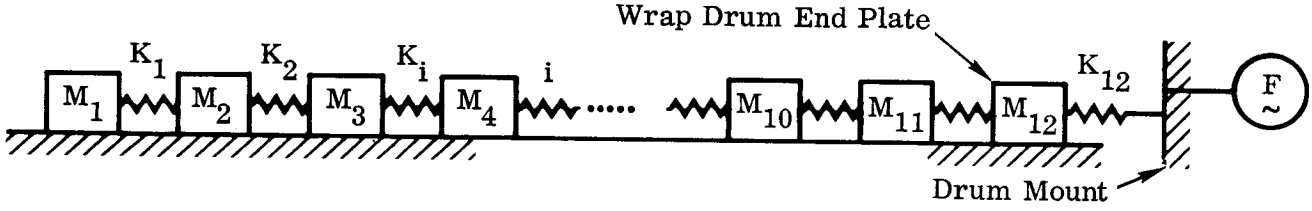

K_i is the shear spring rate between the substrate layers and M_i is the mass of the idealized substrate layer per wrap. M_{12} and K_{12} represent the effect of the wrap drum end plate and was included as part of the system since the input excitation is a shear base motion input through the drum mount. The effect of shear deflection and modulus of the unidealized substrate has been considered negligible for this analysis. This latter effect is due to the fact that the substrate is continuously wound on the wrap drum instead of in concentric layers.

The shear spring modulus was calculated in the following manner as shown in Figure 12.

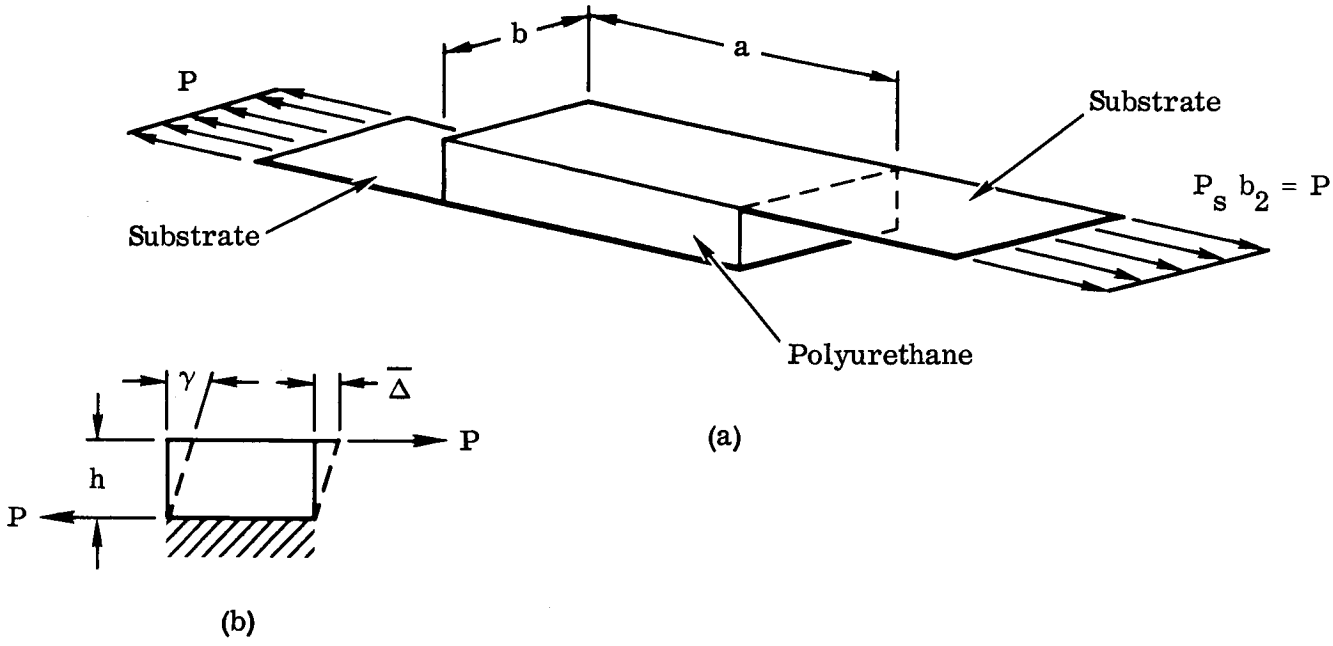

Figure 12 Shear Spring Modulus Schematic

1) $\gamma = f_s/G_s$

2) $f_s = P/kA$

3) $A = ab$

4) k = % area of polyurethane (accounts for cutouts)

5) $\Delta = \gamma h$ Figure 12 (b) above

6) $P = K_s\ \Delta$

Rewriting equation 6) and substituting equations 1) through 5) in 6) as follows:

$$K_s = P/\Delta = P/(\gamma h) = P/h(f_s/G_s)$$

$$K_s = P/h \ (P/kab\ G_s)$$

$$K_s = kab\ G_s/h$$

It was necessary to experimentally determine G_s for polyurethane (1.68 lb/ft^3) from laboratory tests. "G_s" was determined starting with equation 1) as follows and substituting equations 1) through 5)

$$G_s = f_s/\gamma = (P/kab)/(\Delta/h)$$

$$G_s = Ph/kab\ \Delta$$

G_s was determined to be 4.0 (lb/in^2)/RAD., for the material used.

The mass of material was:

Panel Assembly	10.92 lbs.
Solar Cell Inst.	47.50 lbs.
Total Weight	58.42 lbs.

The weight was allocated to each wrap layer in proportion to the mean wrap circumference. The spring rate and mass of the end plate were taken from Section 2.2.3.2 and Section 2.3 respectively.

The basic matrix equation for the vibrating multidegree or freedom system is:

$$\left[W_i\right] \left\{X_i\right\} = \left(g/\omega^2\right) \left[K_i\right] \left\{X_i\right\}$$

The above equation was computer solved to obtain the following first three undamped natural frequencies.

1) $f_n = 29.6$ cps First Mode

2) $f_n = 82.2$ cps Second Mode

3) $f_n = 134.5$ cps Third Mode

With natural frequencies it would be possible to calculate the displacements or the damped system by using mobility equations. However, since the damping factor of the polyurethane is not known and would have to be determined by laboratory tests, it was decided to wait for the vibration tests of the wrap drum test unit. It was also concluded that the time required would be lengthy, in consideration of the value and reliability of the calculations.

2.2.5.3 Wrapped Panel Layer Separation Medium Requirements for Dynamic Sinusoidal Vibration Normal to Requirements

The polyurethane damping pad areas given in Figure 18 of the first Quarterly Report have been revised in this section for:

a. Excessive solar cell temperature (> 600°F) where pad areas were up to 87%, resulting in a deficiency of electrical power. Thermal studies performed in Section 3.3.2.9 of the first Quarterly Report suggest that by limiting damper pad areas to approximately 40% of the solar cell area, a solar cell operating temperature of less than 131°F at 1 A.U. can be met, resulting in a required electrical power output of at least 10 watts/ft^2, at 1 A.U.

b. Greater values for structural dynamic damping at sinusoidal resonance for the wrapped panel and the wrap drum. A decrease in dynamic transmissability from 10:1 to 4:1 and 5:1 respectively were found to be more realistic in 1) Ryan tests presented in Section 2.4.1 and 2) as a result of sinusoidal vibration testing of the Ryan 50 ft^2 Deployable Solar Array.

Also of interest is 1) that the polyurethane sponge foam intended for use has an actual density of 1.68 lbs/ft^3 instead of 2 lbs/ft^3 and 2) pad spacing will be limited to 2.5 inches maximum instead of 3.0 inches, which, by investigation of specimen samples, appears to be more satisfactory for the limitation of the wrapped panel deflection between pads.

Dynamic Analysis

An integration of dynamic transmissibility, Q, between spacecraft mount interface and wrapped panel at maximum excursion area (center of wrap drum), with sinusoidal excitation normal to wrapped panel axis, are given below for wrapped panel response accelerations based on 1) a wrap drum bending fundamental frequency of 50 cps and Q of 5.0 2) a spacecraft mount fundamental frequency of 160 cps and Q of 16.7 and 3) a wrapped panel Q of 4.0

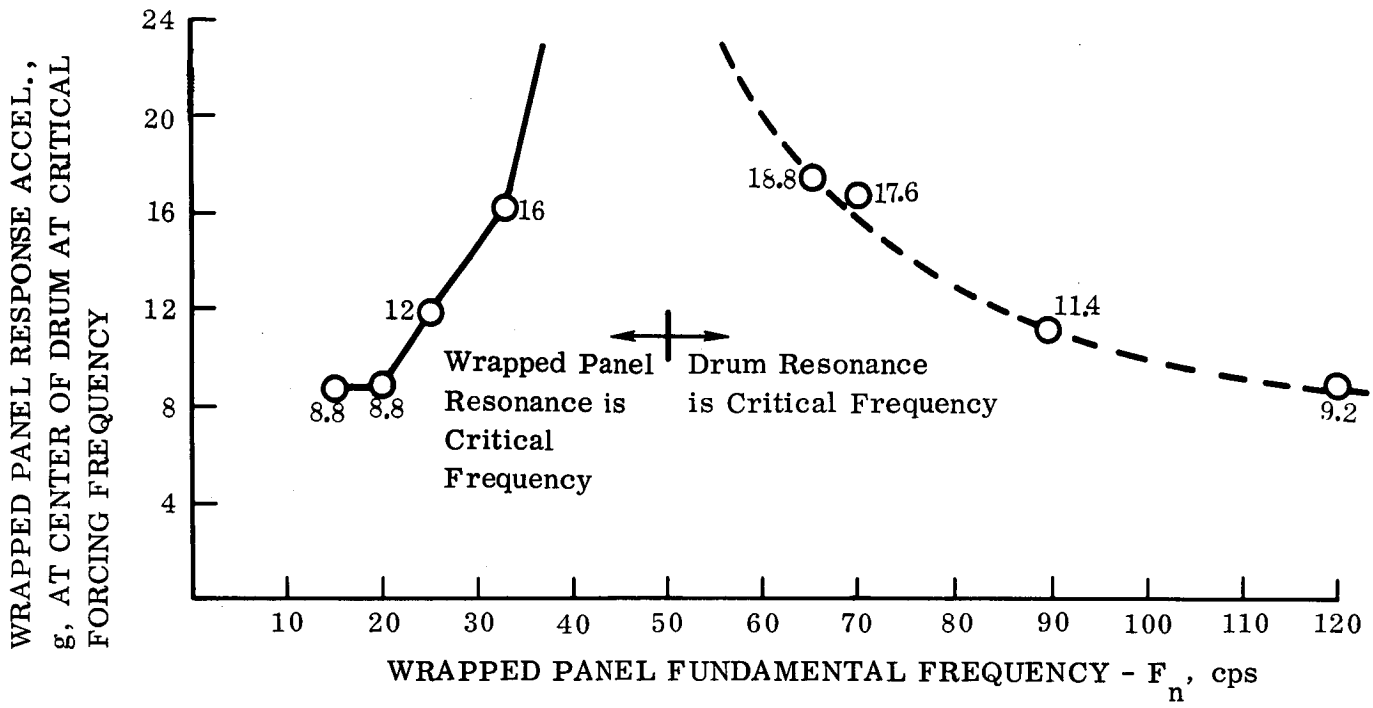

Critical loads for analysis are based on dynamic loads on the wrapped layers (1.53×10^{-3} lbs/square inch per wrap layer which gives a static load of 1.83×10^{-2} lbs/square inch on inner wrap layer separation medium) assuming all layers above the layer in question act as a rigid body on that wrap layer separation medium. Cylindrical stiffening effects of the wrapped substrate will be considered negligible in this analysis, which is probably only sighly conservative for a foil thick Kapton (or fiberglass) substrate. A maximum permissible

deflection of the wrap layer in question will be limited to 0.10 inch to prevent edge contact of adjacent solar cells at that respective layer (in-plane movement of adjacent solar cells limited to 0.013 inch); this is a conservative approach since it is based on a perfect radial breathing mode of vibration which is highly improbably with induced sinusoidal vibration in one axis. However, this appears to be a more realistic design constraint since, as is shown in the above analysis, the G level required to induce solar cell fracture is large (larger than the optimum design will experience).

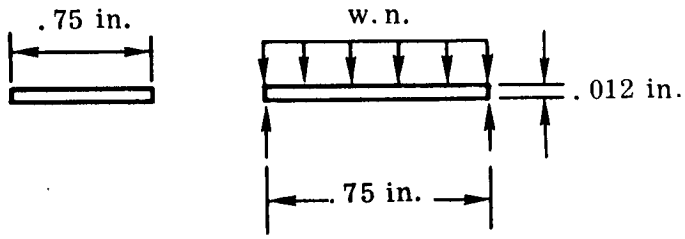

Loads on Solar Cell

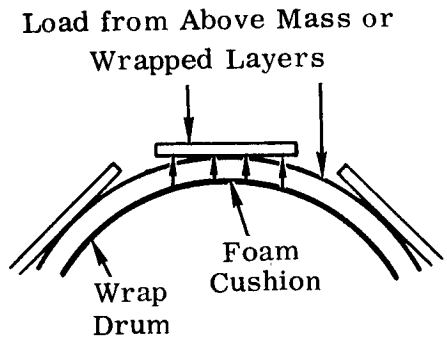

$$f_b = F_{t(glass)} = \frac{g.M \times .006}{1} = 5000 \text{ psi}$$

$$M = \frac{w\ell^2 n}{8} = \frac{1.15 \times 10^{-3} \times .75^2 \, n}{8} \qquad I = \frac{.75 \ (.012)^3}{12} = .108 \times 10^{-6} \text{ in}^4$$

$$M = .081 \times 10^{-3} \, n$$

Then

$$g = \frac{5000 \times I}{.006M} = \frac{5000 \times .108 \times 10^{-6}}{.006 \times .081 \times 10^{-3} n} = \frac{1111}{n}$$

n = wrap layer numbering from outside layer as 1

Selection of the optimum damping pad design for a sinusoidal vibration system on a minimum weight basis is made from a plot of weight versus frequency for various configurations. These configurations vary in medium thickness, and where the medium is less than a full blanket the variables are pad center distances; pad diameters are held constant at 0.75 in, a diameter which appears to be about optimum for stability reasons. A medium spring rate is based on silicone sponge density of 0.008 pound/cubic inch (which is about the minimum obtainable). Comparison is made with separating medium configurations using 0.00097 pound/cubic inch polyurethane foam sponge. The spring rate is obtainable from the Ryan test curves shown below and in Figure 13.

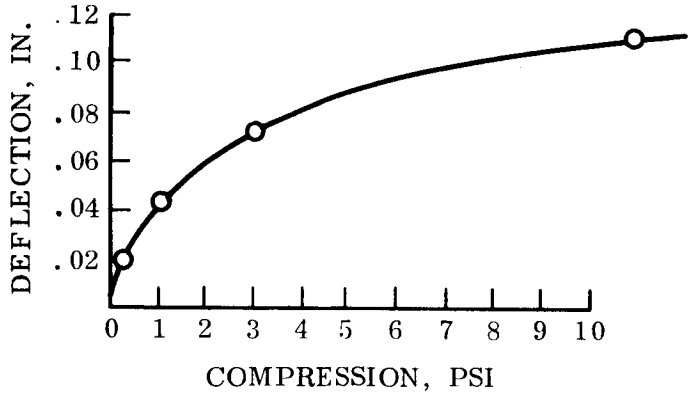

Compression Test of Silicone Sponge Disc .25 in. Thick

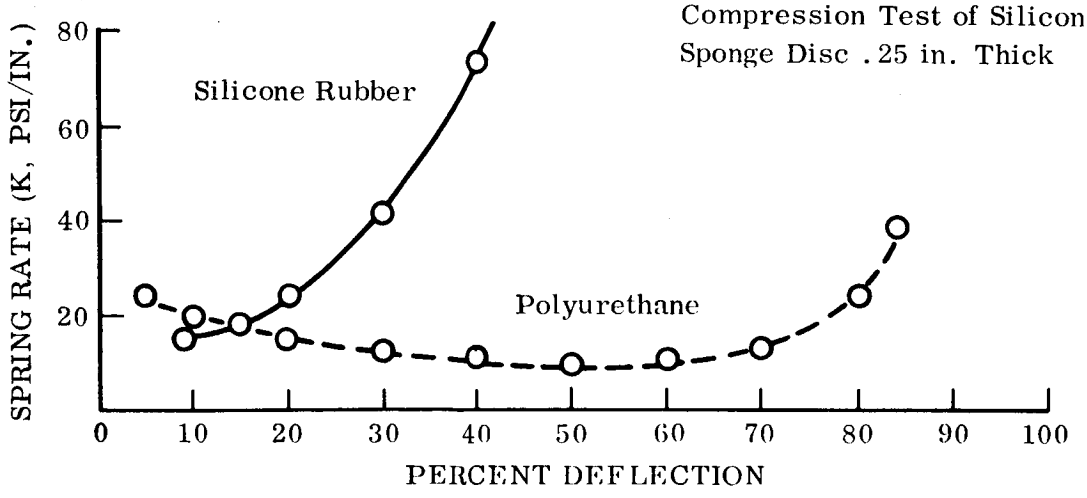

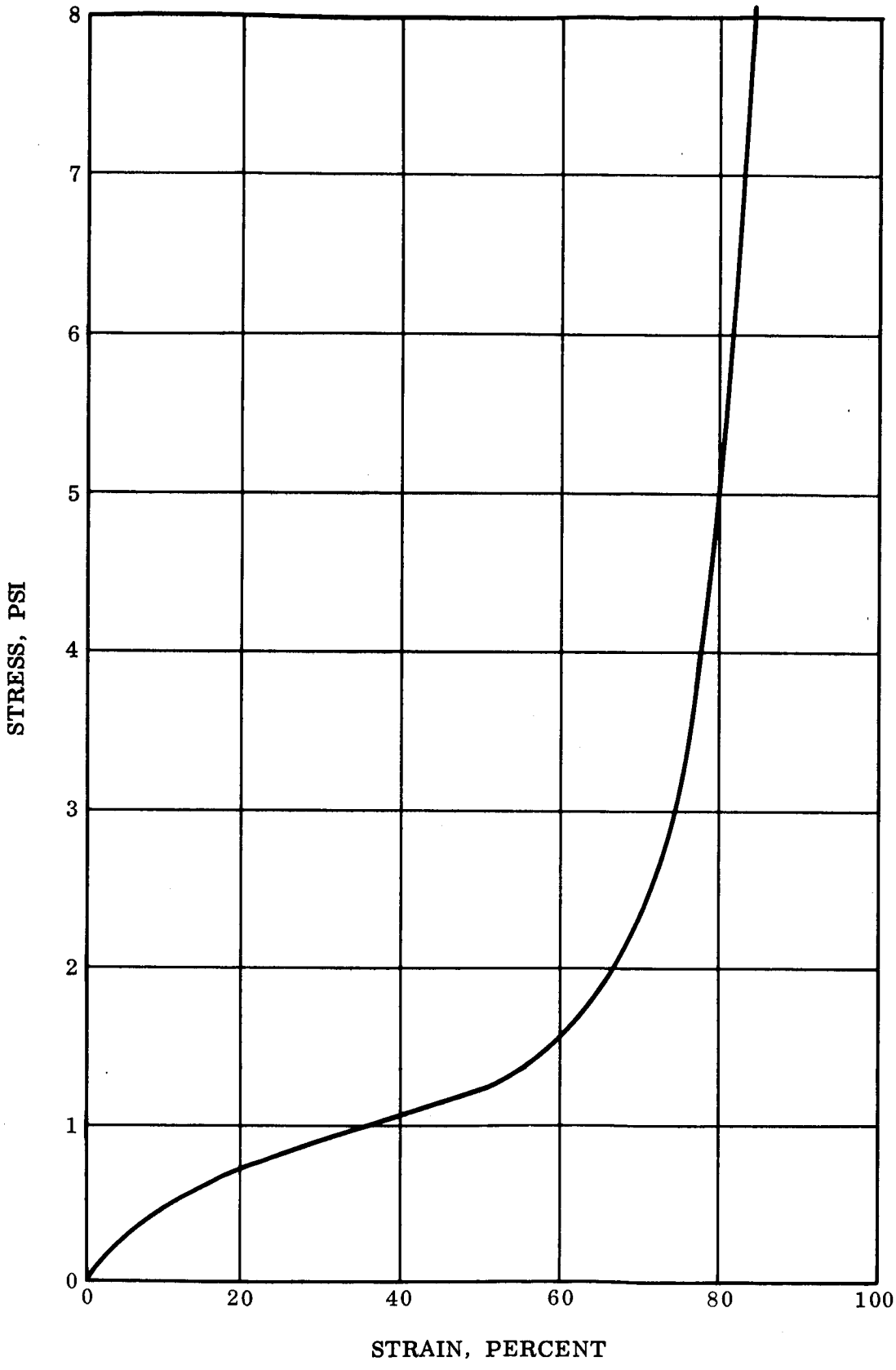

Figure 13 Compression Versus Stress for Polyurethane Foam

Analysis is made by calculating dynamic sinusoidal deflection of a separation medium configuration with a given frequency and then determining its weight based on a thickness equal to its calculated dynamic deflection plus a certain percentage of dynamic deflection which will correspond to the static spring rate, K, used for analysis. This is made possible by limiting spacing between local disc pads, where considered, to 2.5 inches maximum to limit wrapped panel deflection between pads to a negligible magnitude. A minimum medium thickness of 0.05 inch is used as a requirement to prevent solar cell damage when wrapping around the drum, extrapolated from wrap tests conducted by Ryan; Reference 4, p. 70.

In selection of the optimum medium configuration, we shall not consider a thickness greater than 0.15 inch. This limit is made to prevent excess buildup of wrapped panel which forces an excessive weight increase of the guide sleeve mounts.

Analysis of a given silicone foam configuration follows for presentation of the approach taken. Consider an inner wrap layer, disc pad configuration as shown, supporting all 12 wrap layers.

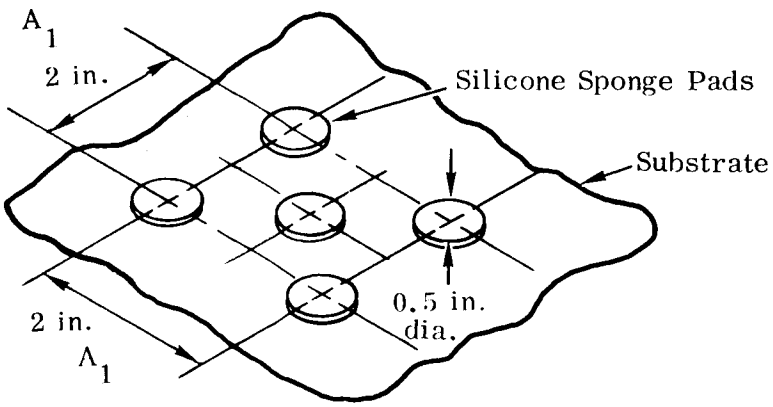

The fundamental frequency, F_n for the separation medium configuration shown on the previous page is calculated by the equation,

$$F_n = \frac{(K/m)^{1/2}}{2\pi} = \frac{(K \cdot g/load)^{1/2}}{2\pi} = \frac{\left(\frac{g}{\text{static defl.}}\right)^{1/2}}{2\pi}$$

K, from compression-deflection curve for 12 wrapped panel layers in 1g field acting on area AA

$$K = \frac{\text{Load}}{\text{Deflection}}$$

Deflection, from Curve.

For $$\frac{\text{Load}}{\text{Pad Area}} = \frac{4 \times 1.53 \times 10^{-3} \times 12}{2\pi \times 0.25^2}$$

$$= \frac{0.073 \text{ lbs}}{0.393 \text{ in}^2} = 0.19 \text{ psi}$$

$$K = \frac{0.073}{0.013} = 5.61 \frac{\text{lbs.}}{\text{in.}}$$

$$F_n = \frac{\left(\frac{5.61 \times 386.4}{0.073}\right)^{1/2}}{2\pi} = \frac{172}{2\pi} = 27 \text{ cps}$$

Dynamic deflection at F_n of the above configuration is calculated by,

$$\delta_{dyn.} = \frac{386.4 g_{(response)}}{(2\pi F_n)^2}$$

$G_{(response)} = 66$ From wrapped panel freq. vs. response accel. curve

$$\delta_{dyn.} = \frac{386.4 \times 66}{(2\pi \times 27)^2} = .89 \text{ in.}$$

Then,

Ther Static thickness for weight purposes = $\delta_{dyn.}$ + A percent of $\delta_{dyn.}$ using K based on 1G deflection (K = constant)

The plots in Figures 14 and 15 show the results of similar calculations for various configurations utilizing silicone or polyurethane foam.

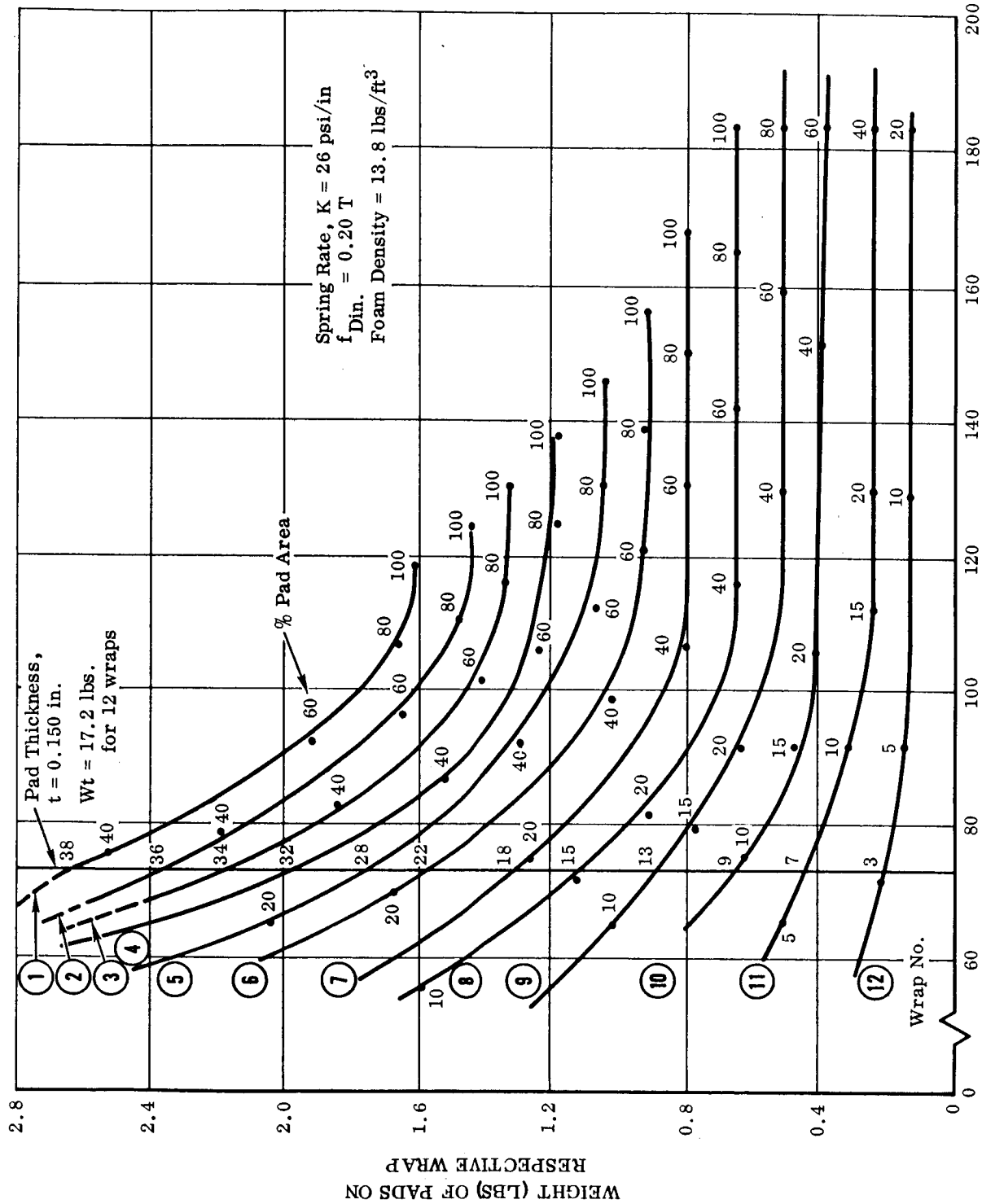

Figure 14 Weight vs. Frequency For Silicone Foam Pads

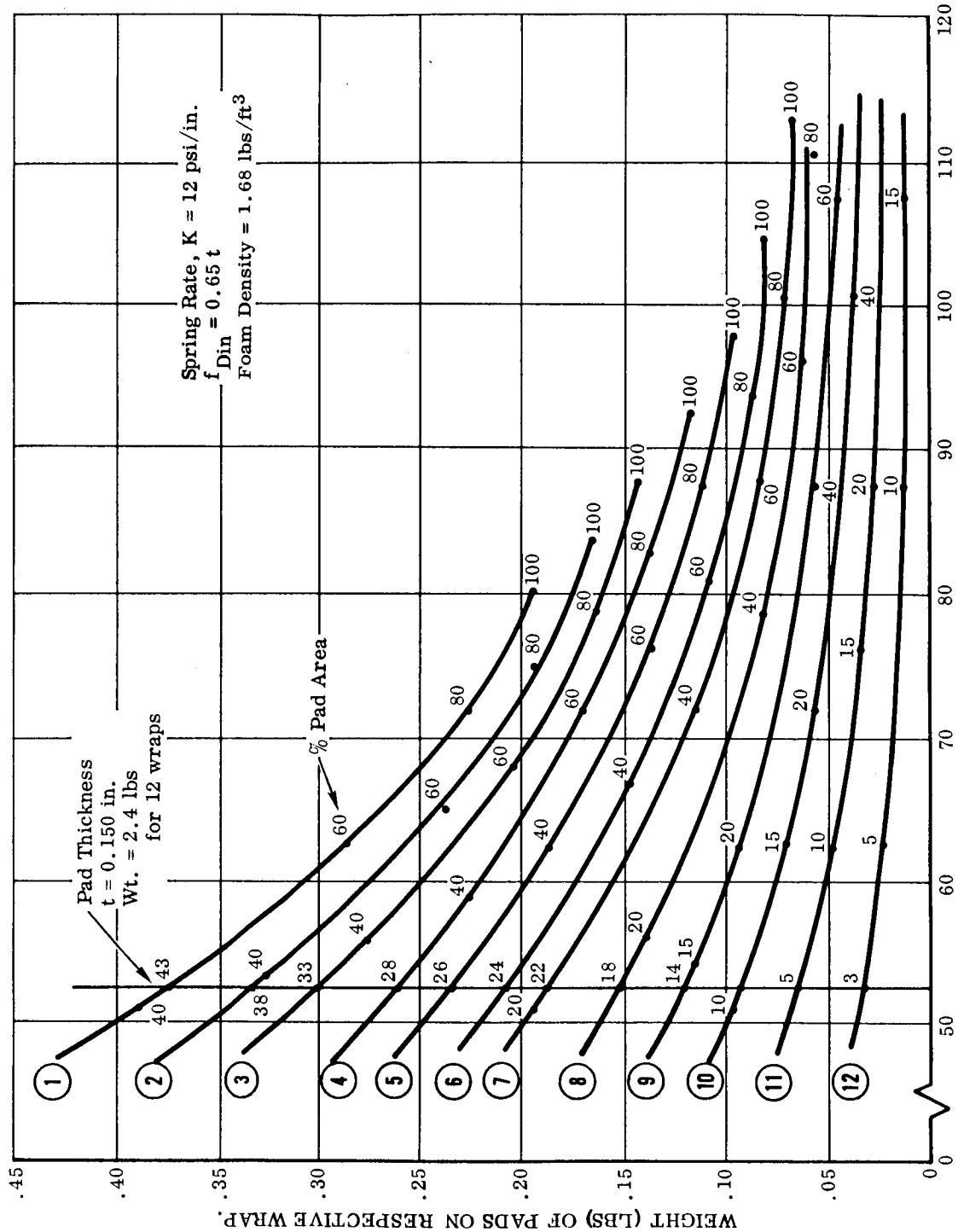

Figure 15 Weight vs. Frequency For Polyurethane Foam Pads

Conclusions

The analysis presented was made to find the lightest weight separation medium configuration using the constraints set forth:

a. Dynamic deflection under sinusoidal excitation at resonance ≤ 0.10 inch to present edge contact of solar cells.

b. Separation medium thickness ≤ 0.15 inch to prevent excessive build-up of wrap thickness, resulting in contact of wrapped substrate and drive torque tube at sinusoidal resonance and possible damage to solar cells.

c. A spacing between disc pads of 2.5 inches so that sinusoidal vibration deflection of the wrapped substrate is negligible between pads; an analysis based on separation medium deflection only is thereby made possible.

d. Separation medium thickness ≥ 0.05 inch to prevent damage to solar cells subject to possible loads during wrapping around drum.

e. A constant thickness separation medium to facilitate ease of tuning (coordinating beam and panel wrap rates).

The plots of frequencies of support medium configurations versus weight for each of the panel wraps shows that the lightest weight medium will result using polyurethane sponge foam. A foam of 1.68 pounds/cubic foot density was considered for the analysis, which is about the minimum obtainable. Utilization of silicone foam of minimum density (13.8 pounds/cubic foot) will result in a total medium weight of approximately 17.2 pounds as compared to 2.4 pounds for polyurethane. A constant thickness design constraint is satisfied by using the minimum thickness possible for the inner wrap, which is 0.15 inch. A thickness less than this would not correspond with the spring rate, K,

for the respective load at that wrap layer. The optimum pads required as a result of this revised analysis and which satisfy the above constraints will not cover such a large substrate area as to force the solar cells to operate above 131°F, thereby jeopardizing a possible electrical power output of 10 watts/ft^2 at 1 A.U.

The results of analytical studies for polyurethane pads are summarized in Table 4.

2.2.5.4 Thermal Studies

This section presents the completion of the thermal studies reported in Section 3.3.2.9 of the first Quarterly Report. In review, the study was conducted to determine the effects on solar cell operating temperatures of the deployed panel utilizing .001 fiberglass substrate versus .001 Kapton substrate. The study was conducted for the sections of the panel representing the extremes in percent radiation blockage areas provided by the sponge foam solar cell protection pads. The essential differences between the configurations analyzed and that selected for design are the foam pad material (silicone was considered here but will be substituted with polyurethane and reported in the next Quarterly Report). Analysis is based on a solar radiation environment normal to the solar cell surface of 260 mw/cm^2 which would be encountered in the vicinity of Venus. Analysis for the panel utilizing Kapton substrate was conducted and presented here to complete the study. Comparison is made with results using fiberglass substrate from the first Quarterly Report.

Figure 16 shows a small section of the outer solar cell wrap which was used for this model. This small testing was reduced into nine smaller sections, which were then divided into isothermal nodes corresponding to layers in Figure 18.

TABLE 4

RESULTS OF ANALYTICAL STUDIES

FOR POLYURETHANE PADS

Wrap No. (Numbering inner as [1]	% Area Pads Required by Analysis	% Pad Area Used	Configuration of Pads Used (Thickness=0.15")
1	43	100	Full Blanket on Drum
2	38	38	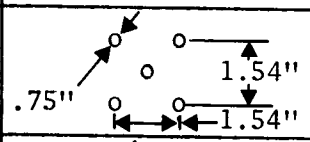
3	33	38	
4	28	28	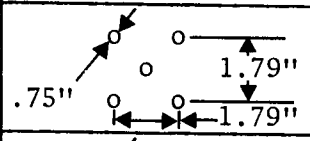
5	26	28	
6	24	24	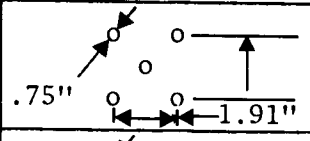
7	22	24	
8	18	18	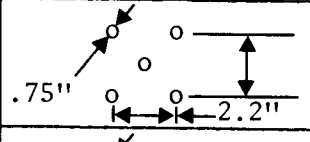
9	14	18	
10	10	14	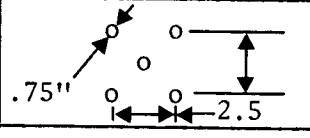
11	5	14	

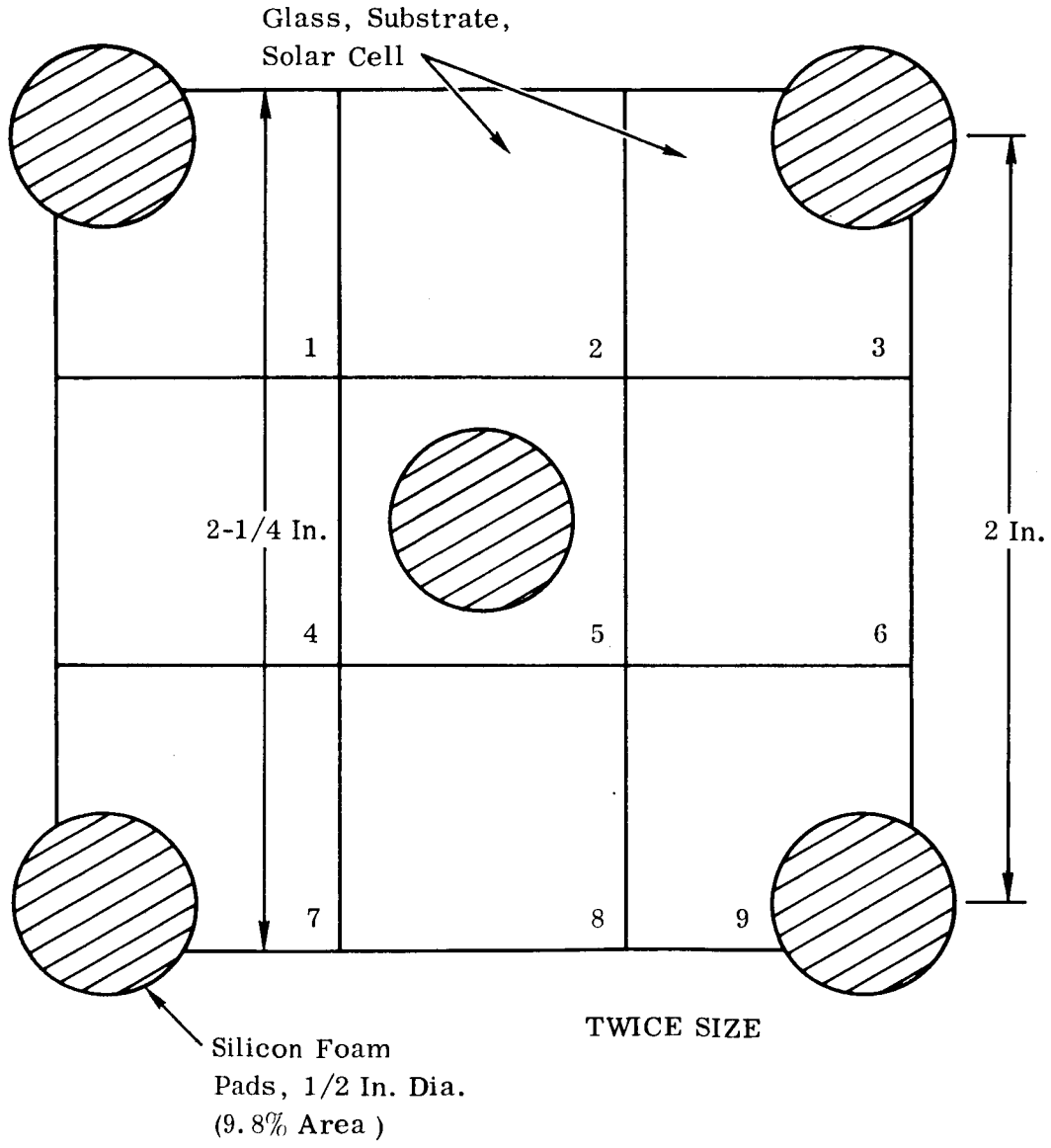

Figure 16 Thermal Model Section - Outer Solar Cell Wrap

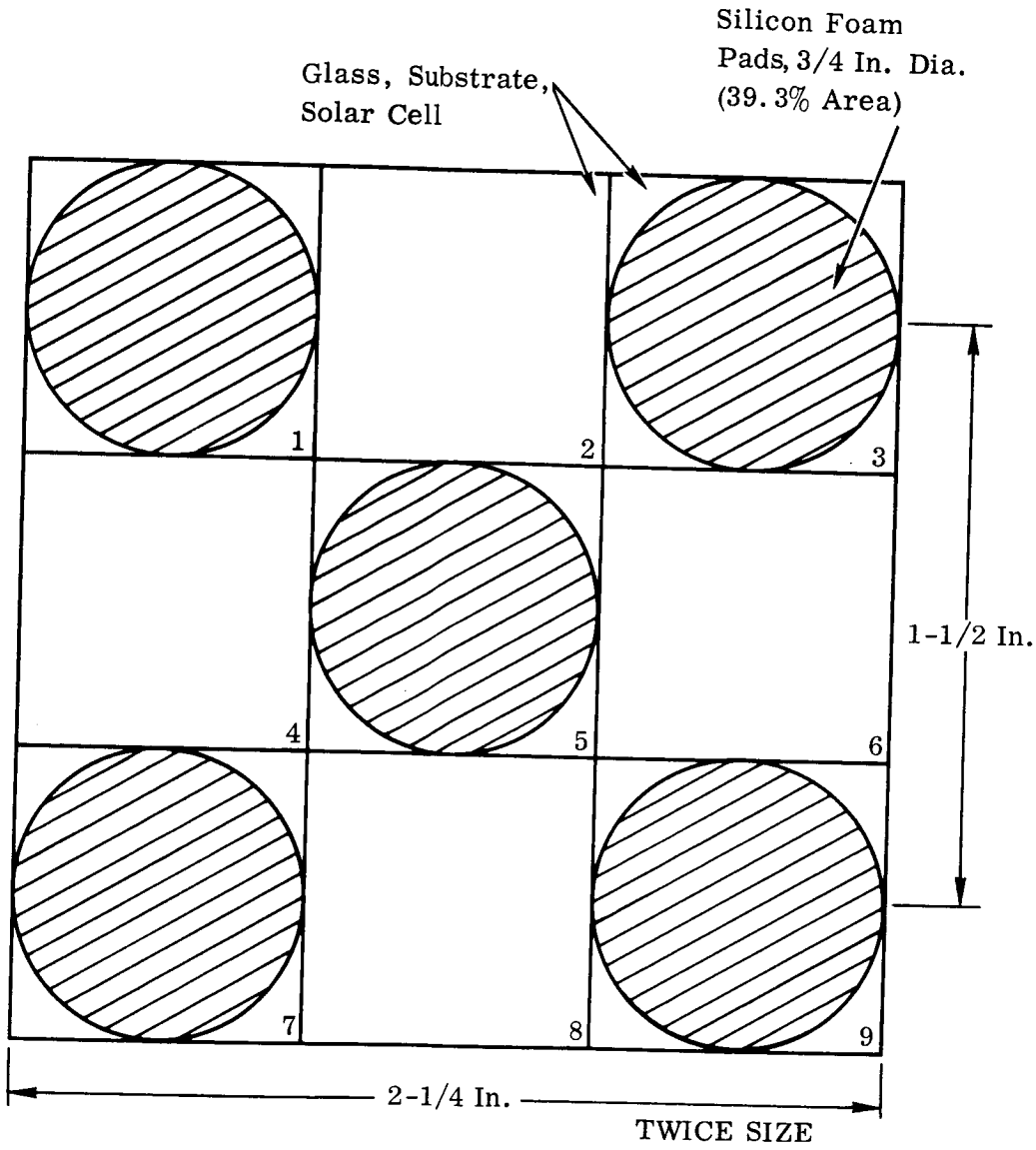

Figure 17 Thermal Model Section - Inner Solar Cell Wrap

Figure 17 shows a small section of the inner solar cell wrap used for the model. The difference between this and the outer wrap is in the size of the cushioning pads.

Assumptions and Material Properties

In the case of both the inner and outer wrap models it was assumed that the adhesive bonding in the layers had little effect on the model and, therefore, these layers were neglected (except for the conductivity). It was also assumed that the substrate was the only material which has an effect on in-plane heat transfer. This is a reasonable assumption since the solar cells are separated on the panel.

The values of the Kapton emissivity and transmissibity were measured in a photospectrometer. The values taken from Figures 18 and 19 of .35 for emittance and .425 for transmittance were used in the substrate model to determine the temperatures of the deployed panel.

The value for the emittance, or ε, was taken as the value of the absorptance of the Kapton at the temperature of 200°F as given in Figure 20.

The value for the emittance, or ε, of the solar cell, was taken as the value of the transmittance of the Kapton at 200°F as taken from Figure 21. This is valid since the solar cell is emitting energy through the Kapton with the Kapton transmitting .425 of the energy striking it.

The materials used in the solar panel and some of their properties are listed in Table 5.

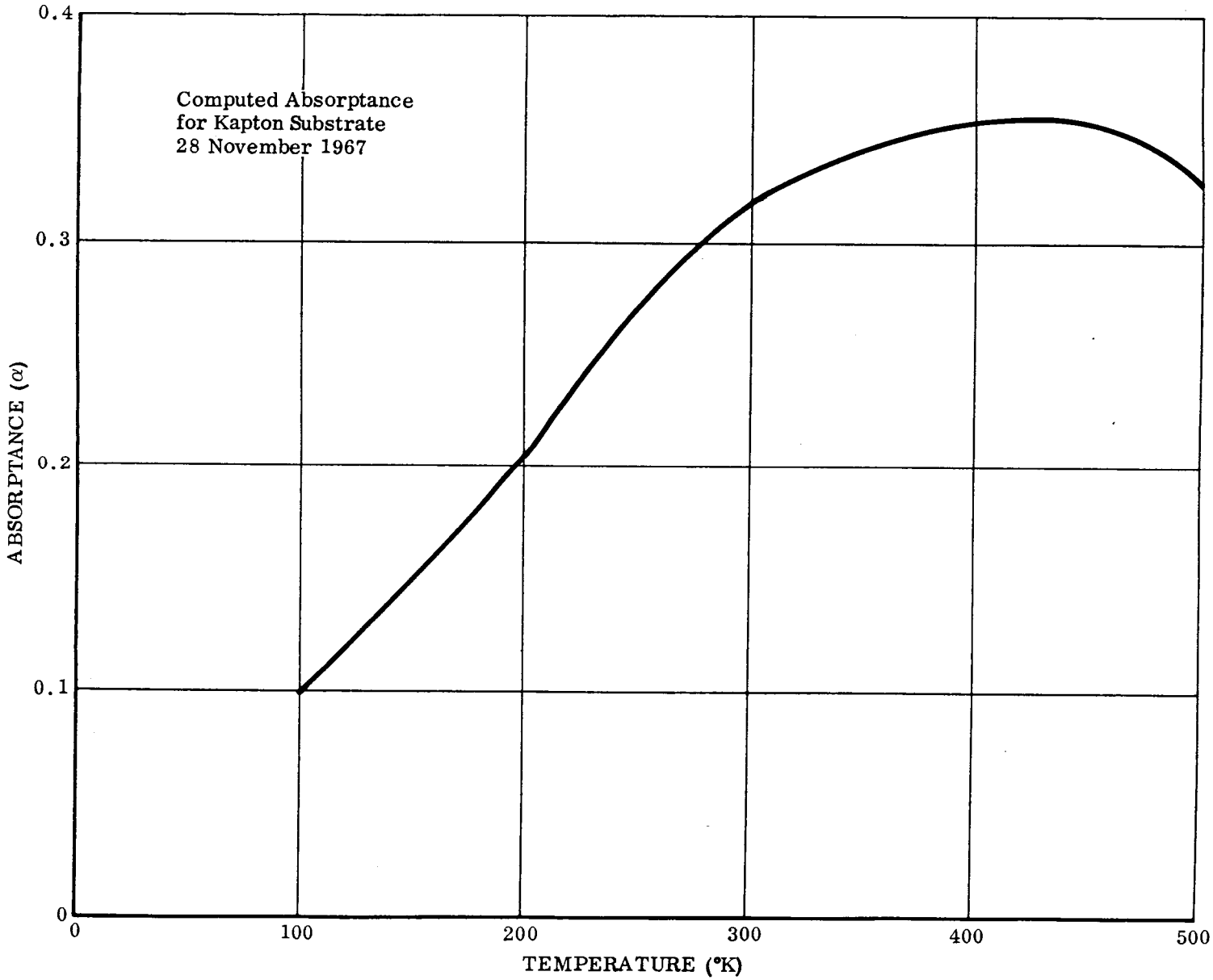

Figure 18 Computed Absorptance for Kapton Substrate, 28 November 1967

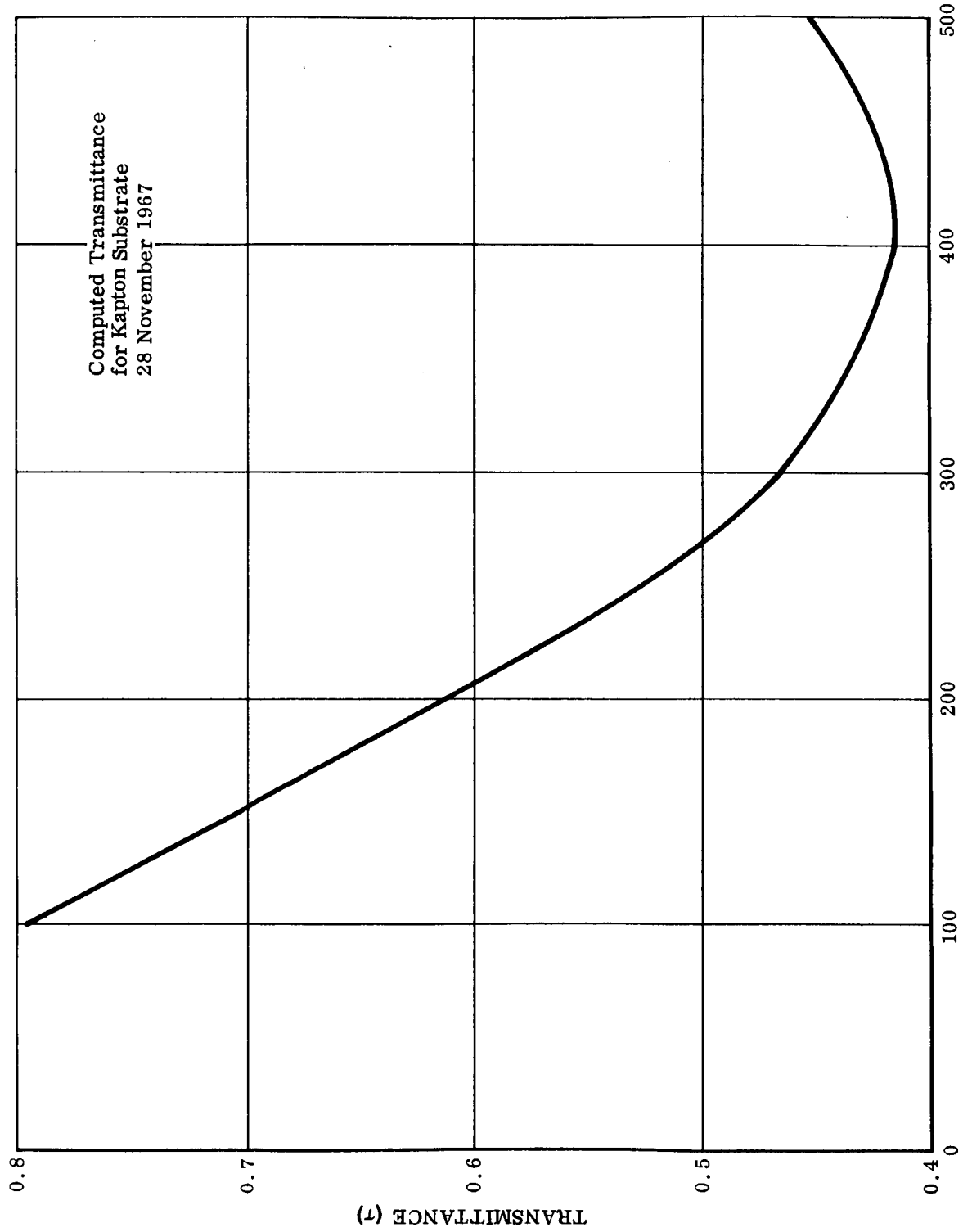

Figure 19 Computed Transmittance for Kapton Substrate, 28 November 1967

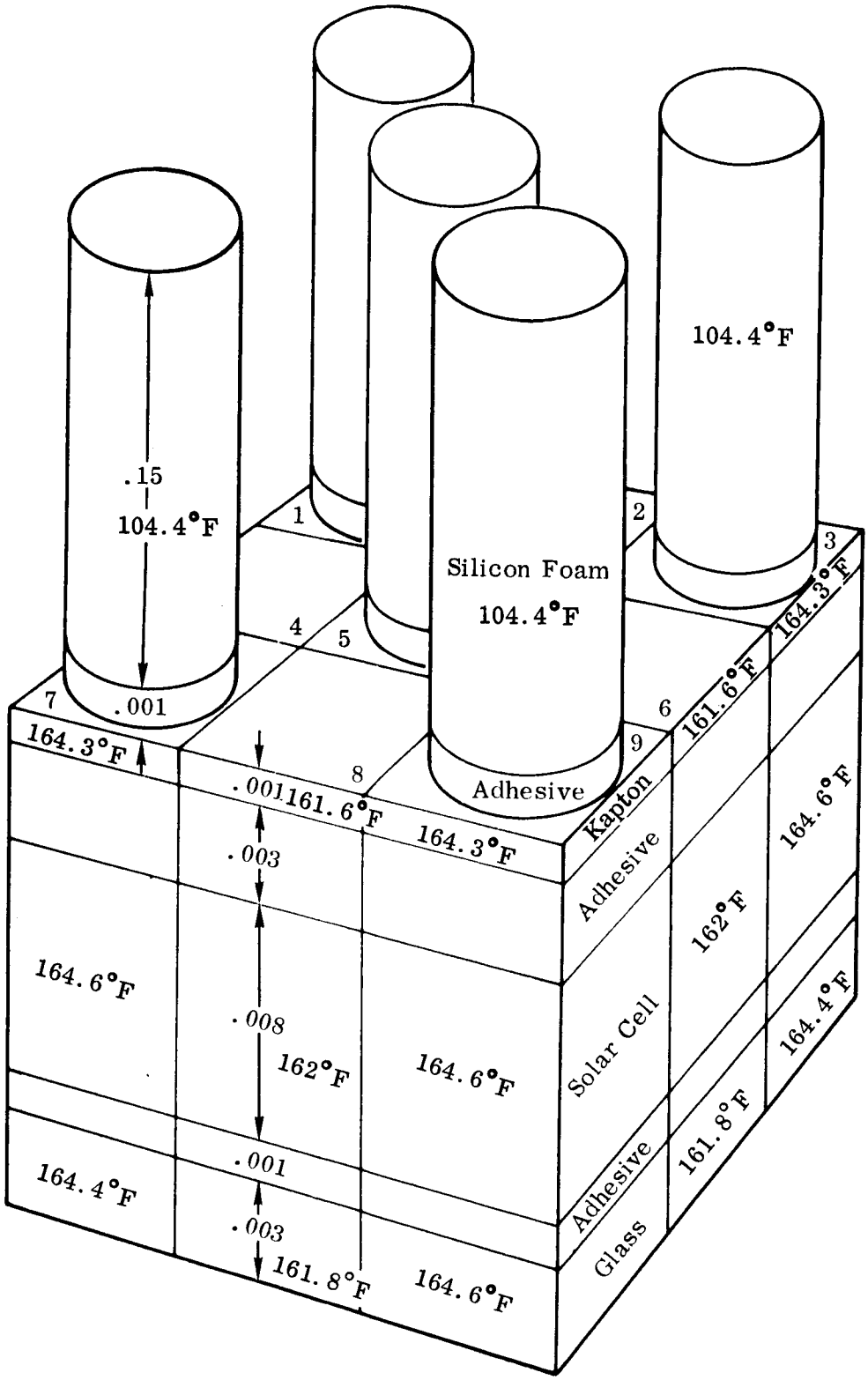

Figure 20 Nodal Temperature - Outer Solar Cell Wrap

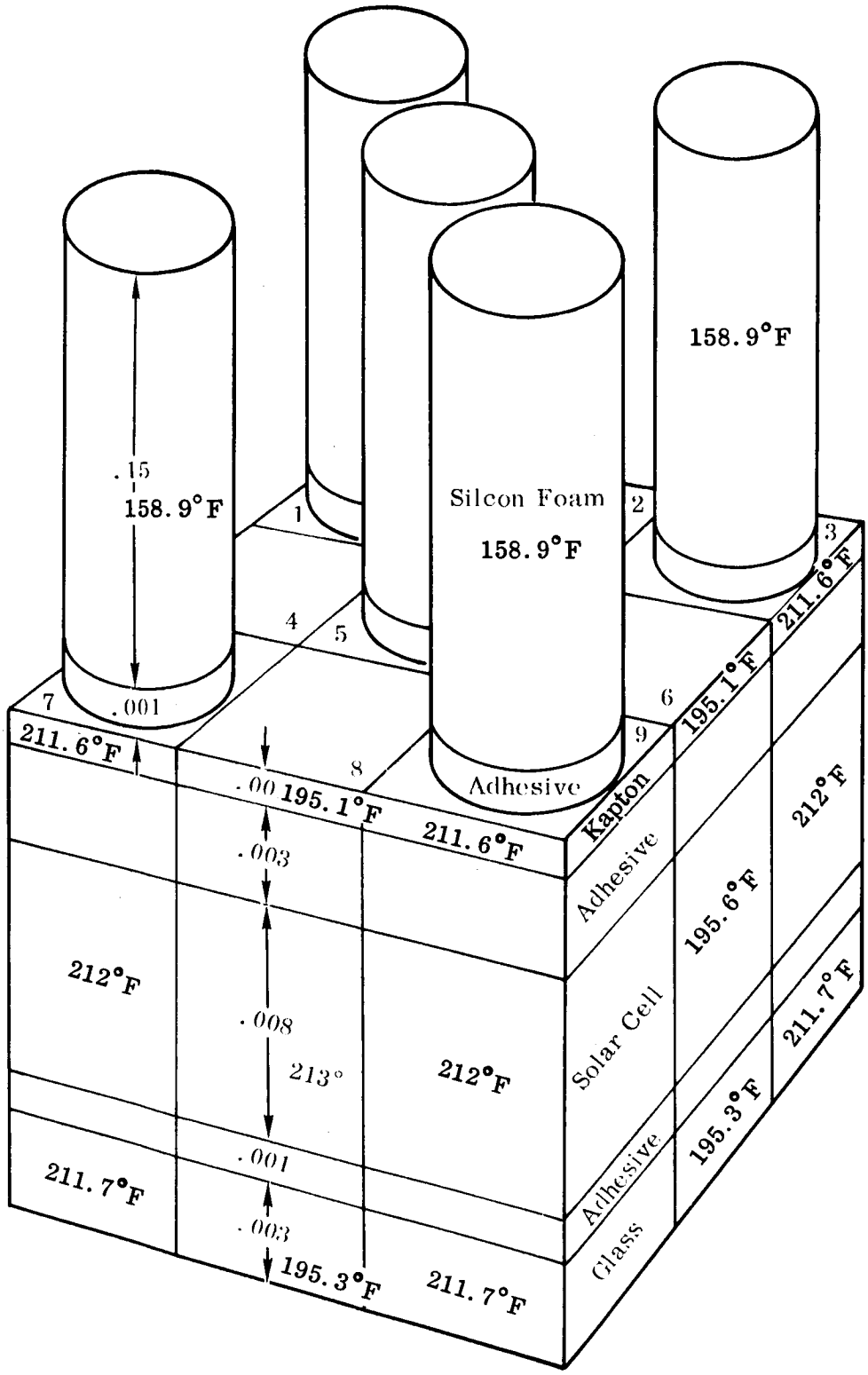

Figure 21 Nodal Temperatures - Inner Solar Cell Wrap

TABLE 5

MATERIALS AND THEIR PROPERTIES CONSIDERED IN THERMAL ANALYSIS

NODE NO.	MATERIAL	SPECIFIC HEAT BTU/LB°R	α	ε
1,5,8,12,15, 19,22,26,29	SILICON GLASS	0.20		
2,6,9,13,16, 20,23,27,30	SOLAR CELL	0.15	.84	.425
3,7,10,14,17, 21,24,28,31	KAPTON	0.261		.35
4,11,18,25,32	SILICON FOAM	0.20		.9

Results

The temperatures of some of the nodes in the outer and inner wraps are shown in Figures 20 and 21. Results of the study, comparing panels with fiberglass substrate versus that with Kapton substrate are given below. Thermal steady state temperatures would be reached in a shortsolar cell operating time, less than .05 hour.

	Temperature, °F, Near Venus	
% Area Pads	Kapton	Fiberglass
39.3	212	231
9.8	164.6	217

Conclusions

Solar cell operating temperatures will be reduced from 231°F and 217°F (inner and outer wraps respectively), using fiberglass substrate to 212°F and 164.6°F using Kapton substrate when subject to a near Venus solar flux. By extrapolation, these temperatures

correspond to 116°F and 109°F utilizing fiberglass substrate versus 106°F and 82°F utilizing Kapton substrate. Any of these temperature levels are well below the upper limit of 131°F, which corresponds to a power output of 10 watts/ft^2 at 1 A.U. With an 8 to 24 percent reduction in solar cell operating temperature possible using Kapton, and further justification due to the weight reduction using Kapton versus fiberglass (see Section 3.3.3.4.2, first Quarterly Report), Kapton substrate is recommended for use.

2.2.6 Deployment/Retraction System Drive Motor Requirements

Calculations and derivation of equation for motor torque and power requirements are presented in this section.

The derivation of the basic equation form motor torque is as follows:

Dimensional Analysis
L = Length, T = Time
lb = Force ~ Weight

a. Torque, Moment (T,M,) = L-lb. (Not Work)

b. Work (W) = L-lb.

c. Power (P) - Work/Time = dw/dt
(P - L-lb./T)

d. W = (Torque, Moment) (Angular Distance)
the Angular Distance (Radians) is non-dimensional

e. Power Out (P_o) = 2 F_b (V) = P_{fr}
F_b = Side Beam Drive Force (#), Thru Guide Bearing. There are 2 Side Beams.

V = L/T. = Velocity (in./sec.) of Side Beam Retraction or Deployment

P_{fr} = Power Lost to Friction

f. Power Input = P_{in} = T (Rad), (in#/sec)

P_{in} = 2tt (RPM) T/30

Equating Input to Output

$P_{in} = P_o = 2\ F_b\ (V) = P_{rf}$

$P_{in} = P_{rf} = K\ P_{in} = 2F_b\ (V)$

K = System Mechanical Friction

$K(P_{in}) = (K)\ [tt\ (RPM)\ T/30] = 2F_b\ (V)$

Solving the above equation for torque (T)

$$T = 60F_b\ (V)/tt(K)\ (RPM) \qquad (1)$$

The side Beam Force (F_b) can be taken from the curve of Figure 22. This curve was derived from experimental data from laboratory tests. The tests were conducted on an .0035, stainless steel (AM355-SCT850) side beam. The constant K_B was experimental obtained for the following equation:

$$F_B = K_B\ EK/R^2$$

K = 44 for beam retraction

K = 23 for beam extension

E = Modulus of Elasticity

I = Moment of inertial of side beam open section

R = Wrap drum radius

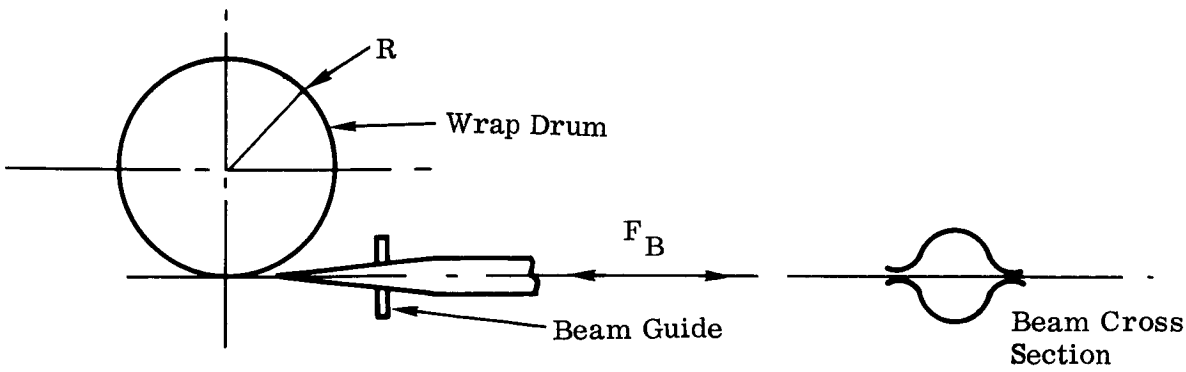

For the following conditions:

$$E = 29.3\ (10^{-6})$$

$$I = .124\ (10^{-6})\ \text{for t} = .004$$

$$K = 44\ \text{maximum retract condition}$$

$$F_b = K_B EI/R^2 = (44)\ (29.3)10^6\ (.124)\ (10^{-6})/R^2$$

$$F_b = 159.86/R^2$$

For a 6 inch drum and .004 Ti. beam F_b is taken conservatively as:

$$F_B\ (\text{Ti.}) = F_B\ (S_T.\ S_T.)\ (E_{Ti}/E_{ST})$$

For a motor output shaft of 6 RPM and a 5:0 inch diameter beam drive sprocket

$$V = (\text{RPM}/60)\ (\pi D_o) = (6/60)\ \pi\ (5)$$

$$V = 1.5708\ \text{in.-lb/sec.}$$

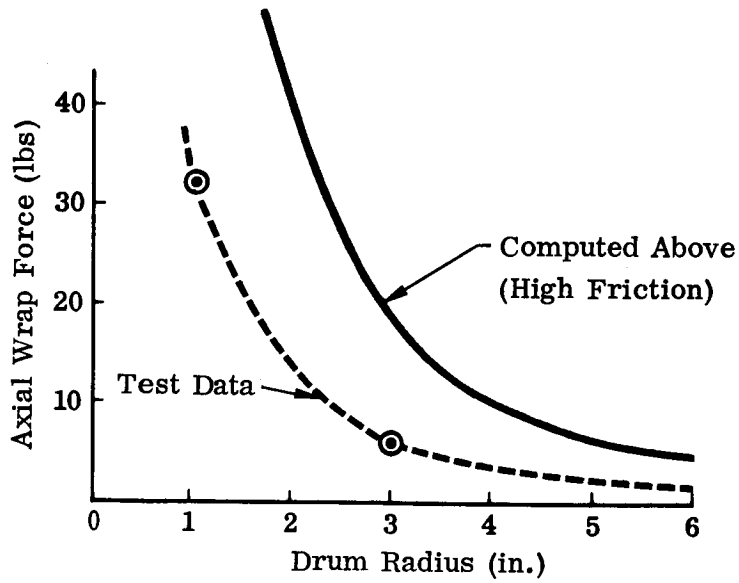

Figure 22 Typical Case of Axial Wrap Force Versus Drum Radius

The drive motor RPM selected under load is 8000 RPM. A mechanical system efficiency of K = .60 is assumed.

$$T = (F_B\ (V)\ 60/\pi\ (K)\ (RPM) \quad \text{Ref: Equation (1)}$$

$$T = (4.0)\ (1.571)\ 60/\pi\ (60)\ (8000)$$

$$T = .025 \text{ in.-lb at } 6.0 \text{ RPM}$$

$$T_6\ (RPM) = T_{8000}\ (RPM)$$

$$T_6 = (.025)\ (8000/6) = \underline{33.33} \text{ in.-lb torque at } 6.0 \text{ RPM}$$

The above torque requirement will be confirmed from drive motor tests on the demonstration model panel array.

2.2.7 Solar Cell Installation

2.2.7.1 Power Analysis and Trade-Off

An additional solar cell has been considered. This solar cell is a non-standard large size cell that offers a significant savings in cost and a power per unit area ratio comparable to that of the corner dart 2 X 2 cm cell. It appears that this special solar cell could be supplied in production quantities within schedule constraints of this contract.

A slight weight saving is also realized due to a reduction in the number of series interconnecting bus bars. The total number of series connected solar cells for one complete circuit would be reduced from 180 cells to 136 cells. The maximum power voltage would be subsequently reduced from 73.7 to 55.7 volts. Open circuit voltage would be reduced from 92.4 to 69.8 volts. The aforementioned voltages are at a temperature of 55°C and an illumination intensity of 1 AU and AMO.

Anticipated performance curves are presented in Figure 23, 24, 25 and 26 for a 2 x 2 cm standard bar contact cell, a 2 x 2 cm corner dart corner dart contact cell, a 2 x 6 cm bar contact cell and the proposed, special 1.042 x 2.384 inch cell, respectively.

2.2.7.2 Unit Weights - Solar Cell Installation

The following unit weight information is reported for the solar cells and related materials that are discussed in this report. It considers the gross solar cell area as 250.72 square feet.

ITEM	WEIGHT (lb/sq ft of gross cell area)
Longitudinal bus (tapered), including adhesive and insulation, (material is 0.001 aluminum)	0.01053
Transverse bus, including adhesive and insulation, (material is 0.002 copper, 0.5 inch wide)	0.00068
Circuit termination, jumpers and solder	0.00032
	0.01153
Solar Cells -	
2 x 2 cm, 8 mil. thick, 0.003 covers	
or,	
2 x 6 cm, 8 mil. thick, 0.003 covers	0.16650
TOTAL	0.17803

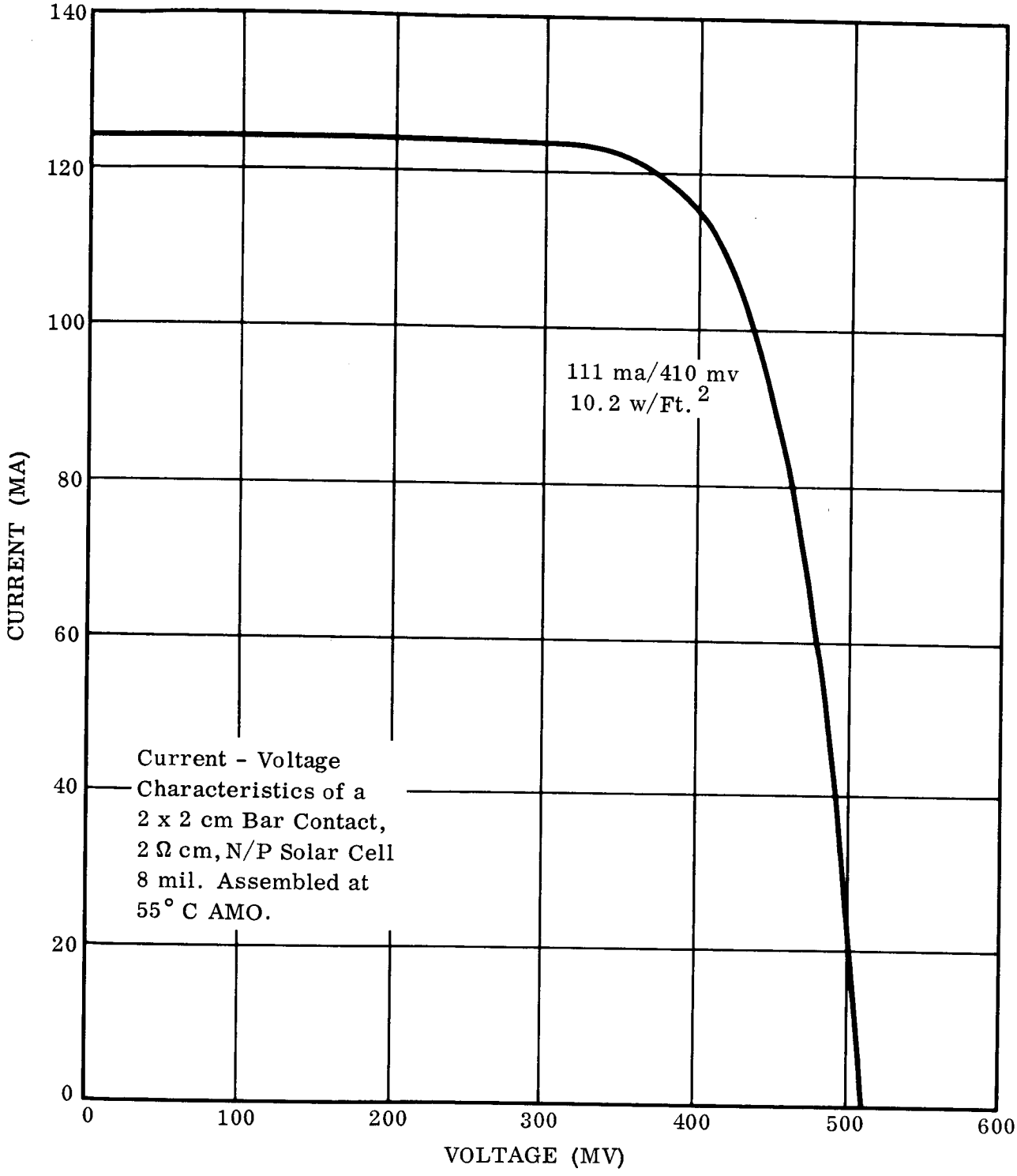

Figure 23 Current-Voltage Characteristics of a 2 x 2 cm Bar Contact 2Ω cm, N/P Solar Cell, 8 Mil., Assembled, at 55°C AMO

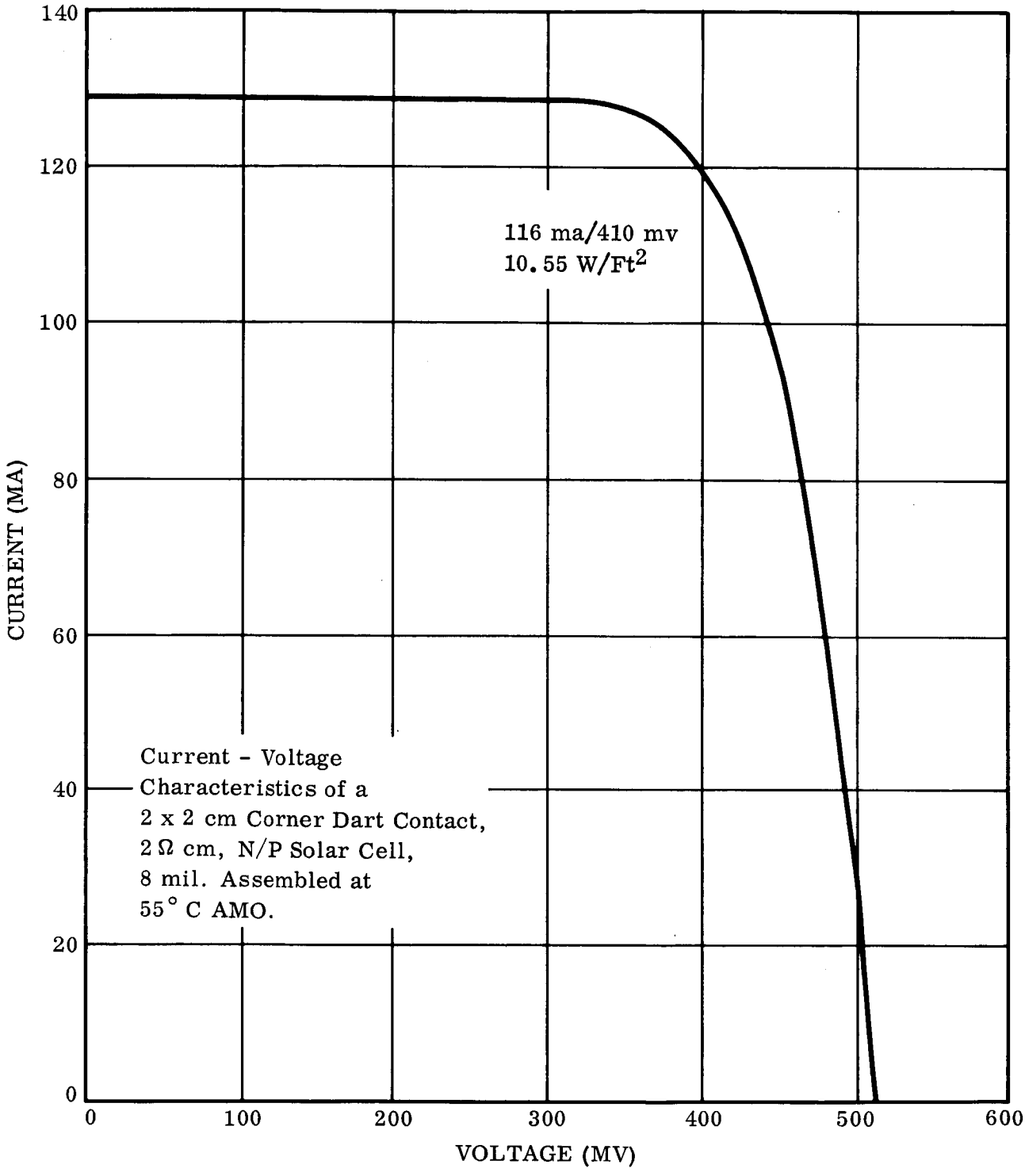

Figure 24 Current-Voltage Characteristics of a 2 x 2 cm Corner Dart Contact 2Ω cm, N/P Solar Cell, 8 Mil, Assembled, at 55°C AMO

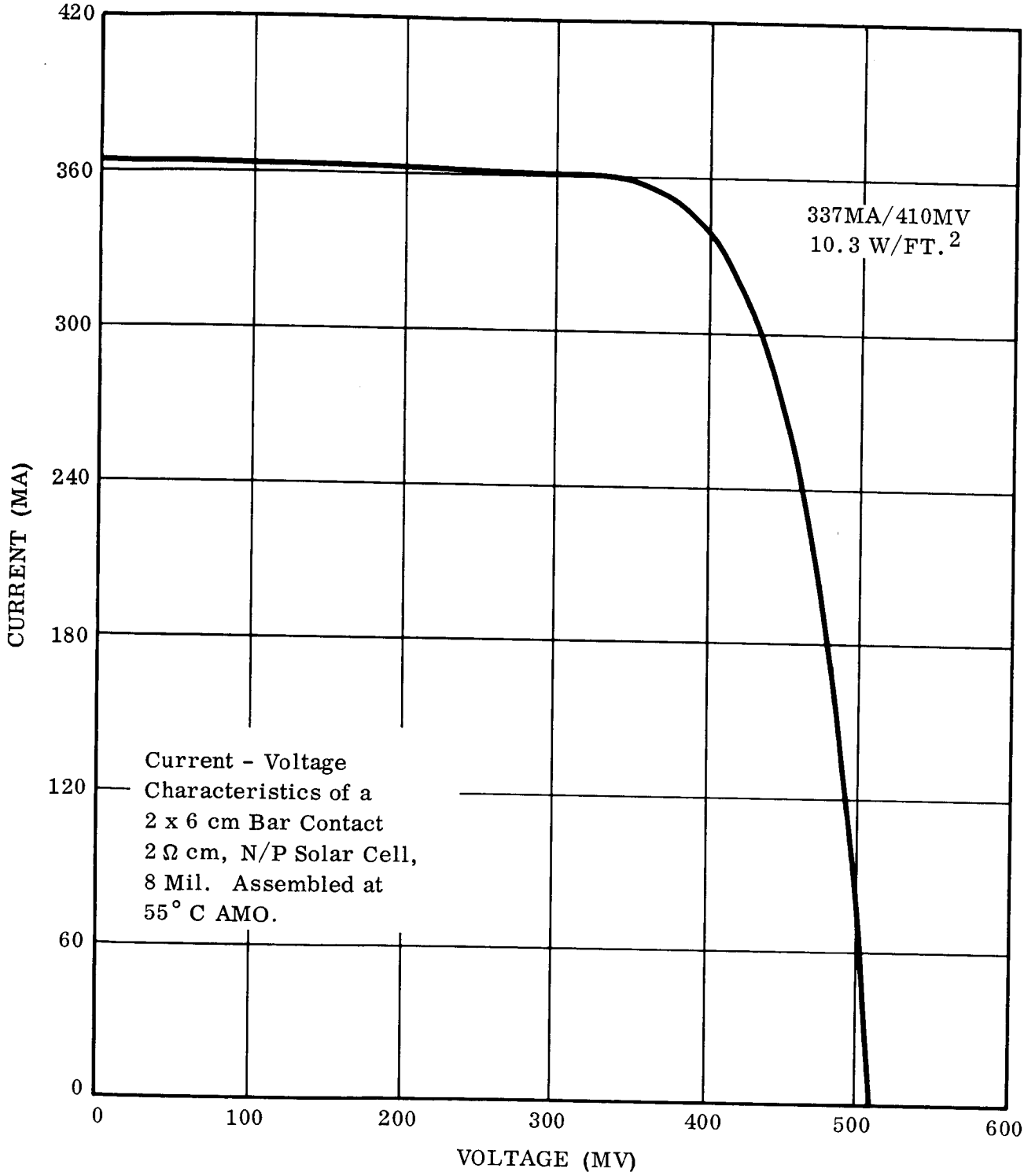

Figure 25 Current-Voltage Characteristics of a 2 x 6 cm Bar Contact 2Ω cm, N/P Solar Cell, 8 Mil., Assembled, at 55°C AMO

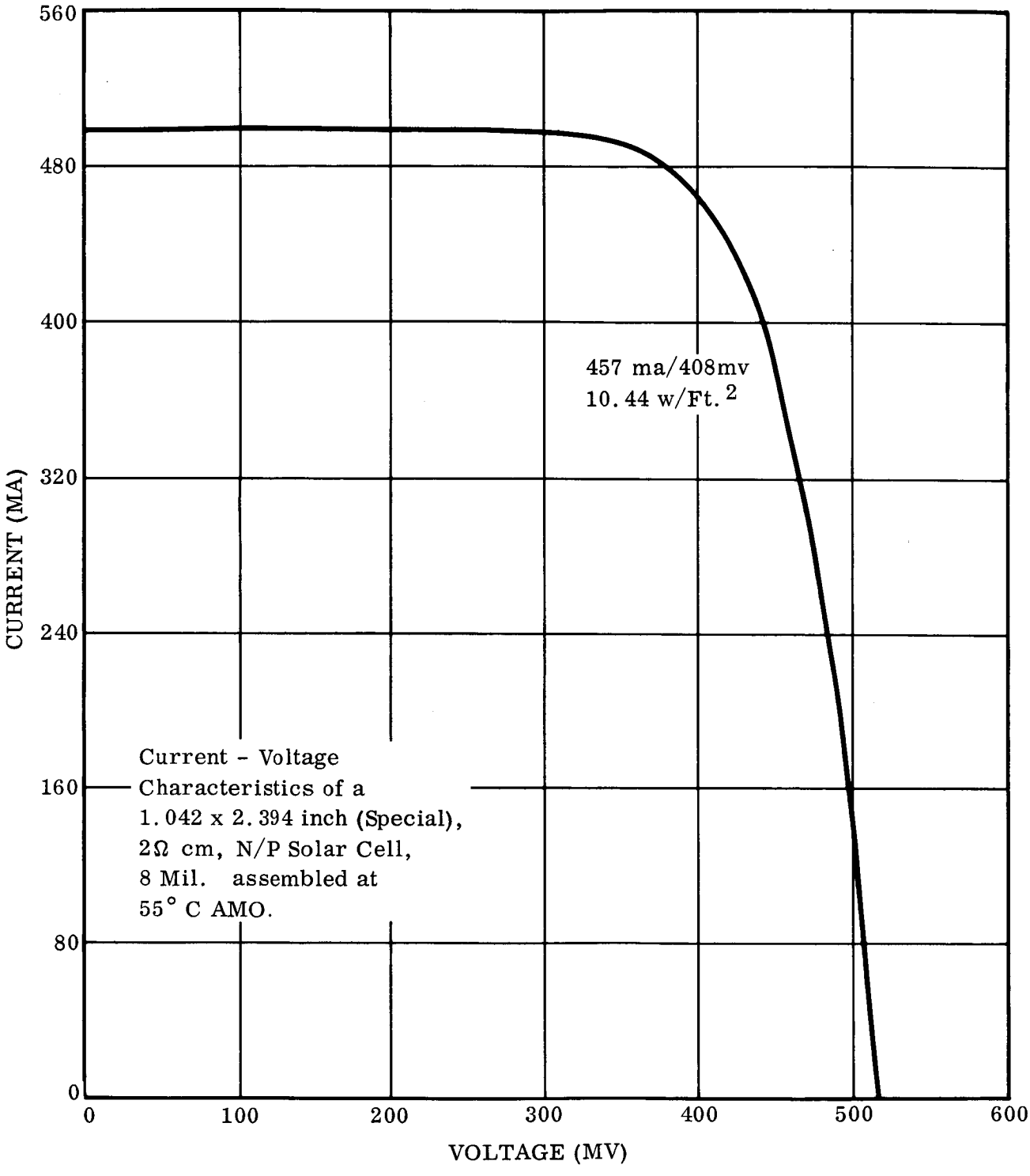

Figure 26 Current-Voltage Characteristics of a 1.042 x 2.384 inch (Special), 2Ω cm, N/P Solar Cell, 8 Mil., Assembled at 55°C AMO

For comparative purposes, equivalent unit weights of the new 1.042 x 2.384 inch solar cell with two coverglass arrangements is given as:

Large cell, 8 mil. thick with 0.003 covers - 0.1639

Large cell, 8 mil. thick with 0.0013 integral covers - 0.1410.

2.2.7.3 Power-to-Weight

Power-to-weight curves for varying solar cell thicknesses and coverglass arrangements have been updated and are presented in Figures 27, 28, 29 and 30. The reader should note that the data presented is exclusive of weight allowances for substrate, array structure and deployment/retraction mechanisms. The data does include weight factors for sub-elements such as bus bars, collector leads, solder and adhesive as well as solar cell and coverglass weight.

A re-evaluation of the power output capabilities of the 2 x 6 cm, 2-ohm base resistivity, solar cell (as reported in the first Quarterly Report) indicated the power output per unit area was high. The 2 x 6 cm cell in reality offers a 1.2% power output per unit area advantage over an equivalent area of 2 x 2 bar contact cells.

2.2.7.4 Magnetic Moment Determination

No significant changes have been made in the overall circuit layout; consequently, the original analysis is still valid, (Pages 121-130, Reference 1).

2.2.7.5 Radiation Degradation

The extent of radiation degradation to solar cells will depend upon the environment of the cell. Hence for purposes of comparison of various coverslides a general environment will be specified which will attempt to represent a realistic situation and at the same time facilitate calculations. For the latter reason pertinent data and graphs are

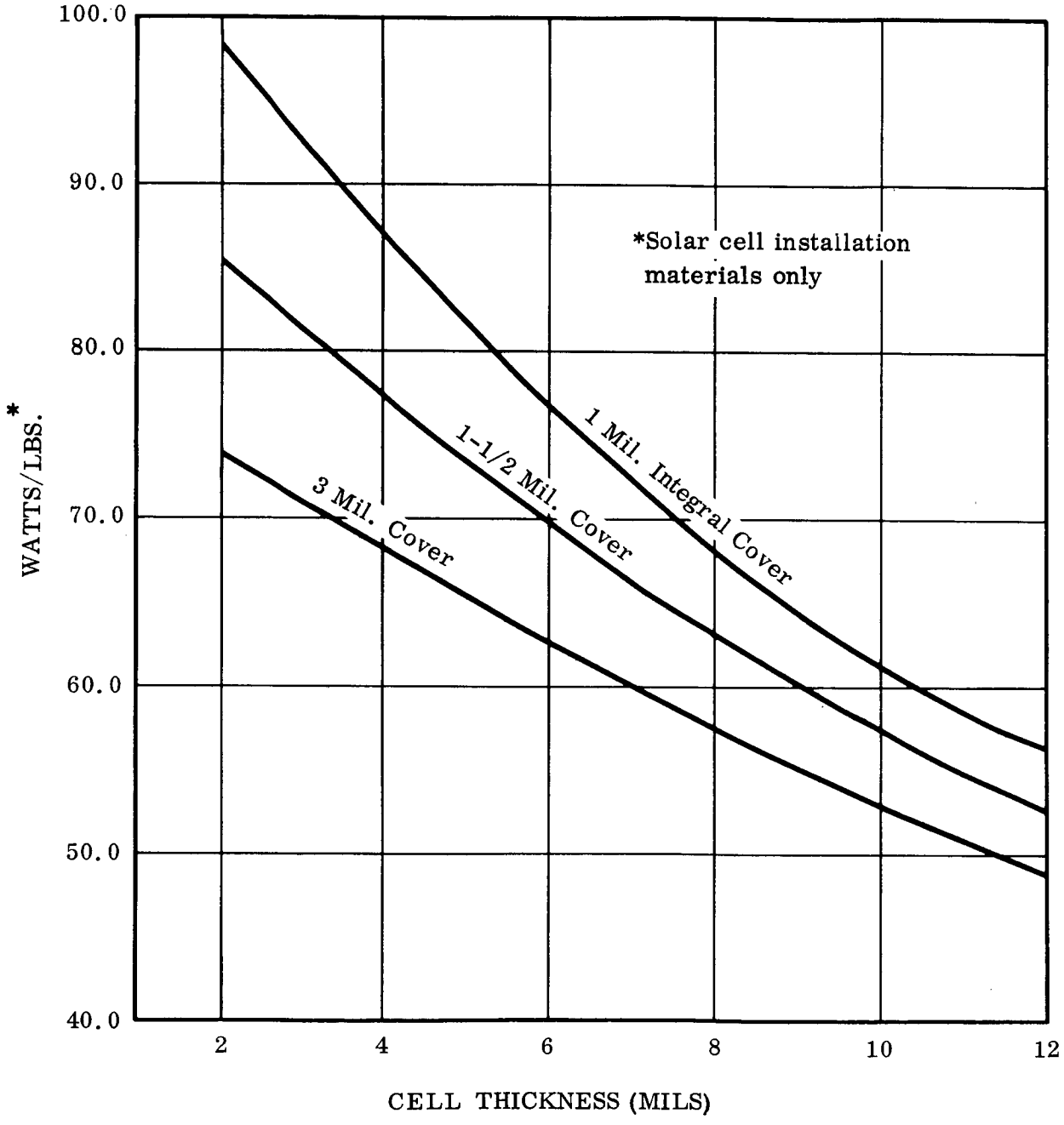

Figure 27 Specific Power Output Per Cell Thickness for 2 x 2 cm Bar Contact, Standard Bus, Cell

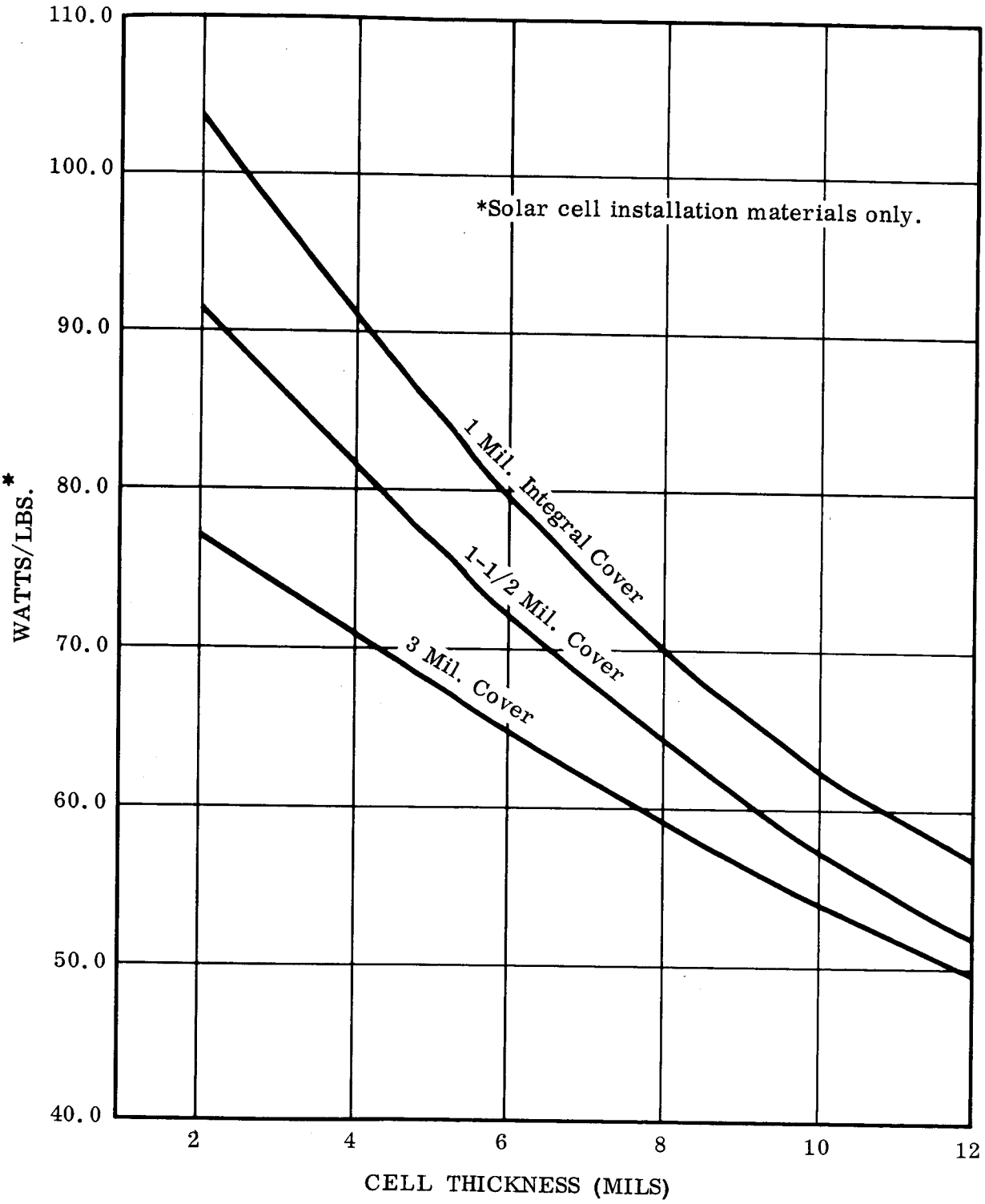

Figure 28 Specific Power Output Per Cell Thickness for 2 x 2 cm Corner Dart, Bus Bar, Cell

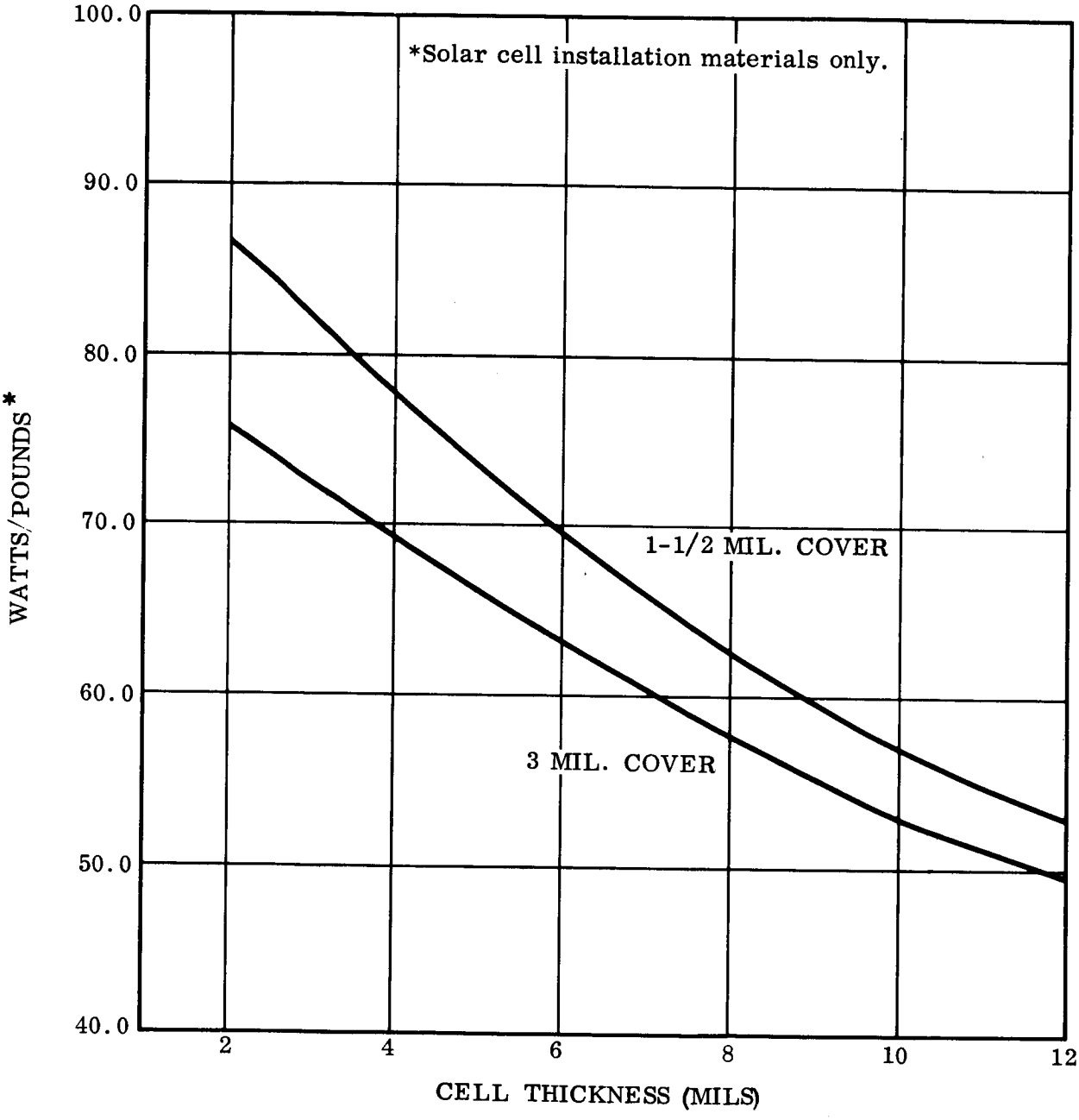

Figure 29 Specific Power Output Per Cell Thickness for 2 x 6 cm, Standard Bus Bar, Cell

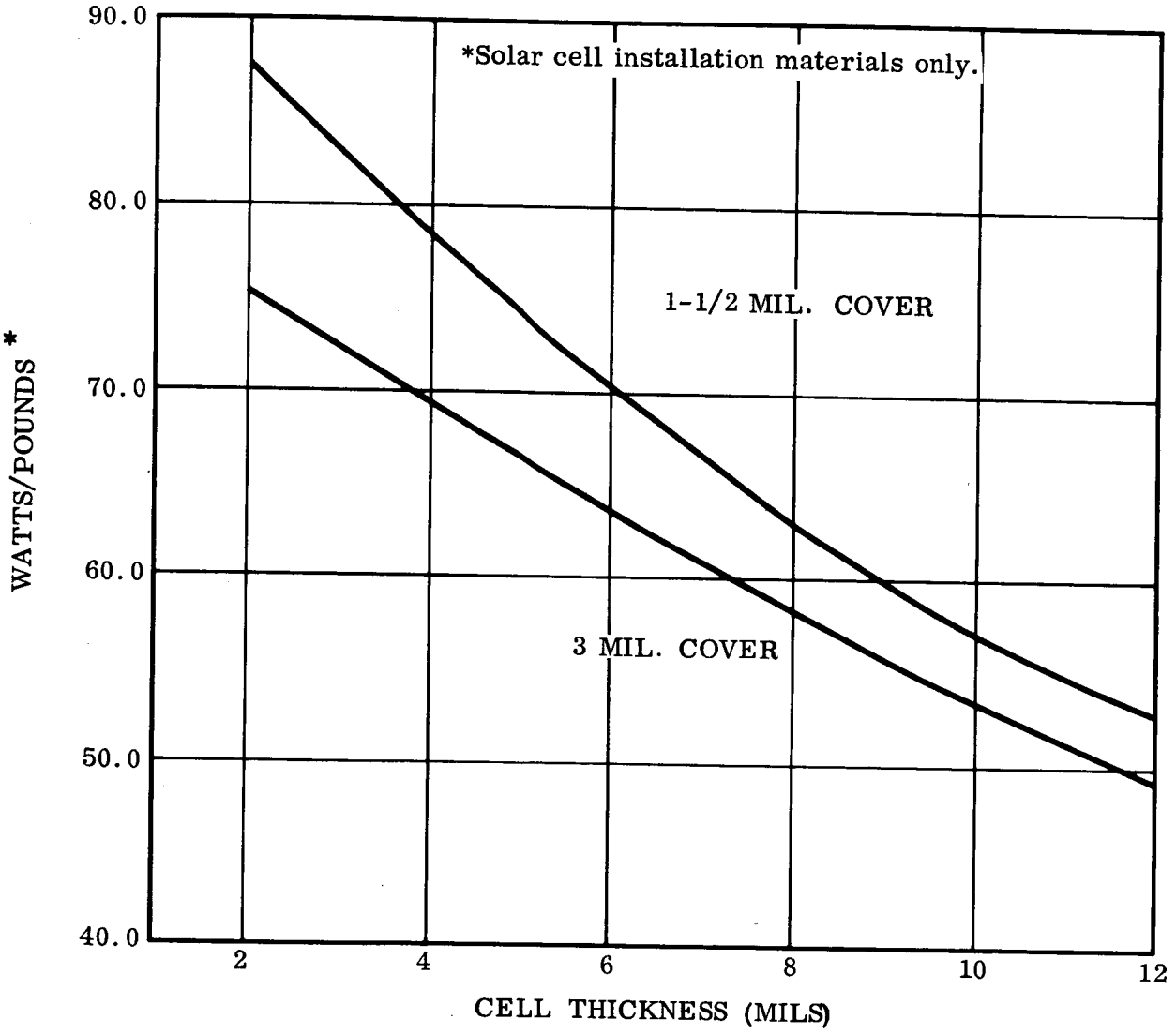

Figure 30 Specific Power Output Per Cell Thickness for 1.042" x 2.384" Cell, Standard Bus Bar

taken from a previous Spectrolab report, No. DR-3A, written by E.L. Ralph, under project number AOSO-3137A.

For this report a 10 ohm-centimeter N/P solar cell in a 1 year solar orbit at 1 A.U. (Astronomical Unit) will be considered. This will neglect the effect of trapped protons and electrons near the earth. Thus radiation damage will occur through protons emitted by solar flares and ultra violet radiation. The former radiation primarily affects the cell by causing defects in the silicon crystal lattice, whereas the U.V. (Ultra-violet) radiation will primarily degrade the coverslide, and coverslide adhesives.

In view of the fact that solar flares can differ widely in both intensity and energy distribution and that measurements of low energy protons (<5 MEV) are not available in any useable quantity, a certain amount of averaging and extrapolating must be made. It should be kept in mind that the numbers thus employed, although not necessarily conforming to any actual realized radiation environment, do represent theoretically plausible conditions based upon the experimental evidence now available.

Figure 31 shows the solar cell coverglass shield thickness as a function of the coverglass thickness with curves for microsheet (Microsheet Silica Corning No. 0211), lead potash (8871), and sapphire. The shield thicknesses for the 3 mil microsheet, 6 mil microsheet and the 1.3 lead potash are obtained from these curves.

Since present data on cell particle degradation is based on experiments with 1 MEV electronics, the proton flux must be converted into an equivalent 1.0 MEV electron flux. Figure 32 contains the information needed to make this conversion. The lead potash curve is labeled 0.015, the 3 mil microsheet is 0.019, and the 6 mil microsheet is 0.035 (their shield thicknesses). For the 6 mil microsheet all protons with energies less than 4.4 MEV are essentially absorbed by the coverglass and

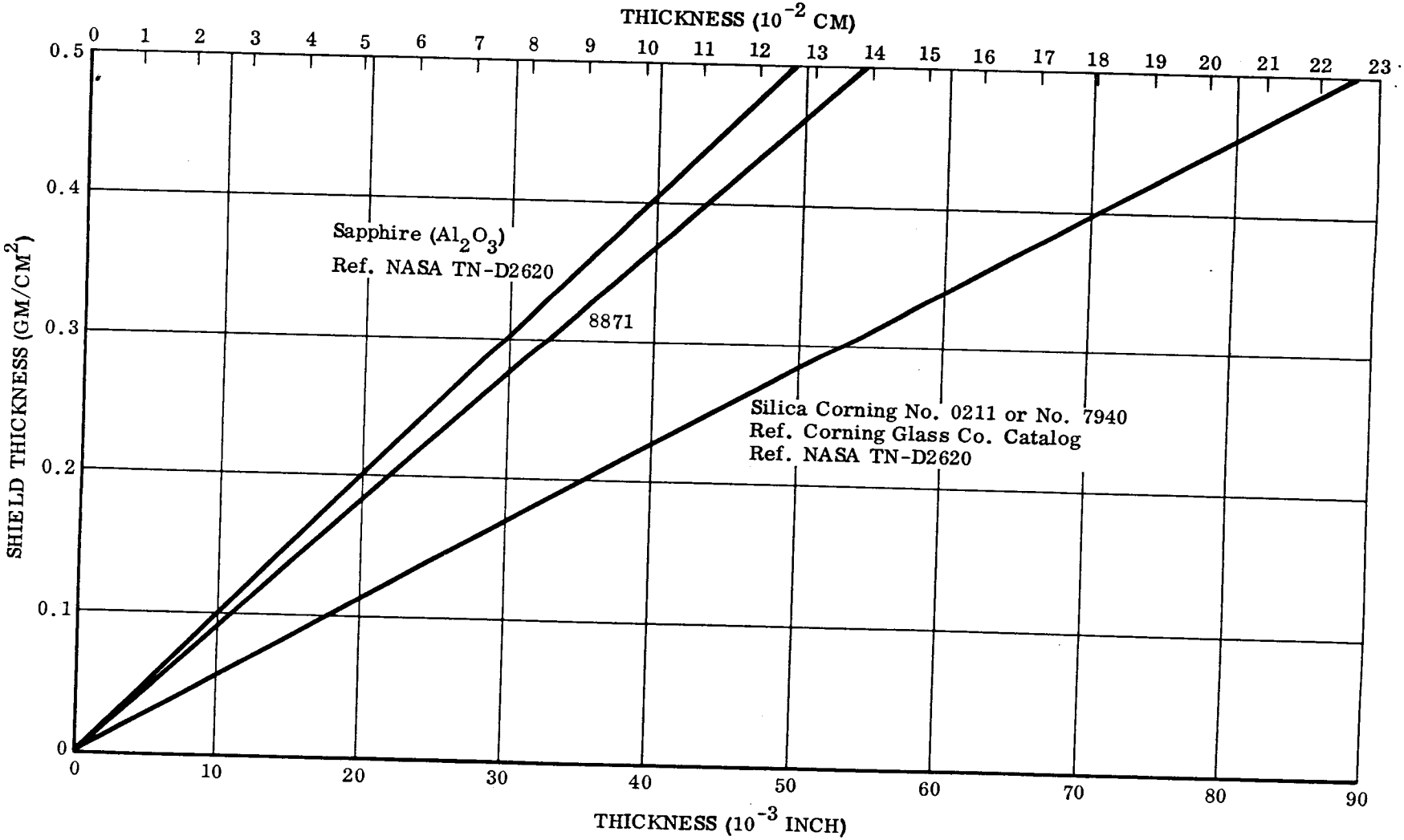

Figure 31 Solar Cell Coverglass Shield Thickness As Function of Thickness of Coverglass

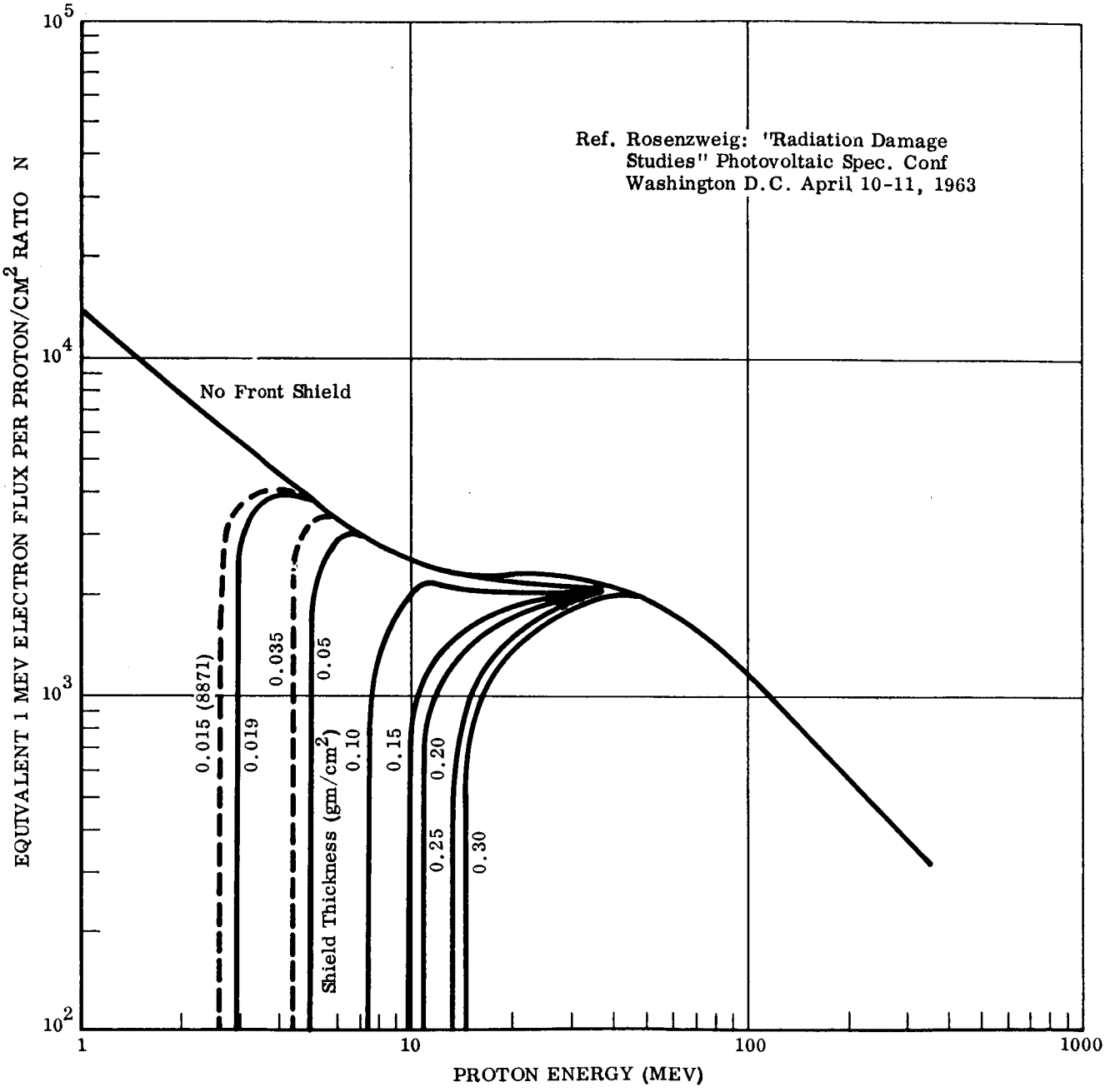

Figure 32 Solar Cell Damage Equivalent to 1 MEV Electrons as Function of Proton Energy Infinate Back Shielding

and do not affect the cell. For the 3 mil microsheet the cutoff is at 3.1 MEV and for the lead potash glass the cutoff energy is 2.7 MEV. The dosage received by the cell is obtained in the following manner. A flux and energy spectrum is assumed for the radiation environment. With a given exposure period the flux can then be converted to a dosage (number of incident particles per area). The proton dosage is then converted by integration (using Figure 2) into an equivalent flux of 1 MEV electrons. Then Figure 33 is used to determine cell degradation.

In the case of the 1 A.U. solar orbit two different flux levels are considered. One will pertain to a probably expected environment and the second will pertain to a highly unlikely high radiation environment (a worst case). Since flux levels can vary widely over short periods of time (with solar flares) the dosage for 1 year will be more meaningful since it will essentially average out the random flux variations. For case 1, a dosage of 8×10^8 protons/cm^2 will be used, and for case 2 a dosage of 4×10^{10} protons/cm^2 will be used. The dosage curves versus time of exposure are shown in Figure 34, where P(<N) means the probability of no more than N particles/cm^2 being "seen" during the specified time interval. We are using curves 1 and 3.

Information on the energy spectrum to be expected is somewhat ambiguous. One reason is that the random solar flares, in addition to exhibiting different flux levels, also have different spectrums. Second, since primary flare measurements have been made on the earth, protons with energies below 4 MEV cannot be measured due to absorption in the atmosphere. By averaging many flares and extrapolating spectral curves, we can expect to find approximately equal numbers of particles in the region 2.7 to 4.4 MEV, 4.4 - 30 MEV, and 30 MEV and greater. These approximations appear to be reasonable on the basis of the limited data in the low energy regions.

The results are summarized in the following charts.

PROTON DOSAGE	EQUIVALENT 1 MEV ELECTRON DOSAGE		
	1.3 Mil Lead Potash	3 Mil Microsheet	6 Mil Microsheet
$8 \times 10^8 P/cm^2$	6×10^{12}	5×10^{12}	2.8×10^{12}
3.5×10^{10} P/cm^2	3×10^{14}	2.5×10^{14}	1.4×10^{14}

% DEGRADATION FOR 1 YEAR DOSAGE (Using Figure 33)

	$8 \times 10^8 P/cm^2$	$3.5 \times 10^{10} P/cm^2$
1.3 Mil	1.2%	18%
3 Mil	1.0%	17%
6 Mil	0.6%	13.5%

This degradation will represent the effect then of protons on the solar cell itself. The ultraviolet radiation will also produce some degradation. For 3 and 6 Mil microsheet coverslides this will be of the order of 3% for one year, depending on adhesives, filters and coatings used. For the lead potash no quantitive data is presently available although browning of the coverslide has been noticed. Measurements are now being made to determine the magnitude of the discoloring for various exposure times and will be considered when available.

2.2.7.6 Reliability Calculations For The 1.042 inch by 2.384 inch Solar Cell (2.647 cm by 6.055 cm)

A chart can be prepared which will compare fracture losses for various cell sizes. This is as follows (see page 294 of Reference 1):

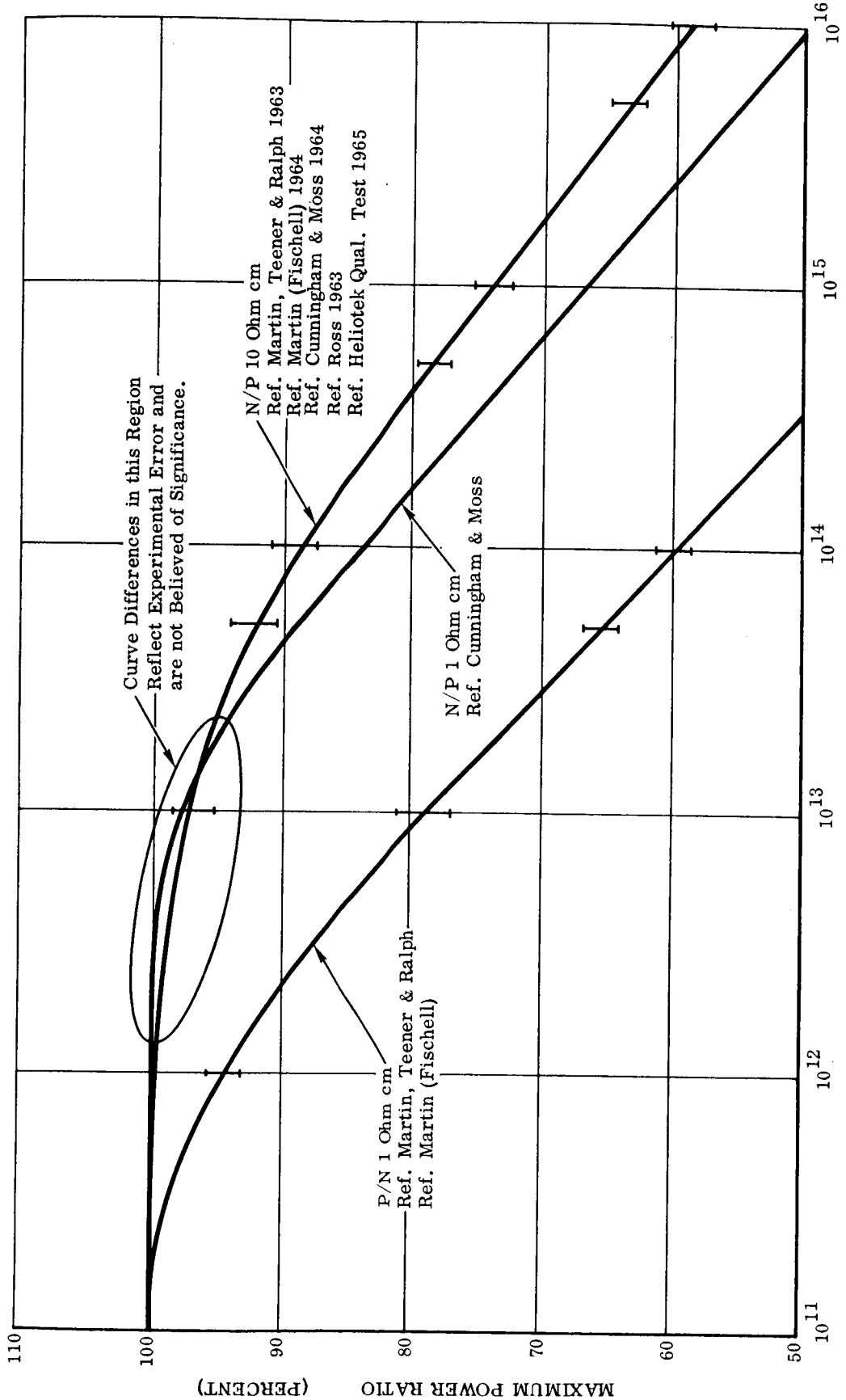

Figure 33 Effect of 1 MEV Electron Irradiation on Silicon Solar Cell Maximum Power Curves Derived From Experimental Studies Performed In Various Laboratories With Air Mass Zero Equivalent Sunlight, 28°

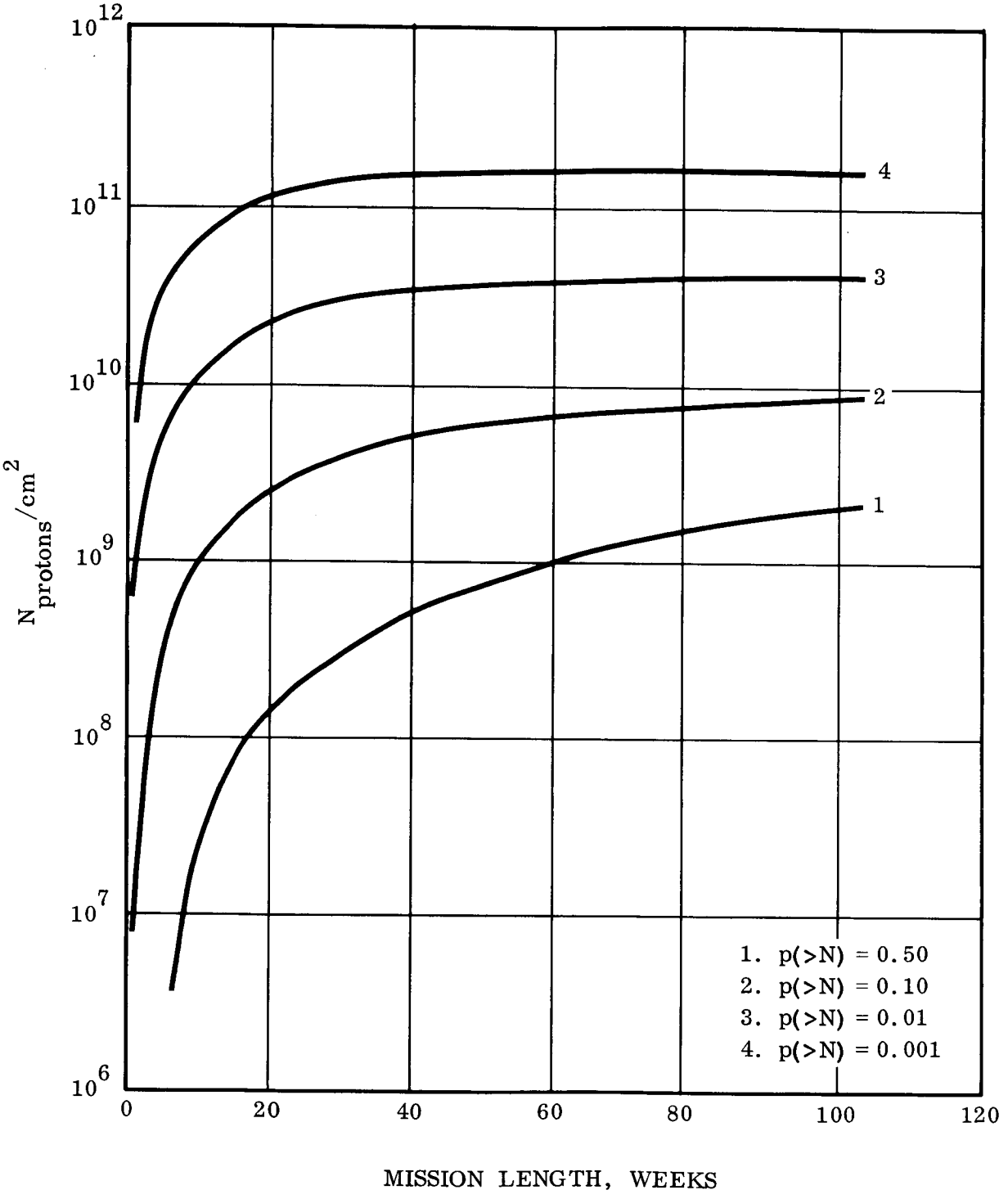

Figure 34 Mission Durations From 1 to 104 Weeks

Type Solar Cell	2 x 2 cm	2 x 6 cm	2.647 x 6.055 cm
Total Area (A)	4 cm^2	12 cm^2	16.097 cm^2
Maximum Area Loss Per Fracture	2.4 cm^2	3.5 cm^2	7.006 cm^2
Average Area Loss Per Fracture	1.2 cm^2	1.2 cm^2	2.341 cm^2
Average Percent Area Loss Per Fracture	30%	10%	14.5%

FOR THE RELATIVE FAILURE FACTOR WE OBTAIN

SOLAR CELL	P = (%) A
2 x 2	1.2
2 x 6	1.2
2.647 x 6.081	2.3

The proposed layout for the 2.647 x 6.055 cell would be 13 modules of 8 circuits consisting of 136 cells in series. This gives a total of 14,144 cells. This compares with 56,160 cells for the 2 x 2 cell configuration and 18,720 cells for the 2 x 6 cm cell configuration. Therefore in order to achieve a total array reliability of 0.99975 14 fractures will be necessary which is the same as for the 2 x 6 cm cell configurations. However, each fracture will produce approximately twice the loss in cell area as for the 2 x 6 cm cell configurations. Therefore, an array power loss of approximately 0.1% would occur with the 14 cell fractures.

The connector for the 2.647 x 6.055 cm cell will have 4 tabs on the N side and 5 tabs on the P side (Solaflex). This will give the same connector reliability per cell as did the connector for the 2 x 6 cm cell (i.e., a probability of failure for two years of 10^{-27} for

the N side and 10^{-33} for the P side). Overall a very slight increase in connector reliability would occur due to the fewer connectors in the special cell configuration. However, this effect is extremely slight.

The length of the long tabs on the back surface should be lengthened from the standard 2 x 6 configuration to an equivalent length for the 2.647 x 6.055 to yield the above reliability figures.

2.3 WEIGHTS ANALYSIS

This section presents calculated weights of sub-elements of the solar array (based on nominal sheet thickness and engineering tolerances) for the concept selected in the trade-off study phase of the program. These calculations are compared with initial estimated weights which served as target weights for design control purposes. Data is summarized in Table 12. Tables 6 through 11 present weight calculations for subelements of the array.

Little change has resulted from those weights presented for the selected concept described in the first Quarterly Report. Those items which are affected by design changes are denoted by asterisk (*) in the tables. The structural design changes which have been made have reduced structure weight, thereby increasing the electrical power/weight ratio.

The power to weight capabilities of the solar array are calculated considering various solar cell power output levels, combined with nominal and maximum expected solar array weights. These values establish a reasonable envelope of obtainable performance and indicate that the objective of the contract can be achieved. The equation used for these calculations is:

$$\text{Watts/Pound} = \frac{(\text{Cell Output})\ (\text{Gross Cell Area})}{(\text{Nominal Array Wt.})\ (K)}$$

TABLE 6

DRUM SUPPORT AND GUIDE SLEEVE MOUNT ASSEMBLY

Item	Cal. Wt. Machined Structure Concept	Target Weight
1. Support Channels	0.375	0.456
2. Slide Guide		0.200
3. Slide	0.102	0.171
*4. Slide Guide Fitting	0.808	
5. Slide Retaining Angles	0.052	--
6. Bulkhead and Adjustment Screws		0.108
7. Springs	0.140	0.140
8. Spring Fittings	0.014	0.027
9. Mount Lugs		0.074
10. Shims		
11. Mount Bolts	0.046	
12. Helicoil Inserts	0.024	
13. Retaining Screws	0.026	
14. Stop Mechanism	0.303	
TOTAL WEIGHT	1.891	1.176

* This weight has been revised from first Quarter Report, Reference 1.

TABLE 7

BEAM GUIDE SLEEVES

Item	Cal. Wt.	Target Wt.
1. Side Plates O/B	0.3203	0.3130
2. Side Plate I/B	0.2014	
3. Top Plates	0.1764	0.2660
4. Bottom Plates	0.0559	
5. End Plates I/B	0.1457	0.0540
6. End Plate O/B	0.0148	
7. Internal Bulkheads	0.1184	0.1310
8. Attach Angles	0.0380	
9. Frame Angle	0.0409	
10. Closing Angle	0.0096	
11. Guide Inserts	0.0842	0.4290
12. Top Plate (Support)	0.0432	
13. Support (Guide Insert)	0.2284	
14. Angles (Clutch End)	0.0075	
TOTAL	1.4847	1.1930

TABLE 8

WRAP DRUM ASSEMBLY

	Item	Cal. Wt. Slip Ring Concept	Target Wt.
1.	Skin (Mag.)	4.794	5.696
2.	Intermediate Rings	0.111	0.115
3.	Harness Retaining Ring		0.106
4.	End Plate Rings		0.113
*5.	End Plates	2.746	1.786
6.	Harness Spool		0.101
7.	Roller Brgs	0.160	
8.	Electrical Harness		1.600
9.	Electrical Wiring	0.600	
10.	Bushing Supports		0.167
*11.	Spindle and Bolt Attachment	0.260	
12.	Snap Rings	0 .009	
13.	Sleeve Holder	0.076	
14.	End Caps	0.065	
15.	Sleeves	0.246	
16.	Sleeve Flanges	0.056	
17.	Contact Rings	0.098	
18.	Ring Holders	0.164	
19.	Insulator	0.005	
20.	Contacts		
21.	Screws	0.010	
	TOTAL WEIGHT	9.400	9.684

* This weight has been revised from first Quarter Report, Reference 1.

TABLE 9

SPACECRAFT MOUNT ASSEMBLY

Item		Cal. Wt. Alumin. Support Structure Concept	Target Wt.
1. Top and Bottom Plates	(.025)	1.0470	0.466
2. Side Plates	(.028)	0.6966	0.368
3. Internal Bulkheads	(.020)	0.3498	0.074
4. Closure Angles		0.2596	0.093
5. Spacecraft Mount Fttg's	(2)	0.0669	0.033
6. Drum Mount Fttg's	(4)	0.0374	0.039
7. Center Attach Fttg's	(2)	0.0366	0.098
8. Truss Tubes	(4)	0.2491	1.787
9. Center Truss Tubes	(2)	0.0827	0.029
10. Truss Pins	(12)	0.1176	0.132
11. Fasteners Attach Fttg's (#6 alum. huckbolts)	(24)	0.0960	
12. Corner Bracket	(2)	0.0406	
TOTAL WEIGHT		3.0799	3.119

TABLE 10

PANEL ASSEMBLY

	Item	Cal. Wt. Kapton Substrate Concept	Target Wt.
1.	Substrate (0.001 Kapton)	2.016	3.233
2.	Substrate (0.001 Fiberglass)		
*3.	Substrate-Beam Attach Medium (Silicone Impregnated 0.004 Fiberglass)	0.089	0.050
*4.	Substrate Intersheet Attach Medium (Silicon Impregnated 0.004 Fiberglass)	0.047	0.045
5.	Side Beams (Basic)	3.029	3.272
6.	Tip Intercostal	0.263	0.502
7.	Stop Damper Pad	0.012	
8.	Substate Doublers (240)	0.061	0.082
9.	Drive Strips (1/2" Wire)	0.536	0.599
10.	Damper Pads	1.914	2.527
11.	Adhesive (Item 10)	0.764	
12.	Outer Wrap Blanket		0.158
	TOTAL WEIGHT	8.731	10.469

* This weight has been revised from first Quarter Report, Reference 1.

TABLE 11

DEPLOYMENT/RETRACTION SYSTEM

	Item	Cal. Wt. Redundant System Concept	Target Wt.
	Extension System		
1.	Drive Motor and Pinion	2.000	0.756
2.	Motor Brace	0.021	0.017
3.	Motor Mount	0.017	0.023
4.	Idlers	0.240	0.240
5.	Torque Tube Shaft	0.234	0.090
6.	Drive Sprockets	0.208	0.230
7.	Torque Tube End Caps	0.106	0.111
8.	Torque Tube	1.481	1.607
9.	Torque Tube Support	0.234	
10.	Bushings and Retainers	0.033	0.071
11.	Roll Pins	0.013	
12.	Attach Bolts (Shaft)	0.060	
13.	Attach Bolts (Motor)	0.040	
14.	Limit Switch and Drive	0.200	0.100
15.	Electrical Wiring	0.200	
	Retraction System		
16.	Drive Shaft-Pulley	0.107	
17.	Drum Pulley and Clutch	0.206	
18.	Spring Belt	0.150	
19.	Belt Retainer	0.021	
20.	Fasteners	0.035	
	TOTAL WEIGHT	5.606	3.245

TABLE 12

WEIGHT SUMMARY

Array Subassembly Item	Cal. Wt. Selected Configuration	Target Wt.	Cal. Wt. as percent of total
* Drum Support and Guide Sleeve Mount Assembly	1.891 (1.921)	1.176	2.5
Beam Guide Sleeves	1.485	1.193	1.9
* Wrap Drum Assembly	9.400 (9.135)	9.684	11.9
Spacecraft Mount Assembly	3.080	3.119	4.0
* Panel Assembly	8.731 (10.919)	10.469	14.2
Deployment/Retraction System	5.606	3.245	7.3
* TOTAL STRUCTURAL WT.	30.193 (32.146)	28.886	41.8
Solar Cell and Electrical Installation Wt. (2 x 2 x 0.008 with 0.003 CG. - 250.7 ft^2 @ 0.178 lb/ft^2)	44.627	47.636	58.2
TOTAL ARRAY WT.	74.820 (76.773)	76.522	100.0

* Brackets ( ) represent calculated weights as shown in first Quarter Report, Reference 1.

Power/Weight Summary

The watts/pound capability of the solar array configuration, as influenced by the various considerations discussed in this section, is determined as follows:

a. Nominal solar array weight with 10.0 watts per square foot solar cell power output.

$$\text{Watts/Pound} = \frac{(10)\ (250.72)}{74.820} = 33.51$$

b. Maximum solar array weight which allows for a 5% growth of the array during detail design and a 4% tolerance for material and fabrication tolerances with power at 10 watts/square ft.

$$\text{Watts/Pound} = \frac{(10)(250.72)}{(74.820)(1.04)(1.05)} = 30.69$$

Solar Array with

1. Nominal weight = 74.820 pounds
2. 2 x 2 - 0.008 cells, 0.003 coverglass with power of 10.2 watts/ft^2 as calculated for proposed design - Reference: Figure 23.

$$\text{Watts/Pound} = \frac{(10.2)(250.72)}{74.820} = 34.18$$

c. Maximum solar array weight as defined in 2.0 above with a power output of 10.2 watts/ft^2.

$$\text{Watts/Pound} = \frac{(10.2)(250.72)}{(74.820)(1.04)(1.05)} = 31.30$$

Ryan Selected Configuration

Ryan Selected Configuration

d. Solar Array with

1. Nominal weight = 74.820 pounds
2. 2 x 6 - 0.008 cells, 0.003 coverglass with power output of 10.3 watts/ft^2 - Reference: Figure 25.

$$\text{Watts/Pound} = \frac{(10.3)(250.72)}{74.820} = 34.52$$

e. Maximum solar array weight as defined in 2.0 above with power output of 10.3 watts/ft^2.

$$\text{Watts/Pound} = \frac{(10.3)(250.72)}{(74.820)(1.04)(1.05)} = 31.61$$

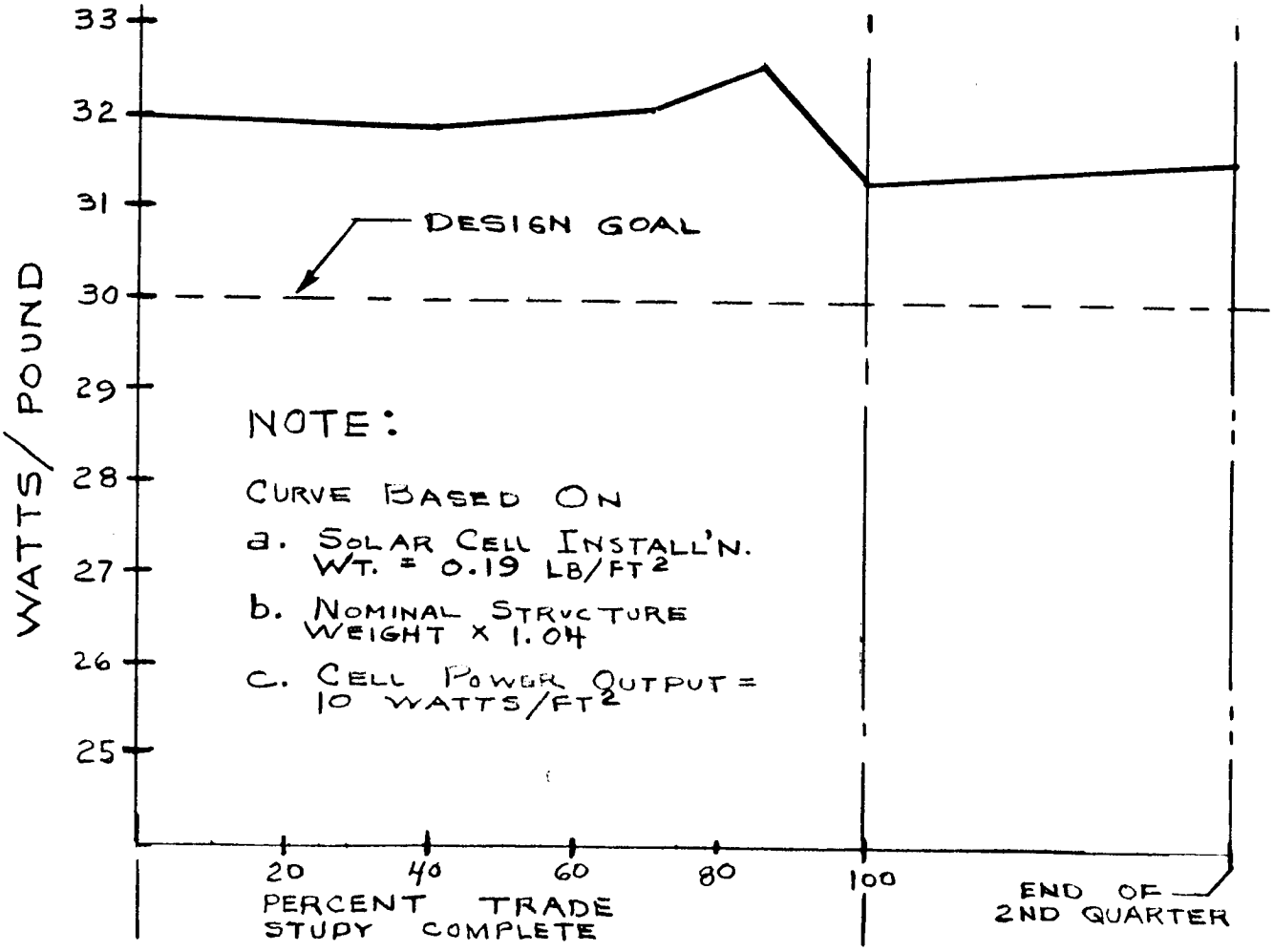

Figure 35 Power/Weight Monitor

Where:

Gross Cell Area = 250.72 Sq. Ft.

K = (Growth Allowance) (Tolerance Allowance) = (1.05) (1.04)

Figure 35 is a power to weight curve that illustrates changes which incurred during trade study activity. The curve has been extended to illustrate the trend that has occured since the last reporting period. The curve considers:

a. An electrical installation weight (cells, wiring, interconnections and adhesives) of 0.19 lb/ft^2 of gross cell area. The 0.19 value is considered a maximum unit weight, utilizing 2 x 2 cm, 0.008 mil cells with 0.003 mil coverglass. This solar cell installation concept will provide 10.0 watts per square foot of power at 1 A.U.

b. Structural mechanical weight at 4% above nominal to account for material and fabrication tolerances.

2.4 TEST DATA

2.4.1 Damping Pad Dynamic Characteristics Test

The intent of this test was to determine the amount of Dynamic Excitation normal to the stowed panel axis at sinusoidal resonance, that can be transmitted through the Polyurethane separation medium pads. The pad configuration used for test simulated that selected in the preceding analysis for support of the inner second and third wraps. Primarily the reason for selecting this pad configuration for test was because of concern for the more critical dynamic loads which occur at the stowed panel inner wrap layers in a compact wrapped panel system. However, we might assume that transmissibility is solely a function of resonant frequency of the respective wrap layer supporting the mass of

the wraps above it and not the total thickness of foam pads the energy must pass through to get to the respective wrap; this may be a conservative assumption, but it allows us to consider the test results as applicable to any wrap layer.

The test specimen consisted of a 9" x 11.5" substrate with the pads bonded to one side. On the other side was bonded one 4 x 14 wired solar cell matrix utilizing 2 x 2 cm x 0.008 solar cells and 0.003 cover glasses; a row of2 cm x 2.75" copper strips each side of the matrix provided complete equivalent mass coverage of specimen at 0.2 lbs/ft^2.

The specimen was draped (to simulate wrapped conditions) over a six inch radius rigid aluminum cylindrical half section fixture and clamped to it as its two ends as shown in Figure 36. The fixture was mounted to a sine wave vibration exciter and the specimen response accelerations monitored (using a miniature accelerometer attached with double back tape to the solar cell coverglass in the center of the specimen in the plane of excitation) at specimen natural frequencies in increments between 1g (0-Pk) and 30 g(0-Pk) input excitation and recorded on an X-Y plot. Input excitation levels were controlled from an accelerometer mounted to the fixture in the plane of excitation. The solar cells were inspected visually for cracks before increasing the input excitation levels between increments.

Test Results

No solar cell damage occured as a result of testing with maximum response accelerations tested to 100 g (0-Pk). The test results are plotted in Figure 37 as a function of dynamic transmissability (response acceleration ÷ input excitation) at specimen resonance for the various excitation levels tested to. The dynamic transmissibility then, from the plot for the resonance frequency of 52.5 cps, calculated in the preceding analysis for the selected pad concept on each

wrap layer is about 3 g's for an input excitation of 6.5 g's

$$\text{Response Acceleration at 52.5 cps from curve in analysis} \div \text{Assumed Pad Transmissability} = 4$$

to the panel wraps. However, a peak transmissability at 52.5 cps is shown to be about 4g on the plot and will be used for design.

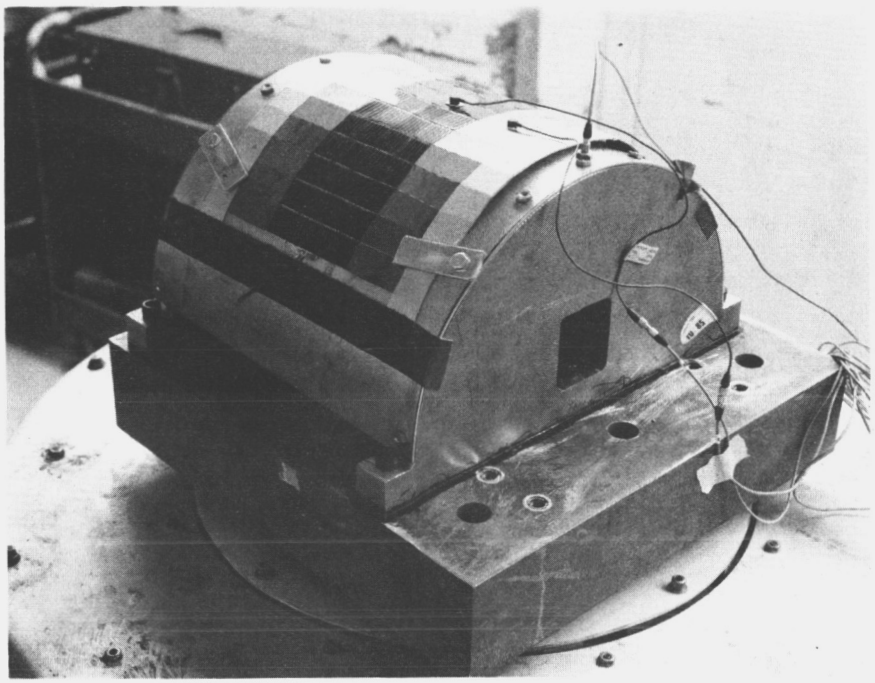

Figure 36 Test Setup on Vibration Exciter

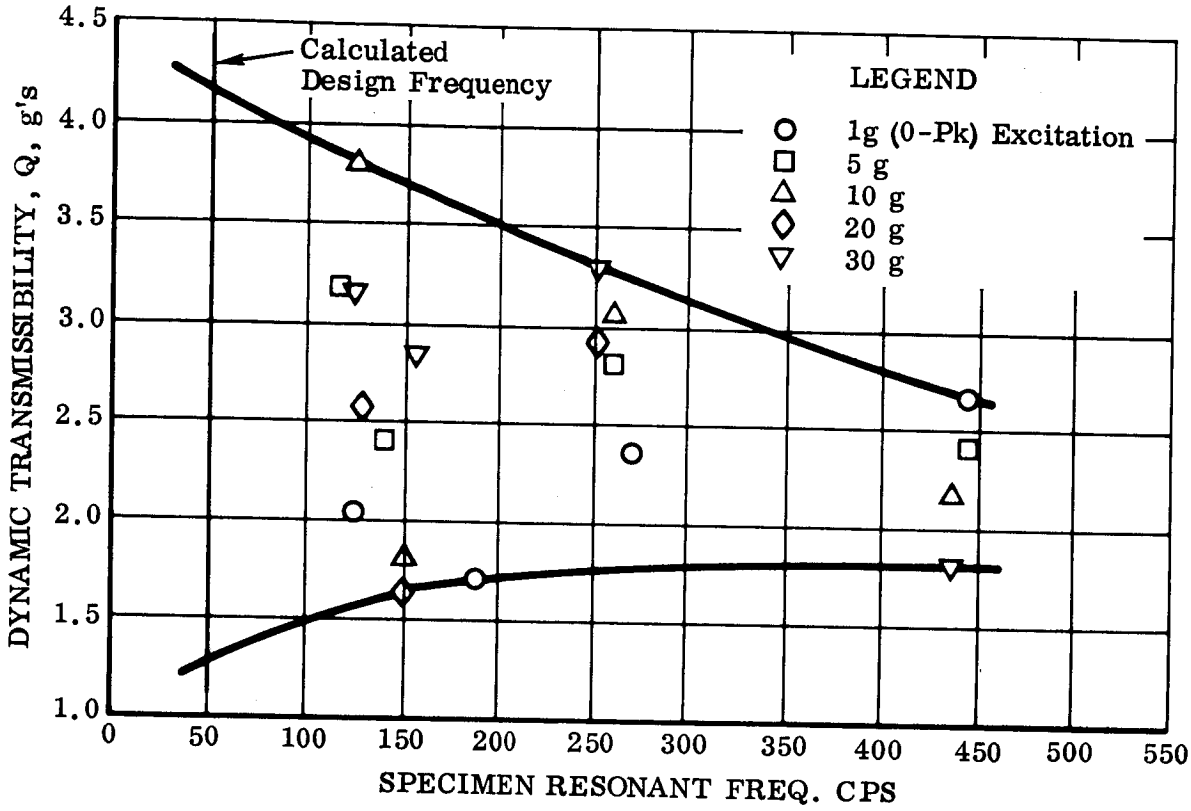

Figure 37 Dynamic Transmissibility Test Results

2.4.2 Test Procedures - Solar Cell Installation

Various test techniques have been reviewed and evaluated and the following procedure is recommended.

2.4.2.1 Test Equipment

a. Primary Standard Cells (four) - to be calibrated in accordance with techniques developed by JPL

b. Special Test Fixture

c. Three kilowatt Electronic load (variable)

d. X-Y Plotter

e. Strip Chart Temperature Recorder

f. Thermocouples

g. Large area AMO Solar Simulator

h. Temperature Bath

i. Mylar covered test chamber

2.4.2.2 Special Test Equipment Review

Primary Standard Cells

These basic silicon chips will be fabricated from the same type of diffused silicon as the solar cells used on the production array. This procedure is necessary due to the spectral response diffusion depth dependence. It is also essential that all aspects of the solar cell coverglass assembly be as nearly identical to the production array as possible to insure a correct spectral response matching.

Special Test Fixture

This fixture will be fabricated to accomodate one complete circuit to facilitate accurate testing. The fixture would feature vacuum hold down and fluid cooling.

Electronic Load

This device would facilitate the tracing of I-V curves of circuits, modules and complete array. Although this piece of equipment is not essential to testing, it would insure accuracy of the tests and save a considerable amount of data reduction and curve generation. Existing equipment is capable of dissipating approximately 250 watts (6.5 amps short circuit current and 60 volts open circuit voltage). An electronic load for an array of 13 modules must be capable of dissipating peak loads of approximately 2.5 KW. A device of this nature could be designed and developed in a span time that is within the constraints of the contract.

Large Area AMO Solar Simulator

A large area simulator of this type is currently available at the Spectrolab facility. A modification in the lens system of the present system is necessary to accomodate the 9 x 36 inch circuits used on the roll-up array. This modification would not be a pacing task.

2.4.2.3 General Test Sequence

Individual Circuits

a. Calibrate simulator using balloon primary standard cells.

b. Position complete circuit serial number 1 in position. Measure and record V_{oc} and I_{sc} and trace I-V curves.

c. Verify simulator using balloon standard.

d. Proceed with testing of all circuits for one complete module utilizing the above technique.

e. Construct a composite I-V curve for 8 circuits (1 module) by summation of average currents for a circuit at a specific voltage.

Individual Modules

a. Install module (with thermocouples attached) and handling frame in mylar covered test chamber.

b. Place primary standard in chamber. Checkout system and close chamber.

c. Stabilize temperature, record primary standard reading and trace three I-V curves. Record primary standard reading.

d. Reduce data and draw a new I-V curve to standard test conditions. Compare new curve to composite of eight individual circuits.

Array (13 Modules Assembled)

This test will be performed after the thirteen modules have been assembled to form a complete array. It will serve the purpose of verifying array operation and confirm results obtained.

Special considerations must be given to handling equipment, test area and test equipment because of the unique nature of this deployed array. The problems associated with handling and testing a complete array will be solved jointly by the Ryan Aeronautical Company and Spectrolab.

3.0 CONCLUSIONS

Work performed to date lends confidence to the concept selection that was presented in the first Quarterly Report. Studies and detail design efforts have not disclosed any deterrents that would constrain the design nor impair achievement of contract objectives.

The structural and mechanical design for deploying an array of 250 square feet solar cells is considered to be the most suitable, considering the design criteria and allowing for state-of-the-art capabilities. Studies relevant to the solar cell installation indicate that whereas existent technology is adequate, new designs in solar cells and coverglass application are feasible that would advance the technology beyond the minimum requirements established for this first phase of ths contract.

4.0 RECOMMENDATIONS

With six months of contracted work completed, this contractor reiterates its recommendation and intention to proceed with the design and analysis and fabrication of a deployment demonstration model of the roll-out solar array. That this work continue in accordance with the program plan that has been submitted; Ryan Report No. 40075-1 dated 11 August 1967; Reference 2.

5.0 NEW TECHNOLOGY

Descriptive Title --

The Application Of Ultra Thin Solar Cell Coverslides

Names of Innovators --

Robert Oliver

Edward Zimmerman

Progress Report Disclosure --

Brief description included in this second quarterly report for the 30 watt per pound roll-up solar cell array.

Location of Initial Disclosure --

Initial disclosure was on page 22 of the aforementioned report.

Disclosure Date --

A new technology report was submitted to NASA, January 19, 1968

PRECEDING PAGE BLANK NOT FILMED.

6.0 REFERENCES

1. First Quarterly Report On The Feasibility Study, 30 Watts Per Pound, Rollup Solar Array Report 40067-1, Ryan Aeronautical Company, 10 November 1967.

2. Ryan Report 40075-1, Feasibility Study, 30 Watts/Pound Roll-Up Solar Array, Program Plan, 11 August 1967.

3. System Specification No. SS501407A, Roll-Up Solar Cell Array, 30 Watts Per Pound, Detail Requirements For, Jet Propulsion Laboratory, California Institute of Technology, 4 January 1967.

4. Phase I Report On The Development of Deployable Solar Arrays, Report 64B119, Ryan Aeronautical Company, San Diego, California, 15 October 1964.